

# Polarimetric SAR Interferometry

**Konstantinos P. Papathanassiou, Matteo Pardini**

German Aerospace Center (DLR)  
Microwaves and Radar Institute (DLR-HR)

[kostas.papathanassiou@dlr.de](mailto:kostas.papathanassiou@dlr.de)  
[matteo.pardini@dlr.de](mailto:matteo.pardini@dlr.de)

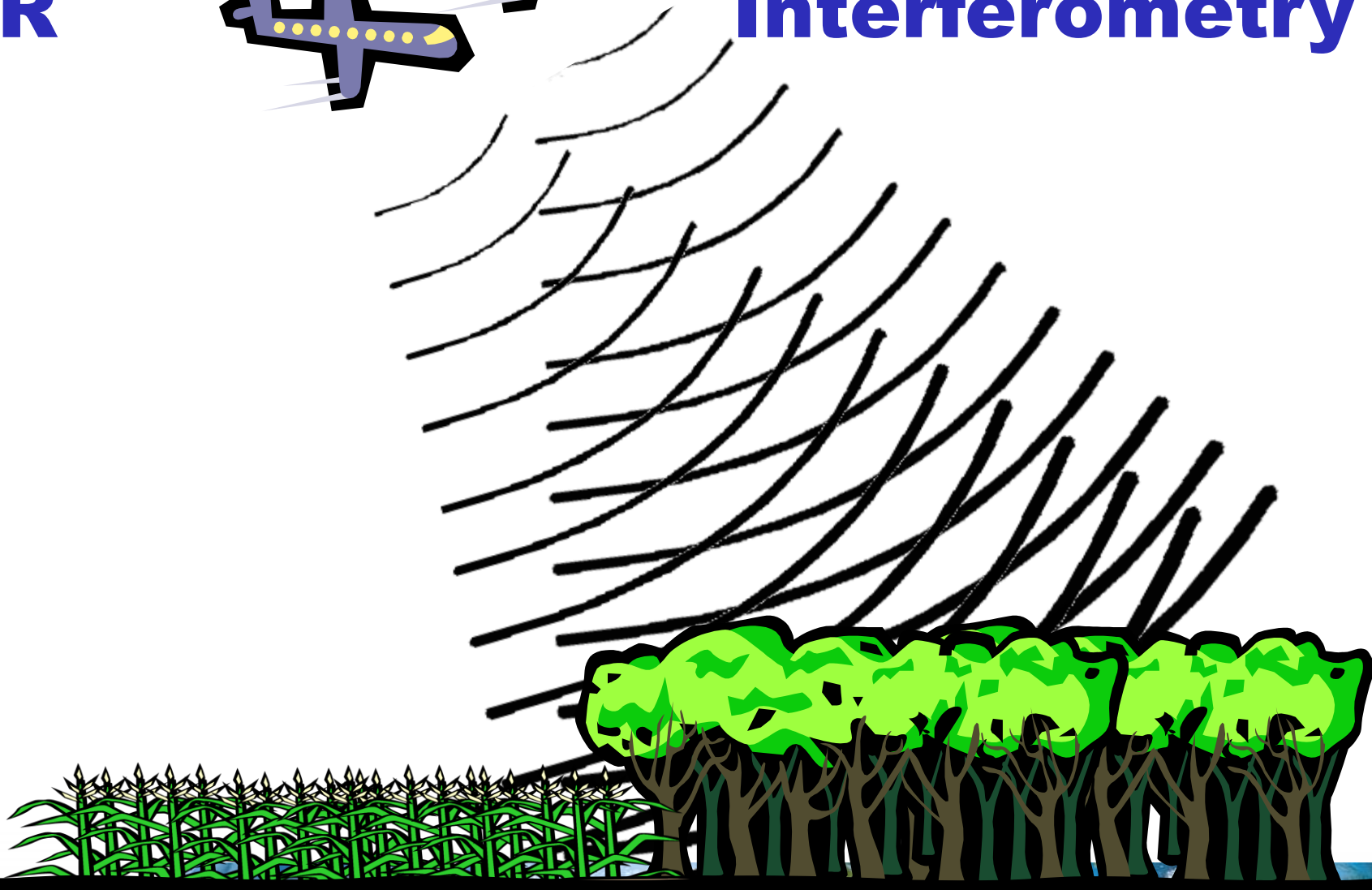


# Polarimetric

# SAR



# Interferometry

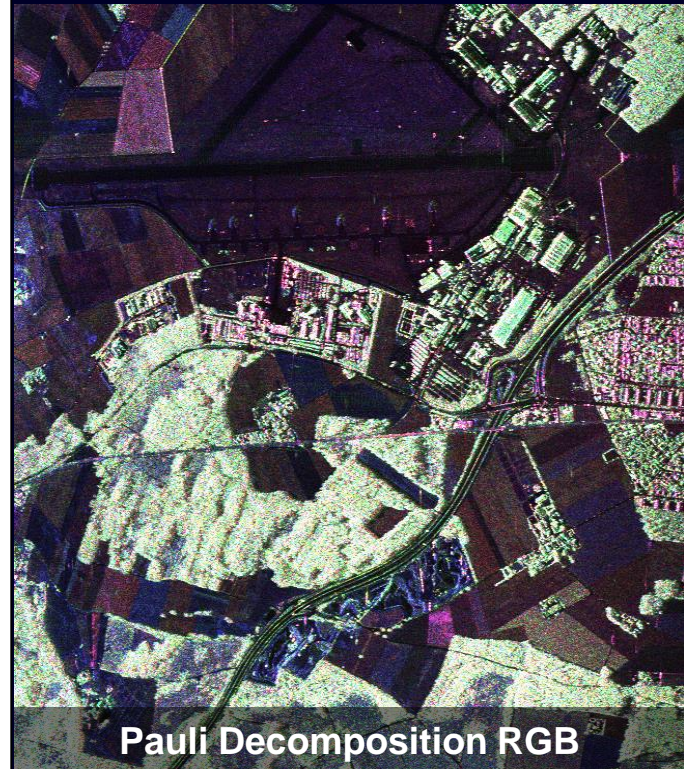




VV Channel Image

# SAR Polarimetry (PolSAR)

Allows the identification / decomposition of different scattering processes occurring inside the resolution cell



Pauli Decomposition RGB



VV Channel Image

# SAR Interferometry (InSAR)

Allows the location of the effective scattering center inside the resolution cell



## SAR Polarimetry (PolSAR)

Allows the identification / decomposition of different scattering processes occurring inside the resolution cell

## SAR Interferometry (InSAR)

Allows the location of the effective scattering center inside the resolution cell



Pauli Decomposition RGB



VV Channel Image



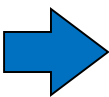
InSAR DEM

## Polarimetric SAR Interferometry (Pol-InSAR)

Potential to separate in height different scattering processes occurring inside the resolution cell.

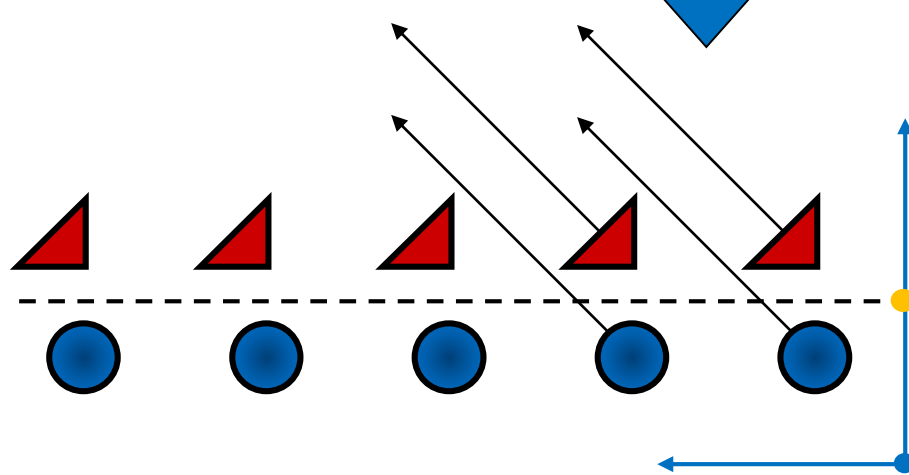
# Interferometry vs. Polarimetry

$$S_{HH}^1 = A_D^1 + A_S^1$$



$$\varphi = \arg\{ S_{HH}^1 \quad S_{HH}^{2*} \}$$

$$S_{HH}^2 = A_D^2 + A_S^2$$

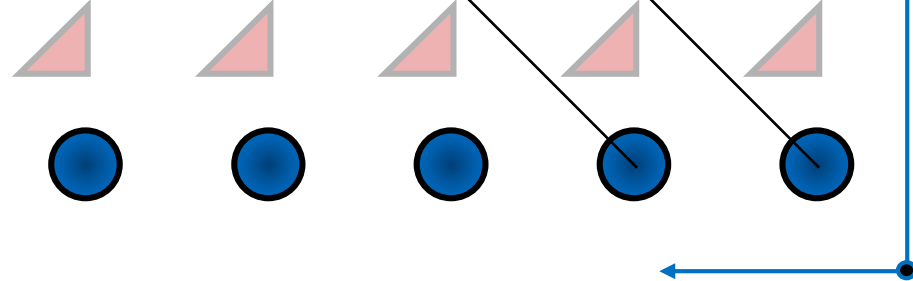


$$[S_D] = \begin{bmatrix} S_{HH} & S_{HV} \\ S_{VH} & S_{VV} \end{bmatrix} = A_D \begin{bmatrix} 1 & 0 \\ 0 & -1 \end{bmatrix}$$

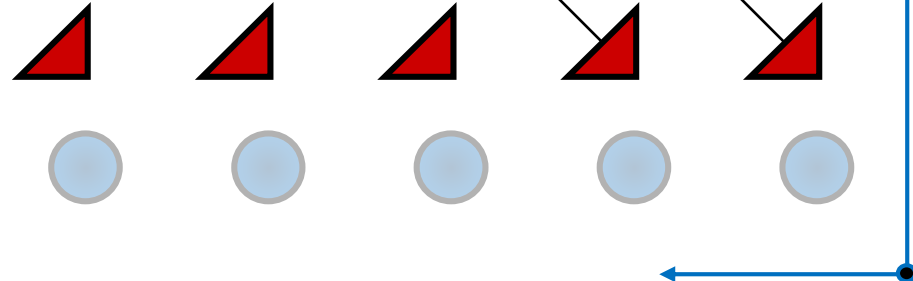


$$[S_S] = \begin{bmatrix} S_{HH} & S_{HV} \\ S_{VH} & S_{VV} \end{bmatrix} = A_S \begin{bmatrix} 1 & 0 \\ 0 & 1 \end{bmatrix}$$

$$S_{HH} + S_{VV} = 2A_S$$



$$S_{HH} - S_{VV} = 2A_D$$

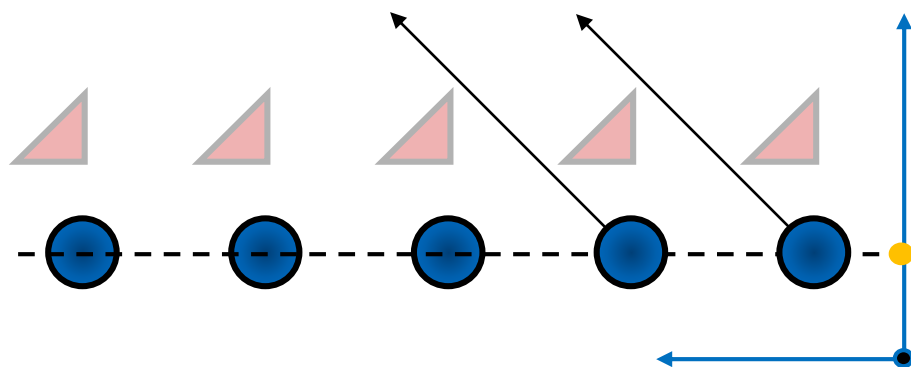


# Polarimetric Interferometry

$$i_{1S} = S_{HH}^1 + S_{VV}^1 = 2A_S^1$$

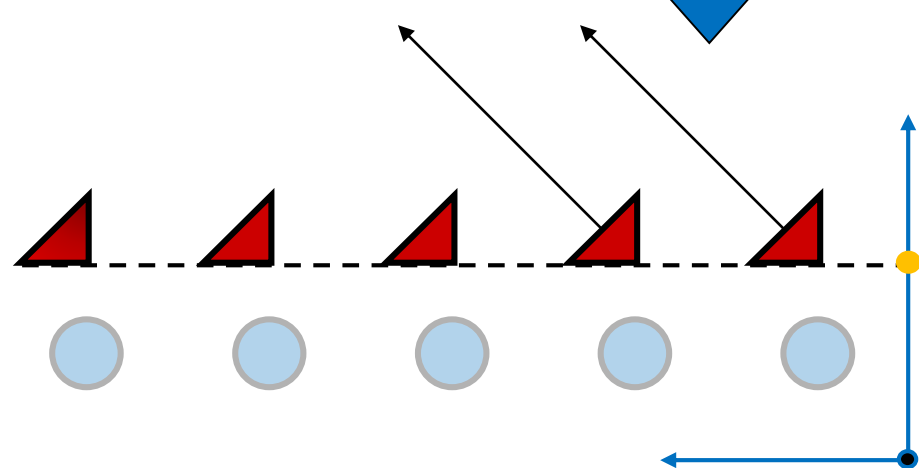
$$\rightarrow \varphi_S = \arg\{ i_{1S} \ i_{2S}^* \}$$

$$i_{2S} = S_{HH}^2 + S_{VV}^2 = 2A_S^2$$



$$i_{1D} = S_{HH}^1 - S_{VV}^1 = 2A_D^1$$

$$i_{2D} = S_{HH}^2 - S_{VV}^2 = 2A_D^2$$



$$[S_D] = \begin{bmatrix} S_{HH} & S_{HV} \\ S_{VH} & S_{VV} \end{bmatrix} = A_D \begin{bmatrix} 1 & 0 \\ 0 & -1 \end{bmatrix}$$



$$[S_S] = \begin{bmatrix} S_{HH} & S_{HV} \\ S_{VH} & S_{VV} \end{bmatrix} = A_S \begin{bmatrix} 1 & 0 \\ 0 & 1 \end{bmatrix}$$



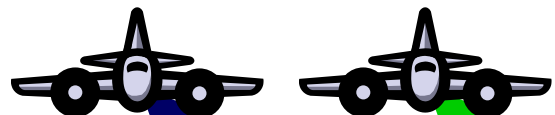


PolSAR

$$[S] = \begin{bmatrix} S_{HH} & S_{HV} \\ S_{VH} & S_{VV} \end{bmatrix} \rightarrow$$

### Polarimetric Coherences

$$\gamma(S_{ij} S_{mn}) = \frac{\langle S_{ij} S_{mn}^* \rangle}{\sqrt{\langle S_{ij} S_{ij}^* \rangle \langle S_{mn} S_{mn}^* \rangle}}$$

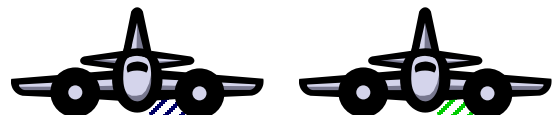


InSAR

$$[S_1 \quad S_2] \rightarrow$$

### Interferometric Coherences

$$\gamma(S_1 S_2) = \frac{\langle S_1 S_2^* \rangle}{\sqrt{\langle S_1 S_1^* \rangle \langle S_2 S_2^* \rangle}}$$



Pol-InSAR

$$[S_1] = \begin{bmatrix} S_{HH}^1 & S_{HV}^1 \\ S_{VH}^1 & S_{VV}^1 \end{bmatrix}$$

$$[S_2] = \begin{bmatrix} S_{HH}^2 & S_{HV}^2 \\ S_{VH}^2 & S_{VV}^2 \end{bmatrix} \rightarrow$$

### Polarimetric / Interferometric Coherences

$$\gamma(S_{ij}^1 S_{mn}^2) = \frac{\langle S_{ij}^1 S_{mn}^{2*} \rangle}{\sqrt{\langle S_{ij}^1 S_{ij}^{1*} \rangle \langle S_{mn}^2 S_{mn}^{2*} \rangle}}$$



# Complex Coherences on the Unit Circle (UC)

$$\tilde{\gamma} := \frac{\sum_{k=1}^N S_1(k)S_2^*(k)}{\sqrt{\sum_{k=1}^N S_1(k)S_1^*(k) \sum_{k=1}^N S_2(k)S_2^*(k)}} = \exp(i \operatorname{Arg}(\tilde{\gamma})) \cdot |\tilde{\gamma}|$$

Correlation Coefficient  $0 \leq |\tilde{\gamma}| = \gamma \leq 1$

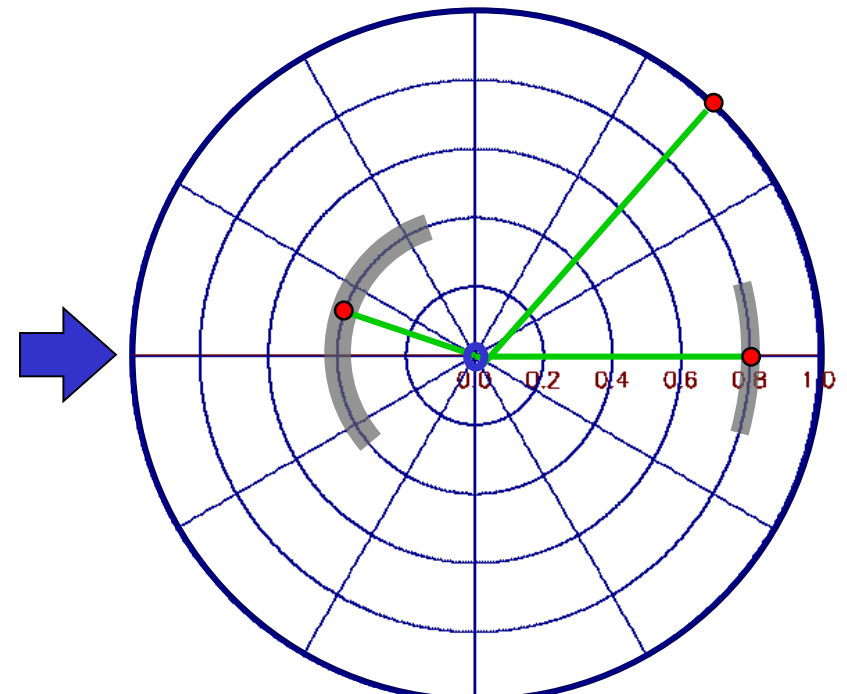
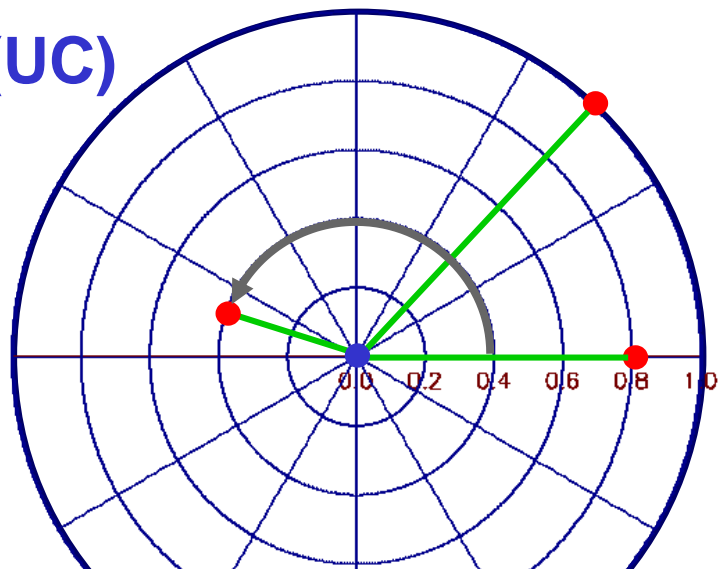
Interferometric Phase  $0 \leq \operatorname{Arg}(\tilde{\gamma}) = \phi \leq 2\pi$

Cramer Rao Bounds:

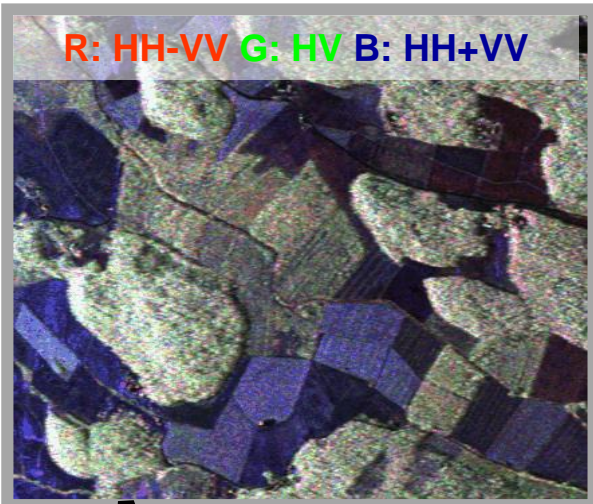
Correlation Coefficient  $\operatorname{VAR}(|\tilde{\gamma}|)_{\text{CR}} = \frac{(1 - |\gamma|^2)^2}{2N}$

Interferometric Phase  $\operatorname{VAR}(\phi)_{\text{CR}} = \frac{1 - |\gamma|^2}{2N|\gamma|^2}$

$\phi = \operatorname{arg}(\tilde{\gamma})$  and N is the number of Looks



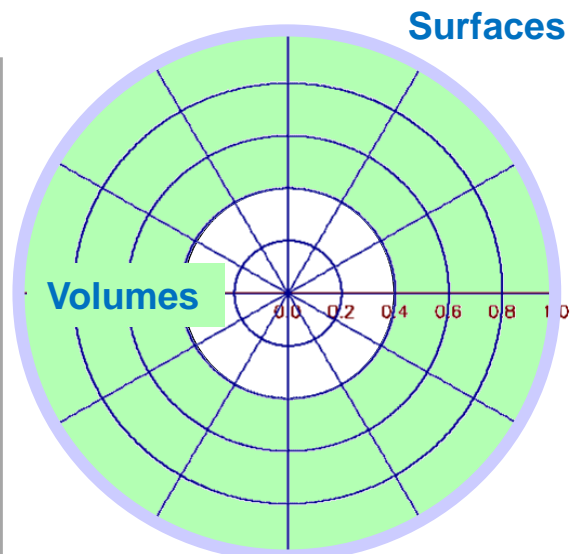
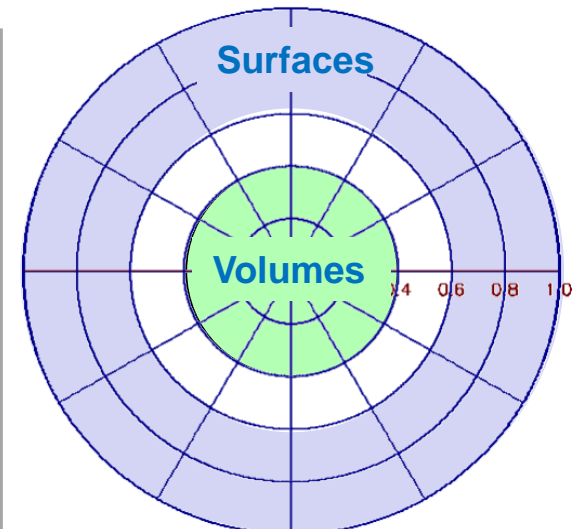
# Why is Interferometry important for Volume Scatterers?

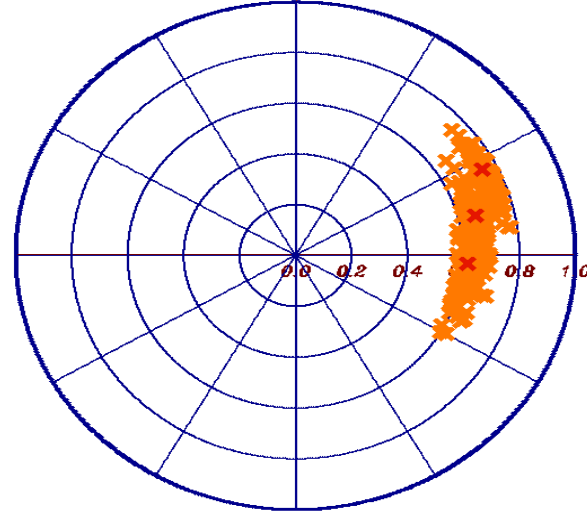
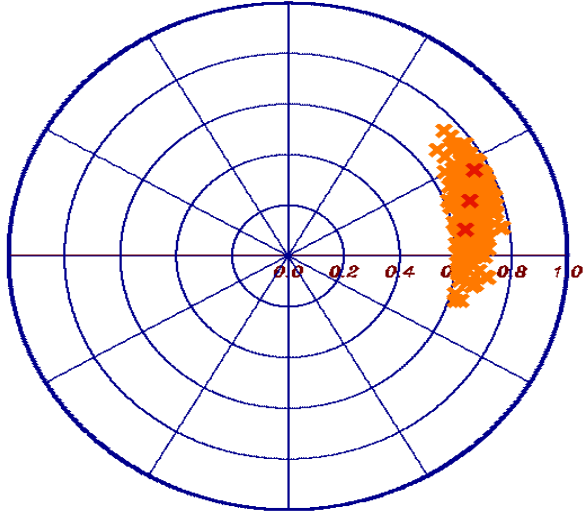
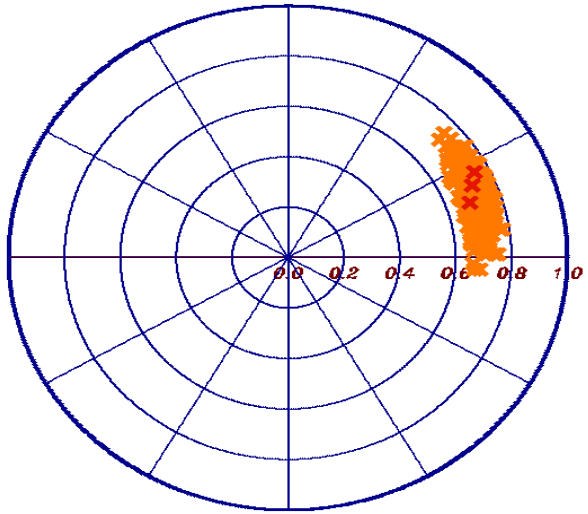


HH-VV Coherence

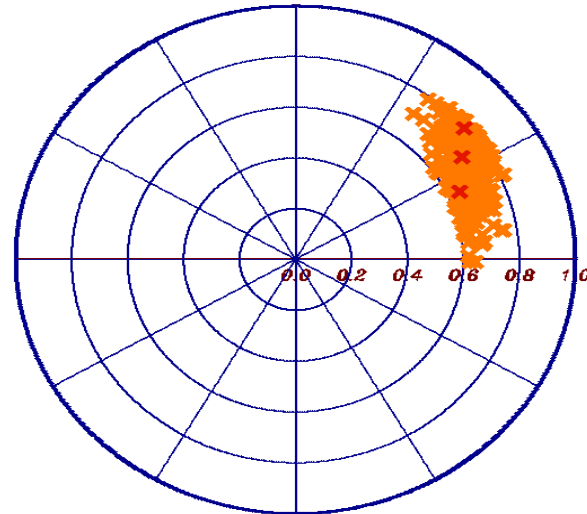
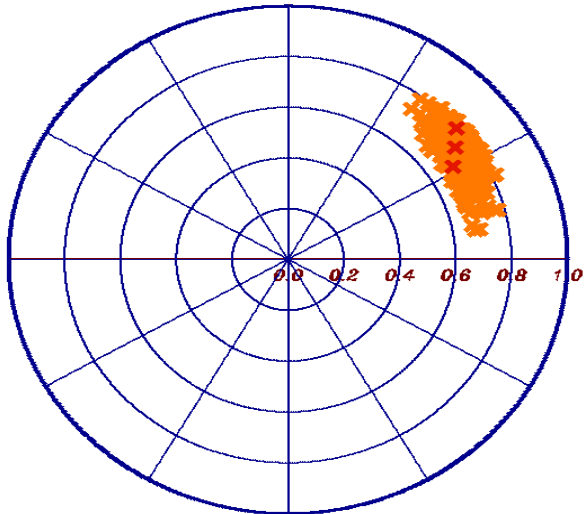
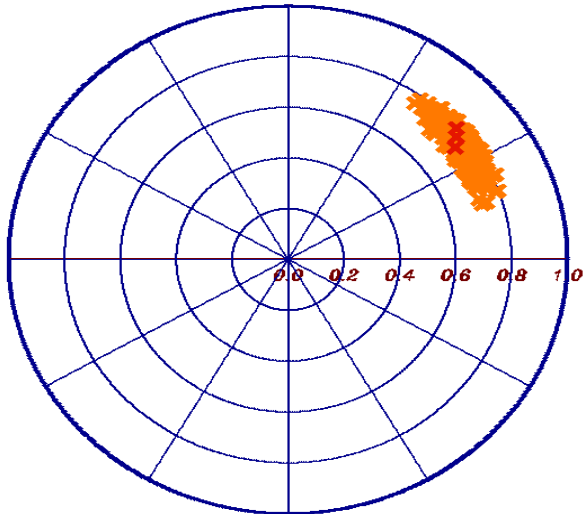


HH-HH Coherence





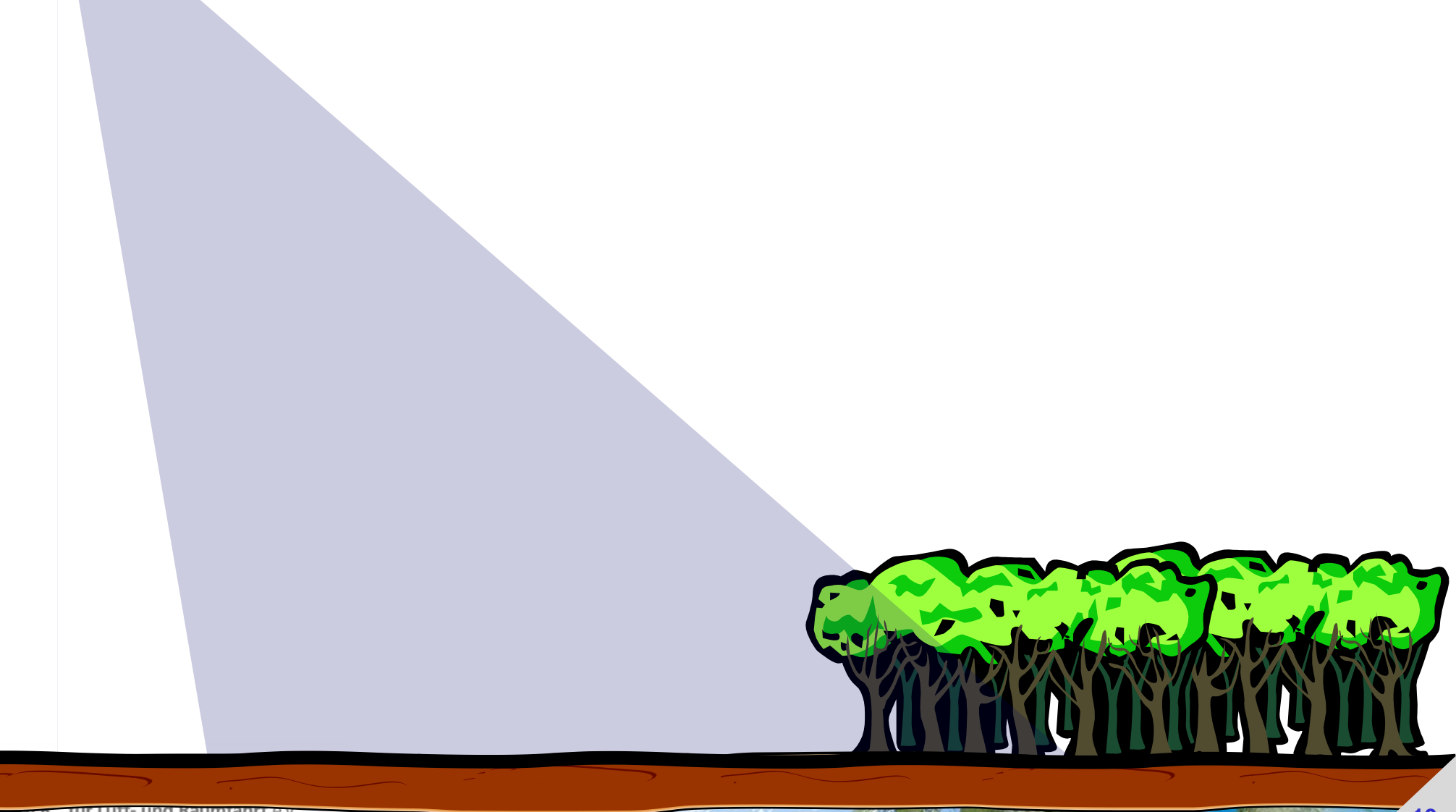
## Pol-InSAR: Basic Principles & Ideas





$S_1$

## SAR Interferometry for Volume Structure



 $S_1$  $S_2$ 

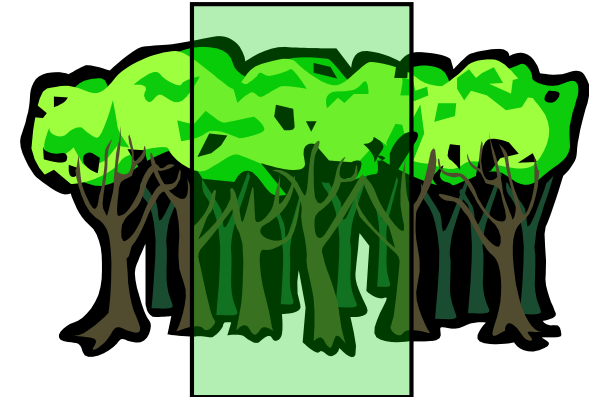
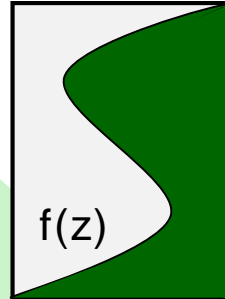
### Interferometric Coherence

$$\tilde{\gamma}(S_1 S_2) = \frac{< S_1 S_2^* >}{\sqrt{< S_1 S_1^* > < S_2 S_2^* >}}$$

## SAR Interferometry for Volume Structure

**Volume Coherence**

$$\tilde{\gamma}_{Vol}(f(z), k_z) = e^{ik_z z_0} \frac{\int_{-h_v}^{h_v} f(z) e^{ik_z z} dz}{\int_{-h_v}^{h_v} f(z) dz}$$



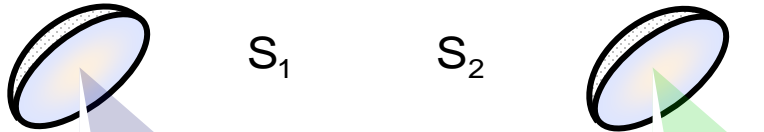
$f(z)$  ... vertical reflectivity function

$$\tilde{\gamma} = \tilde{\gamma}_{Temporal} \tilde{\gamma}_{SNR} \tilde{\gamma}_{Vol}$$

- $\tilde{\gamma}_{Temporal}$  ... temporal decorrelation
- $\tilde{\gamma}_{SNR}$  ... additive noise decorrelation
- $\tilde{\gamma}_{Volume}$  ... geometric decorrelation

$$\text{Vertical Wavenumber: } k_z = \frac{\kappa \Delta \theta}{\sin(\theta_0)}$$





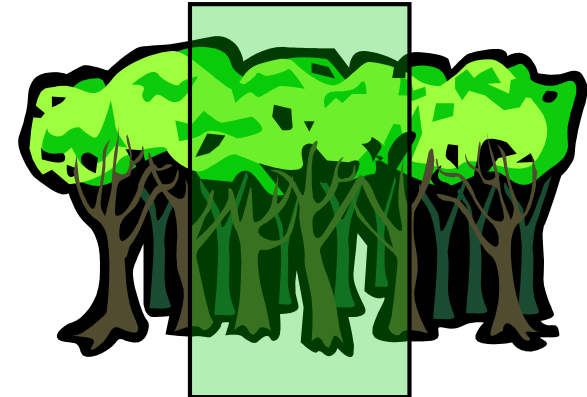
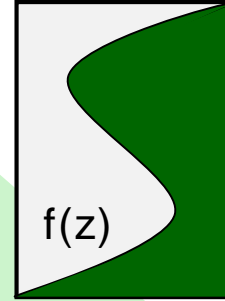
Interferometric  
Coherence

$$\tilde{\gamma}(S_1, S_2) = \frac{< S_1 S_2^* >}{\sqrt{< S_1 S_1^* > < S_2 S_2^* >}}$$

## SAR Interferometry for Volume Structure

Volume  
Coherence

$$\tilde{\gamma}_{Vol}(f(z), k_z) = e^{ik_z z_0} \frac{\int_0^{h_v} f(z) e^{ik_z z} dz}{\int_0^{h_v} f(z) dz}$$



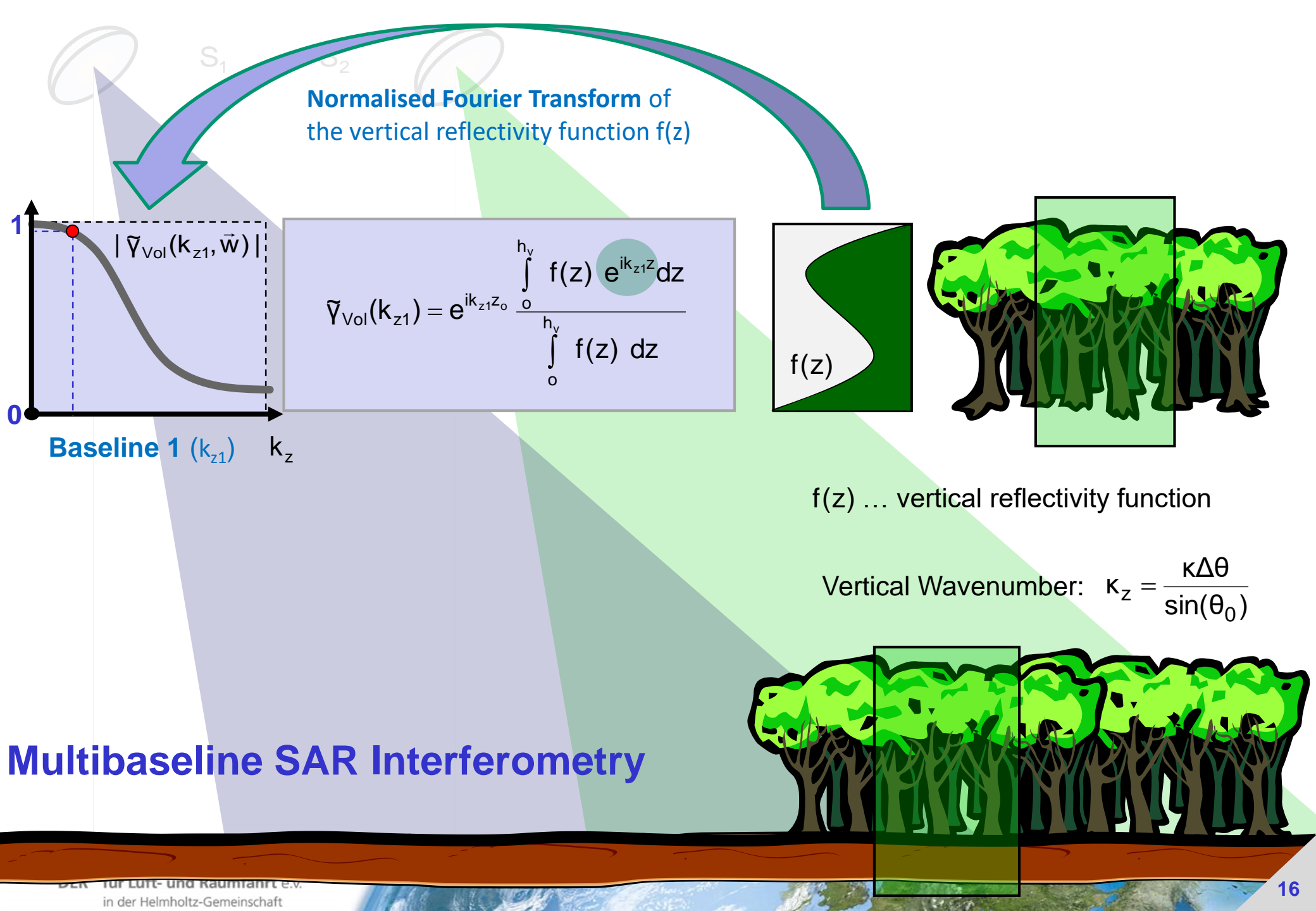
$f(z)$  ... vertical reflectivity function

$$\tilde{\gamma} = \tilde{\gamma}_{Temporal} \tilde{\gamma}_{SNR} \tilde{\gamma}_{Vol}$$

- $\tilde{\gamma}_{Temporal}$  ... temporal decorrelation
- $\tilde{\gamma}_{SNR}$  ... additive noise decorrelation
- $\tilde{\gamma}_{Volume}$  ... geometric decorrelation

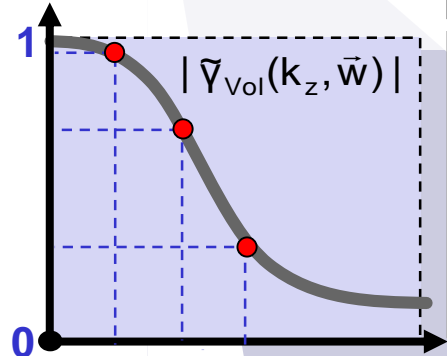
$$\text{Vertical Wavenumber: } k_z = \frac{\kappa \Delta \theta}{\sin(\theta_0)}$$

SAR interferometry allows to reconstruct the vertical reflectivity function  $f(z)$  of a volume scatterer by means of interferometric (volume) coherence measurements at different vertical wavenumbers  $k_z$ , i.e. at different spatial baselines.



  $S_1$   
**Baseline 3 ( $k_{z3}$ )**

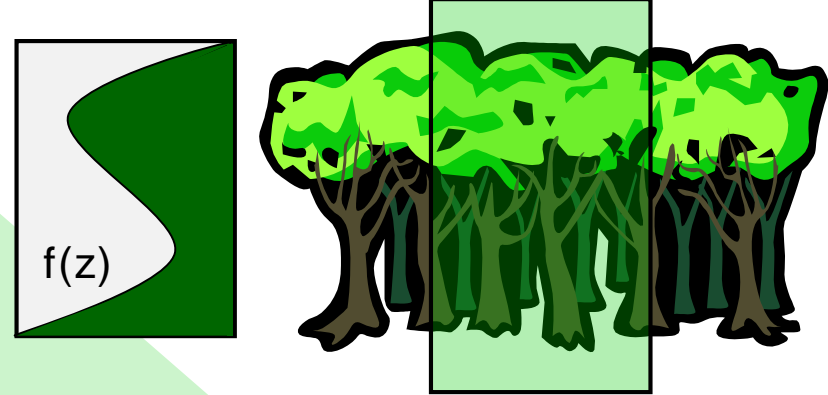
$$\tilde{\gamma}_{\text{vol}}(k_{z3}) = e^{ik_z z_o} \frac{\int_0^{h_v} f(z) e^{ik_{z3} z} dz}{\int_0^{h_v} f(z) dz}$$



**Baseline 2 ( $k_{z2}$ )**

$$\tilde{\gamma}_{\text{vol}}(k_{z2}) = e^{ik_z z_o} \frac{\int_0^{h_v} f(z) e^{ik_{z2} z} dz}{\int_0^{h_v} f(z) dz}$$

$$\tilde{\gamma}_{\text{vol}}(k_{z1}) = e^{ik_z z_o} \frac{\int_0^{h_v} f(z) e^{ik_{z1} z} dz}{\int_0^{h_v} f(z) dz}$$



$f(z)$  ... vertical reflectivity function

Vertical Wavenumber:  $\kappa_z = \frac{\kappa \Delta \theta}{\sin(\theta_0)}$

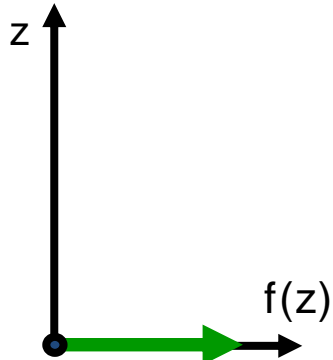


## Multibaseline SAR Interferometry

Multi-baseline measurements allow to sample the spectrum of the vertical reflectivity  $\text{FT}\{f(z)\}$  @ different (spatial) frequencies ( $k_z$ ).

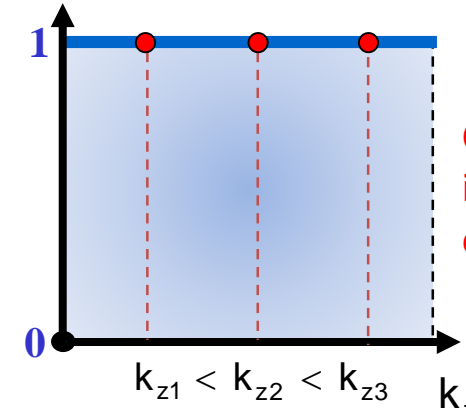
## Vertical Reflectivity Function $f(z)$

Surface Scatterer

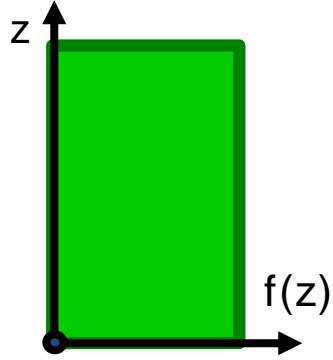
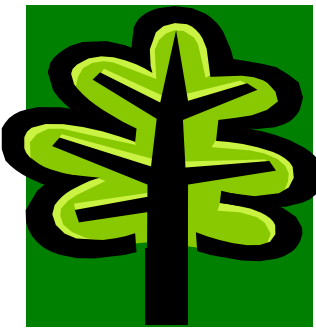


$$|\tilde{\gamma}_{\text{Vol}}(k_z)| = \frac{\left| \int_0^{h_v} f(z) e^{ik_z z} dz \right|}{\int_0^{h_v} f(z) dz}$$

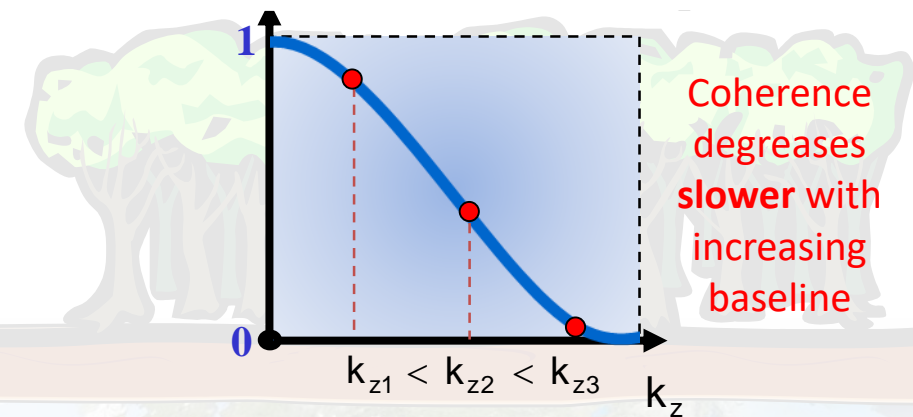
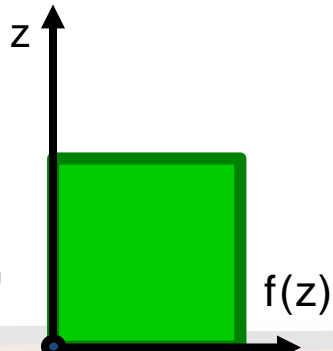
## InSAR Volume Coherence $|\tilde{\gamma}_{\text{Vol}}(k_z)|$



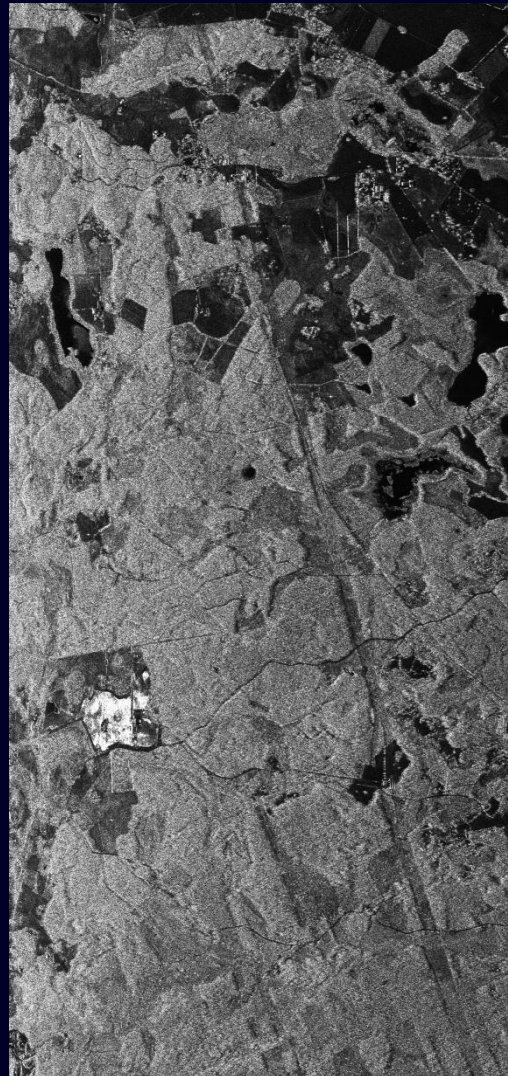
Tall Vegetation



Short Vegetation



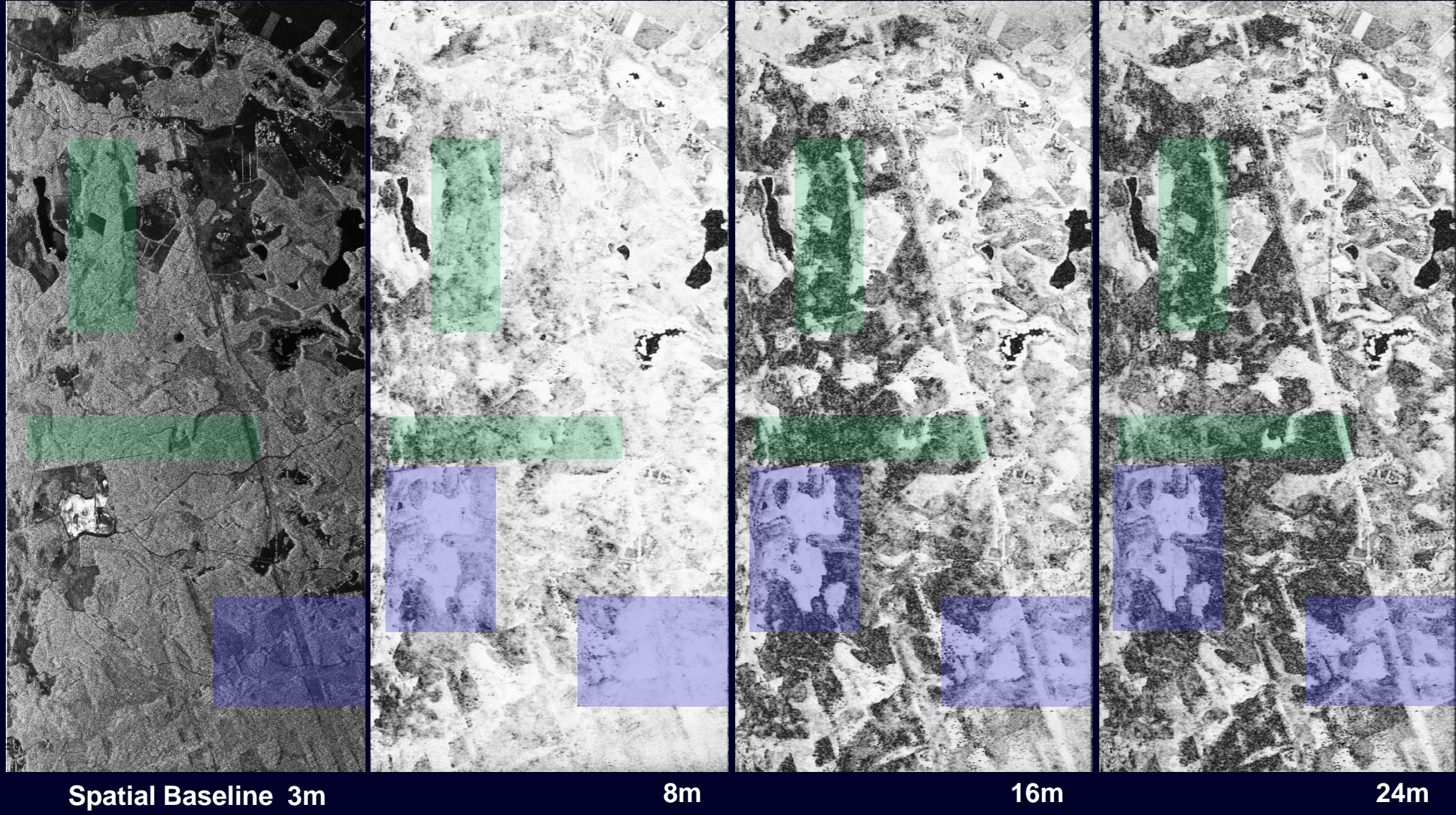
# Amplitude Image



Amplitude Image HH



# Interferometric Coherence: Volume Decorrelation



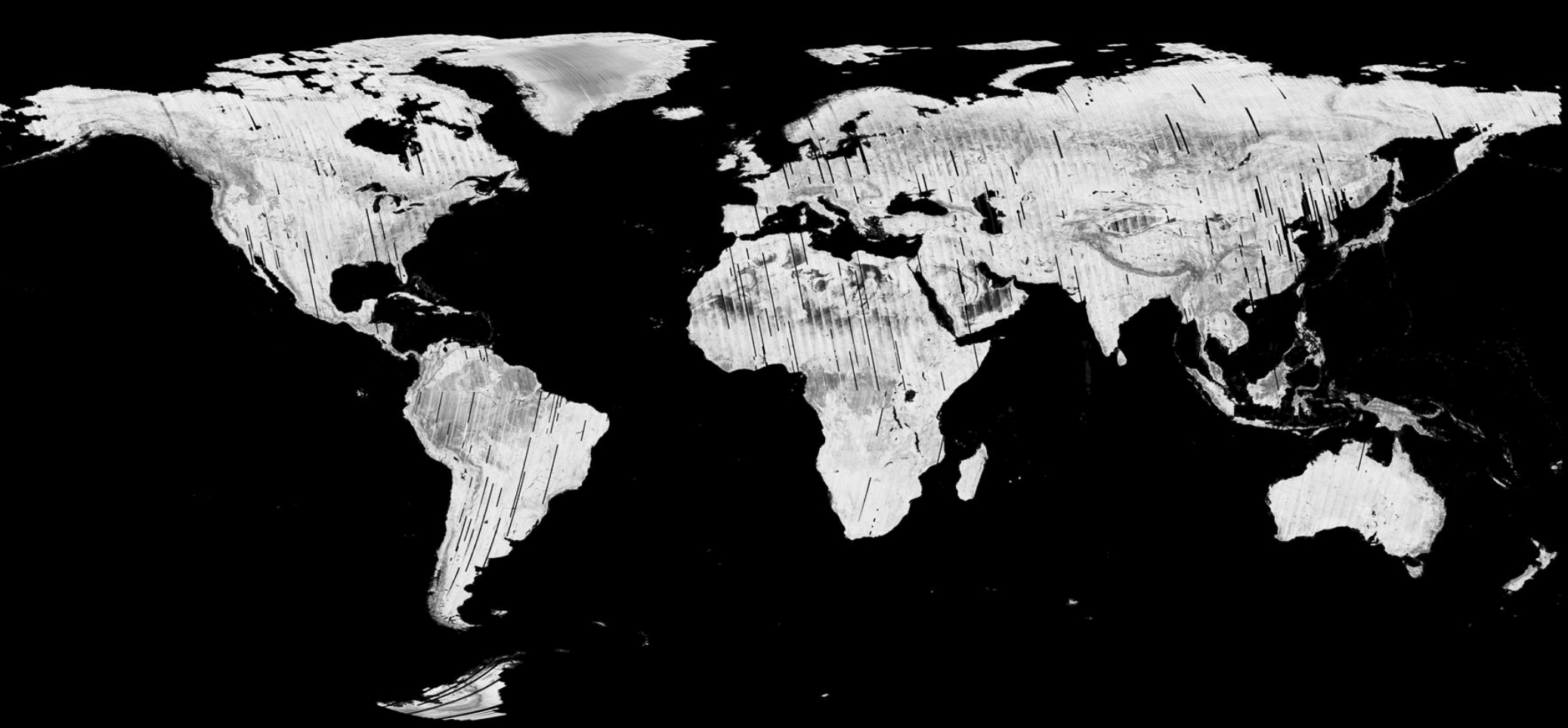
Deutsches Zentrum  
für Luft- und Raumfahrt e.V.  
in der Helmholtz-Gemeinschaft

InSAR Coherence

$$\tilde{\gamma} = \tilde{\gamma}_{\text{Temporal}} \gamma_{\text{SNR}} \tilde{\gamma}_{\text{Vol}}$$

For surfaces:

$$\tilde{\gamma}_{\text{Vol}} = 1 \rightarrow \tilde{\gamma} = \gamma_{\text{SNR}}$$



0

1



By DLR-HR-STL

500x500 m<sup>2</sup> resolution



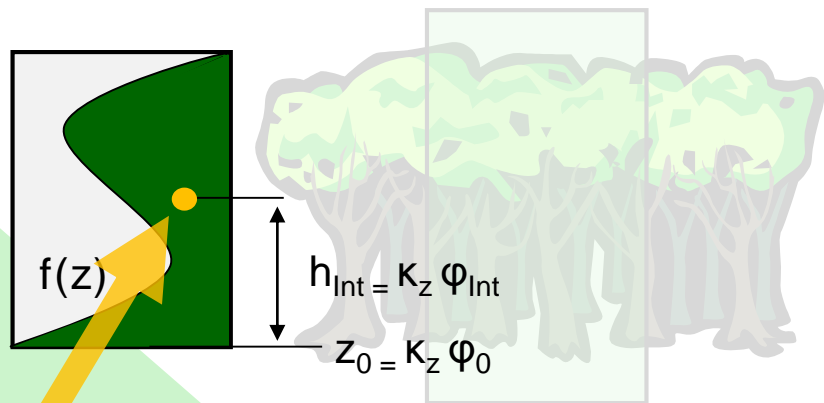
### Interferometric Coherence

$$\tilde{\gamma}(S_1, S_2) = \frac{\langle S_1 S_2^* \rangle}{\sqrt{\langle S_1 S_1^* \rangle \langle S_2 S_2^* \rangle}}$$

## SAR Interferometry for Volume Structure: The Phase Center

Volume Coherence

$$\tilde{\gamma}_{Vol}(f(z), k_z) = e^{ik_z z_0} \frac{\int_0^{h_v} f(z) e^{ik_z z} dz}{\int_0^{h_v} f(z) dz}$$

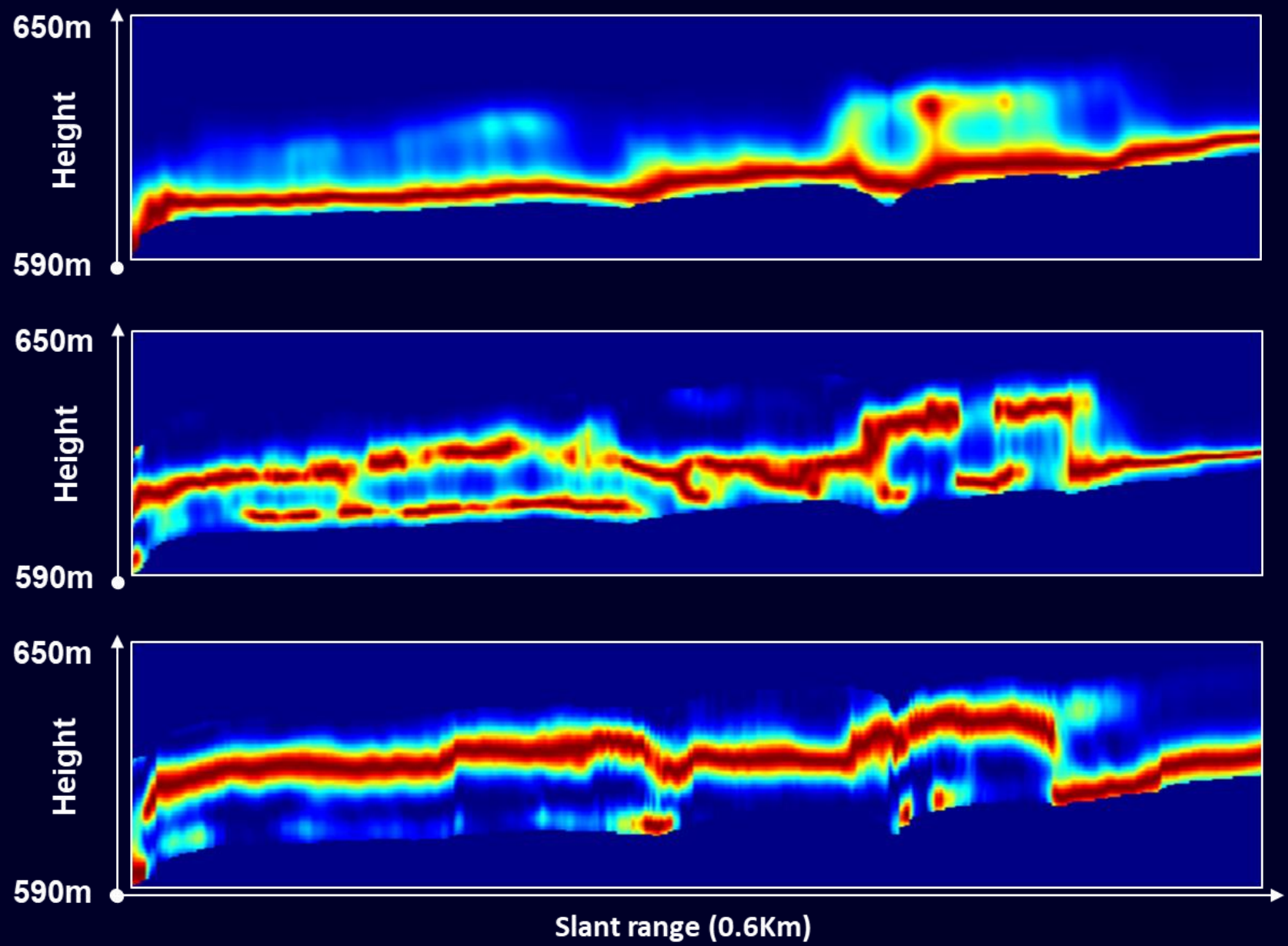


$f(z)$  ... vertical reflectivity function

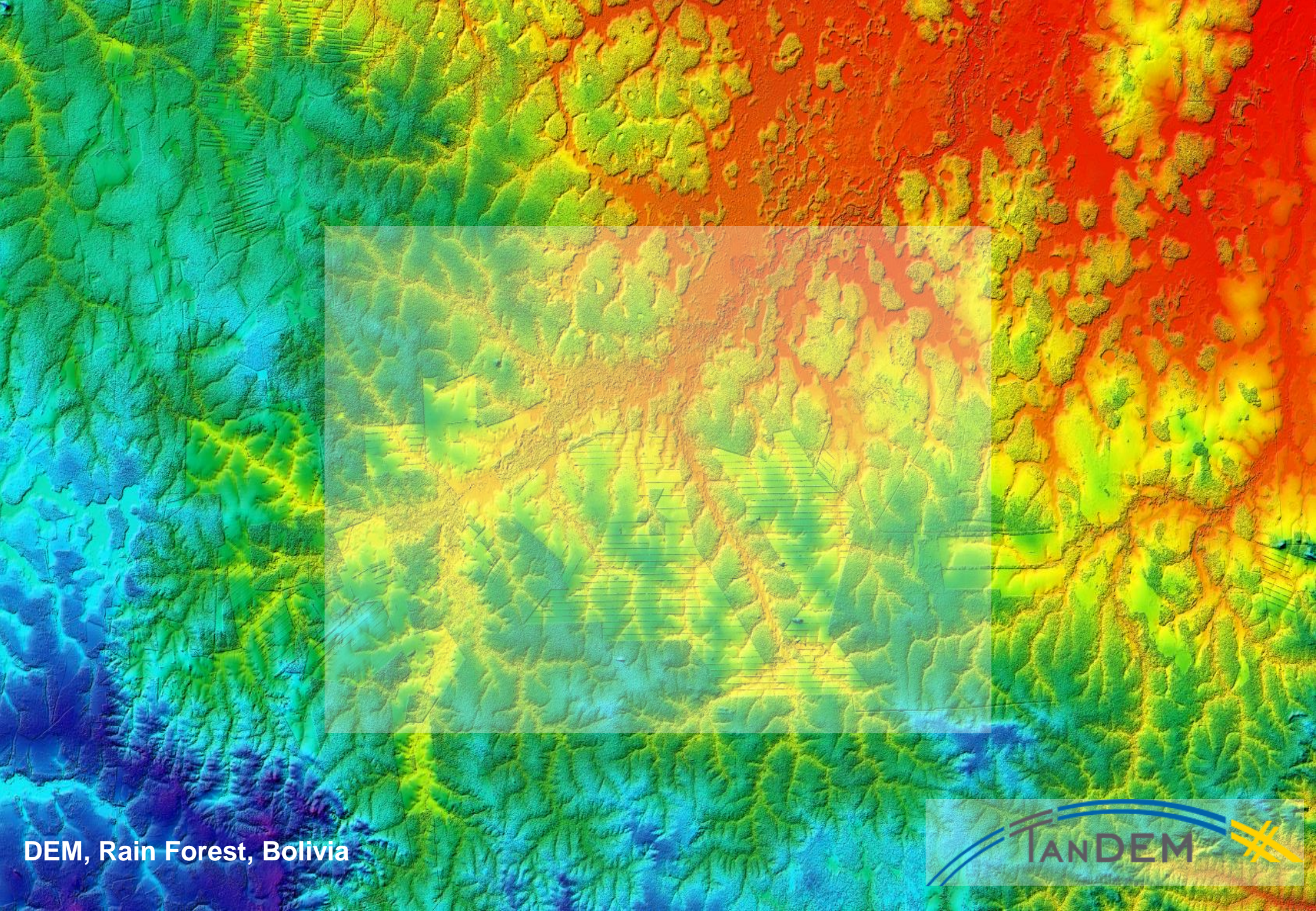
$$\tilde{\gamma} = \tilde{\gamma}_{Temporal} \gamma_{SNR} \tilde{\gamma}_{Vol}$$

- $\tilde{\gamma}_{Temporal}$  ... temporal decorrelation
- $\gamma_{SNR}$  ... additive noise decorrelation
- $\tilde{\gamma}_{Volume}$  ... geometric decorrelation

The **phase (center)** of  $\tilde{\gamma}_{Vol}$  is associated to the **center of mass** of  $f(z)$ : The phase center height  $h_{Int} = K_z \phi_{Int}$  corresponds to the height of the center of mass of  $f(z)$  with respect to  $z_0$  !!!

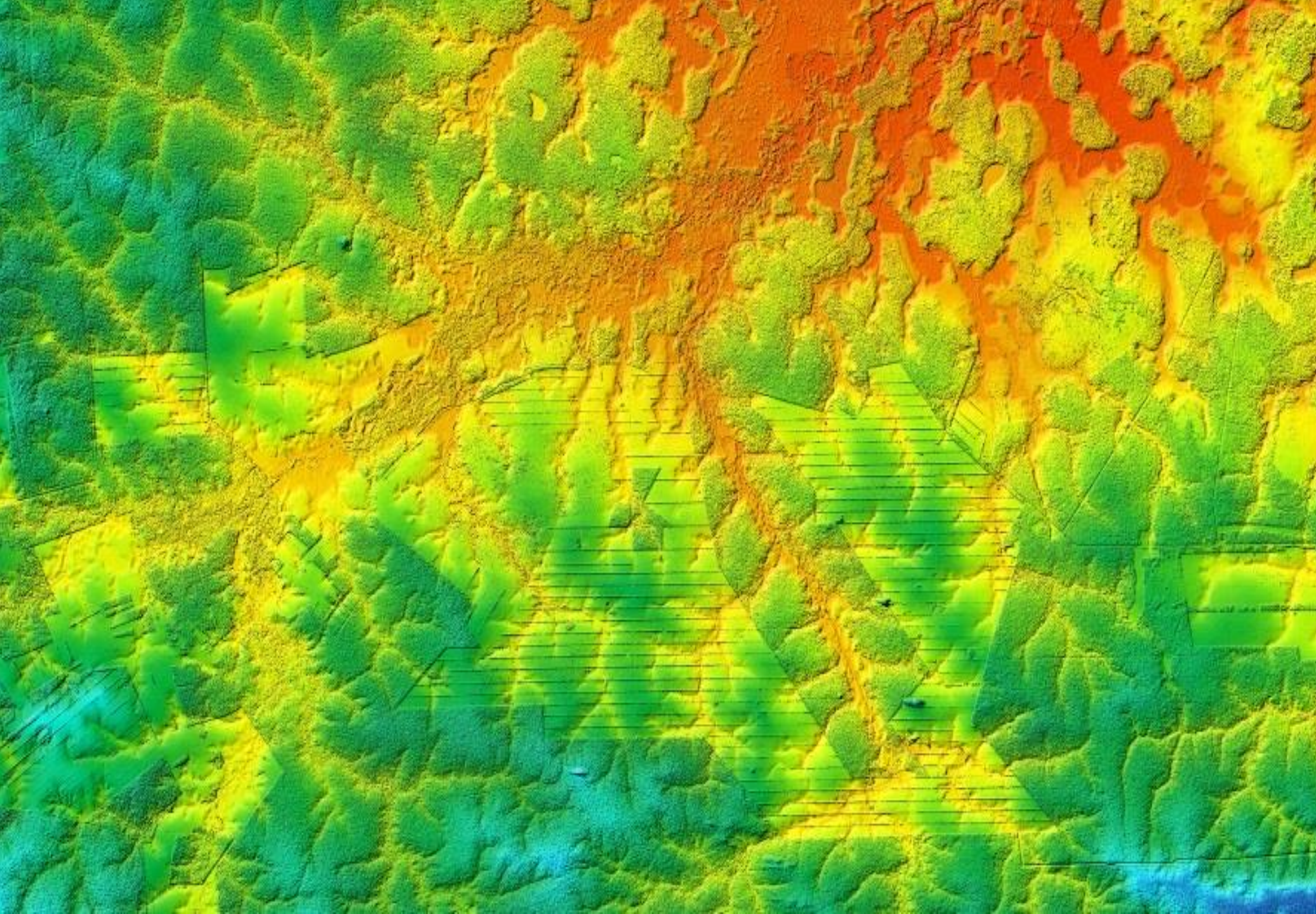


Traunstein forest (Germany) - Capon - HH



DEM, Rain Forest, Bolivia





# Polarimetric SAR Interferometry

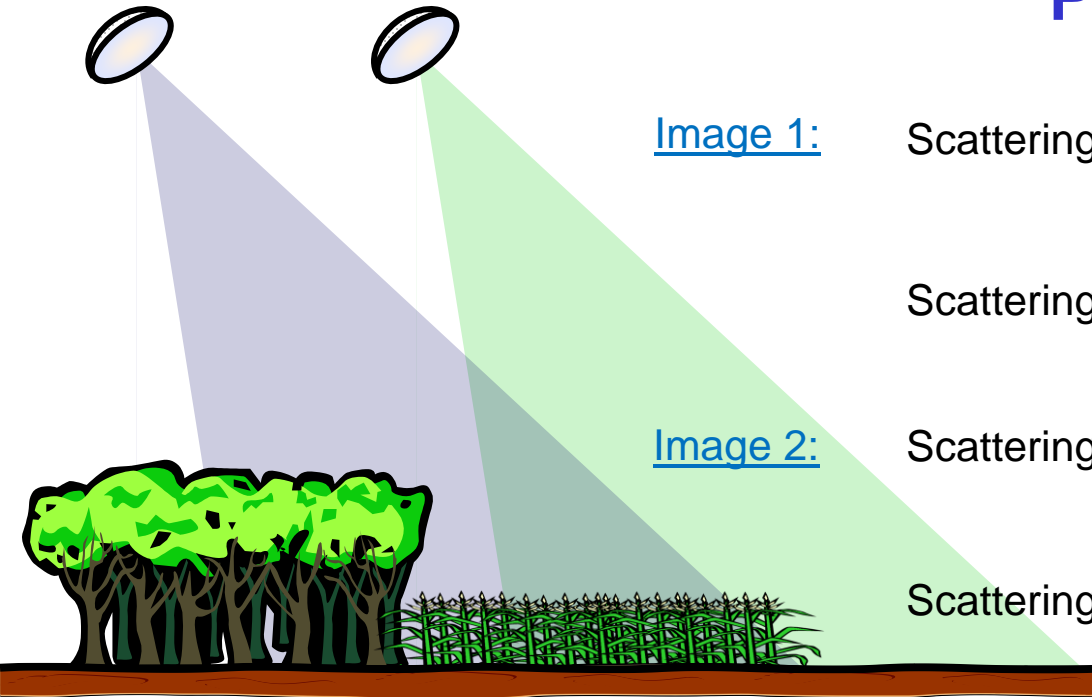


Image 1:

Scattering Matrix:

$$[S_1] = \begin{bmatrix} S_{\text{HH}}^1 & S_{\text{HV}}^1 \\ S_{\text{VH}}^1 & S_{\text{VV}}^1 \end{bmatrix}$$

Scattering Vector:

$$\vec{k}_1 = \frac{1}{\sqrt{2}} [S_{\text{HH}}^1 + S_{\text{VV}}^1 \quad S_{\text{HH}}^1 - S_{\text{VV}}^1 \quad 2S_{\text{HV}}^1]^T$$

Image 2:

Scattering Matrix:

$$[S_2] = \begin{bmatrix} S_{\text{HH}}^2 & S_{\text{HV}}^2 \\ S_{\text{VH}}^2 & S_{\text{VV}}^2 \end{bmatrix}$$

Scattering Vector:

$$\vec{k}_2 = \frac{1}{\sqrt{2}} [S_{\text{HH}}^2 + S_{\text{VV}}^2 \quad S_{\text{HH}}^2 - S_{\text{VV}}^2 \quad 2S_{\text{HV}}^2]^T$$

Image formation:

$$i_1 = \vec{w}_1^+ \cdot \vec{k}_1 \quad \text{and} \quad i_2 = \vec{w}_2^+ \cdot \vec{k}_2 \quad \dots \text{projection of the scattering vector on a (complex) unitary vector } \vec{w}_i$$

$\vec{w}_i$  used to select a given polarisation out of all possible polarisations provided by  $[S]$

Example:  $S_{\text{HH}} + S_{\text{VV}}$  image:  $\vec{w} = [1 \ 0 \ 0]^T \rightarrow i = \vec{w}^+ \cdot \vec{k}_j = \frac{1}{\sqrt{2}} (S_{\text{HH}}^j + S_{\text{VV}}^j)$

$S_{\text{HH}}$  image:  $\vec{w} = [1/\sqrt{2} \ 1/\sqrt{2} \ 0]^T \rightarrow i_j = \vec{w}^+ \cdot \vec{k}_j = S_{\text{HH}}^j$



# Polarimetric SAR Interferometry

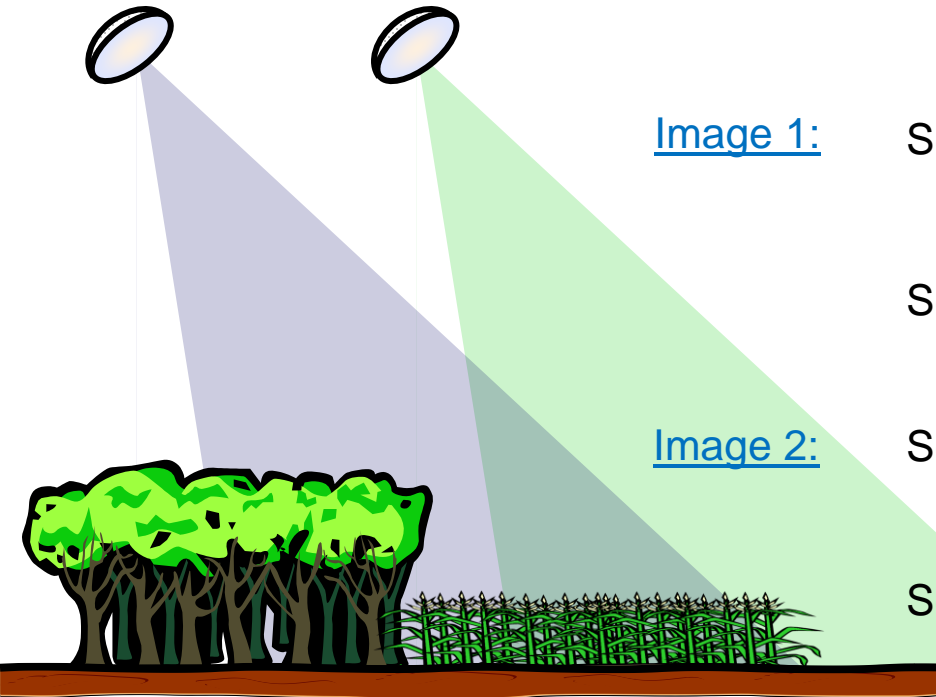


Image 1:

Scattering Matrix:

$$[S_1] = \begin{bmatrix} S_{HH}^1 & S_{HV}^1 \\ S_{VH}^1 & S_{VV}^1 \end{bmatrix}$$

Scattering Vector:

$$\vec{k}_1 = \frac{1}{\sqrt{2}} [S_{HH}^1 + S_{VV}^1 \quad S_{HH}^1 - S_{VV}^1 \quad 2S_{HV}^1]^T$$

Image 2:

Scattering Matrix:

$$[S_2] = \begin{bmatrix} S_{HH}^2 & S_{HV}^2 \\ S_{VH}^2 & S_{VV}^2 \end{bmatrix}$$

Scattering Vector:

$$\vec{k}_2 = \frac{1}{\sqrt{2}} [S_{HH}^2 + S_{VV}^2 \quad S_{HH}^2 - S_{VV}^2 \quad 2S_{HV}^2]^T$$

Image formation:  $i_1 = \vec{w}_1^+ \cdot \vec{k}_1$  and  $i_2 = \vec{w}_2^+ \cdot \vec{k}_2$  where  $\vec{w}_i$  are complex unitary vectors\*

Interferogram formation:

$$i_1 i_2^* = (\vec{w}_1^+ \cdot \vec{k}_1)(\vec{w}_2^+ \cdot \vec{k}_2)^* = \vec{w}_1^+ (\vec{k}_1 \cdot \vec{k}_2^+) \vec{w}_2 = \vec{w}_1^+ [\Omega] \vec{w}_2$$

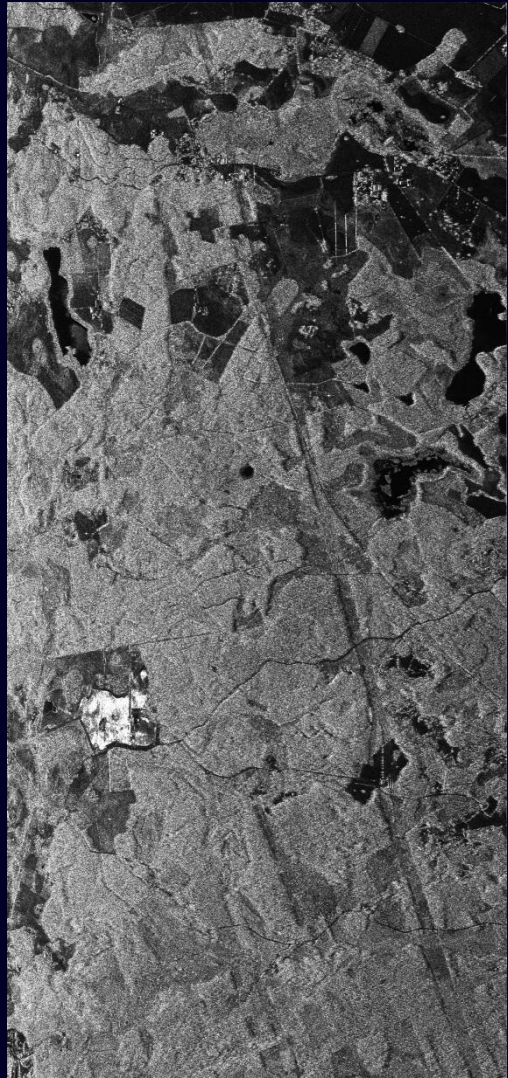
Interferometric Coherence:

$$\tilde{\gamma}(\vec{w}_1, \vec{w}_2) = \frac{\langle i_1 i_2^* \rangle}{\sqrt{\langle i_1 i_1^* \rangle \langle i_2 i_2^* \rangle}} = \frac{\langle \vec{w}_1^+ [\Omega] \vec{w}_2 \rangle}{\sqrt{\langle (\vec{w}_1^+ [T_{11}] \vec{w}_1) \rangle \langle (\vec{w}_2^+ [T_{22}] \vec{w}_2) \rangle}}$$

where  $[T_{11}] = \langle \vec{k}_1 \cdot \vec{k}_1^+ \rangle$   $[T_{22}] = \langle \vec{k}_2 \cdot \vec{k}_2^+ \rangle$  and  $[\Omega] = \langle \vec{k}_1 \cdot \vec{k}_2^+ \rangle$

$\vec{w}_i$  used to select a polarisation state out of all possible polarisations provided by the scattering matrix  $[S]$

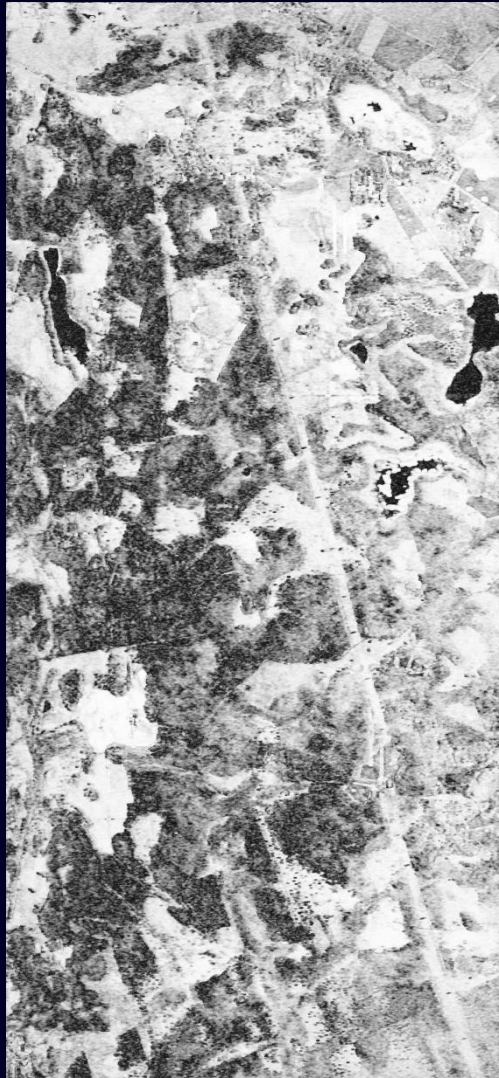
# Interferometric Coherence: Volume Decorrelation



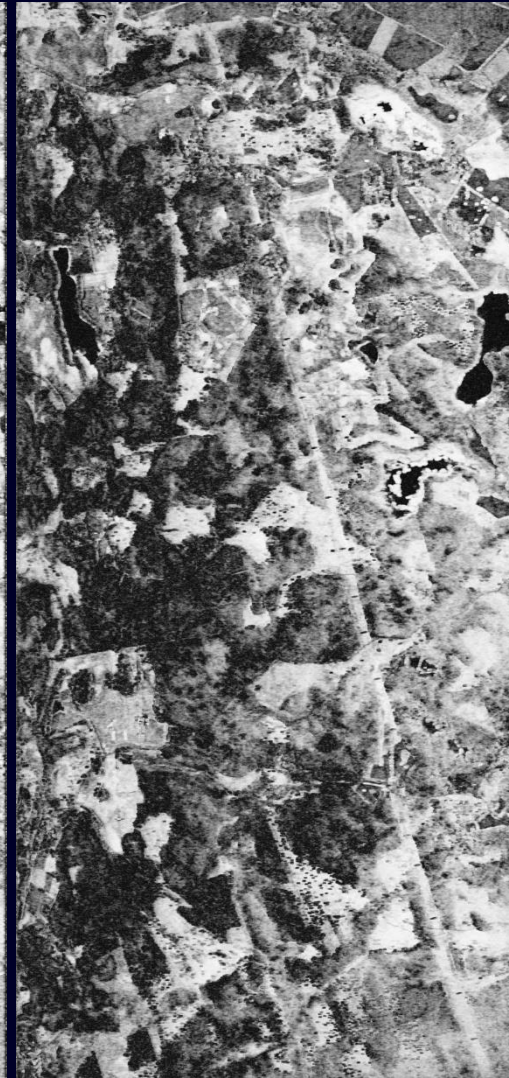
Amplitude Image HH



Sp. Baseline 16m



Opt 1



HH

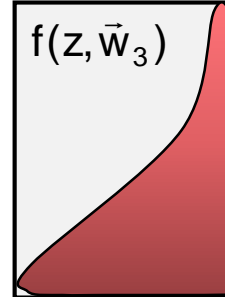
Opt 3





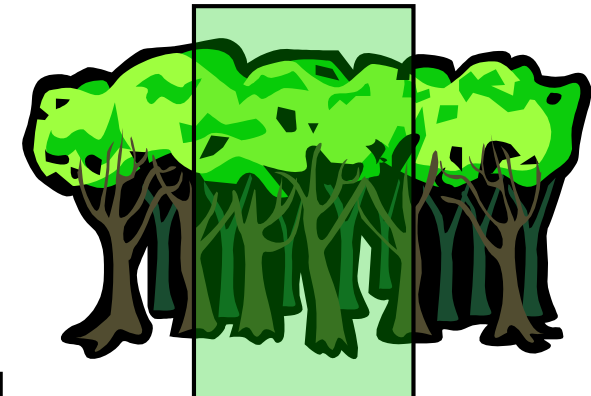
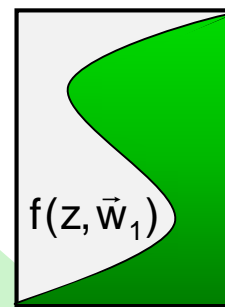
Polarisation 3 (w<sub>3</sub>):

$$\tilde{\gamma}_{\text{Vol}}(f(z, \vec{w}_3)) = e^{ik_z z_0} \frac{\int_0^{h_v} f(z, \vec{w}_3) e^{ik_z z} dz}{\int_0^{h_v} f(z, \vec{w}_3) dz}$$



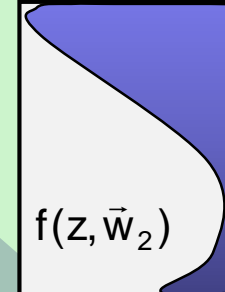
Polarisation 1 (w<sub>1</sub>):

$$\tilde{\gamma}_{\text{Vol}}(f(z, \vec{w}_1)) = e^{ik_z z_0} \frac{\int_0^{h_v} f(z, \vec{w}_1) e^{ik_z z} dz}{\int_0^{h_v} f(z, \vec{w}_1) dz}$$



Polarisation 2 (w<sub>2</sub>):

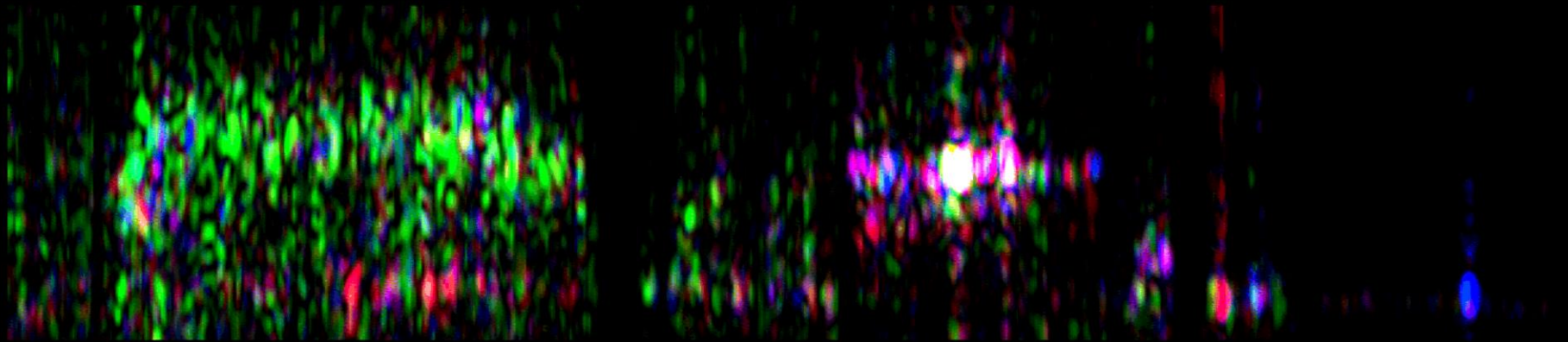
$$\tilde{\gamma}_{\text{Vol}}(f(z, \vec{w}_2)) = e^{ik_z z_0} \frac{\int_0^{h_v} f(z, \vec{w}_2) e^{ik_z z} dz}{\int_0^{h_v} f(z, \vec{w}_2) dz}$$



$f(z, \vec{w})$  ...vertical reflectivity function

## Polarimetric SAR Interferometry





spruce forest

road

building

cars

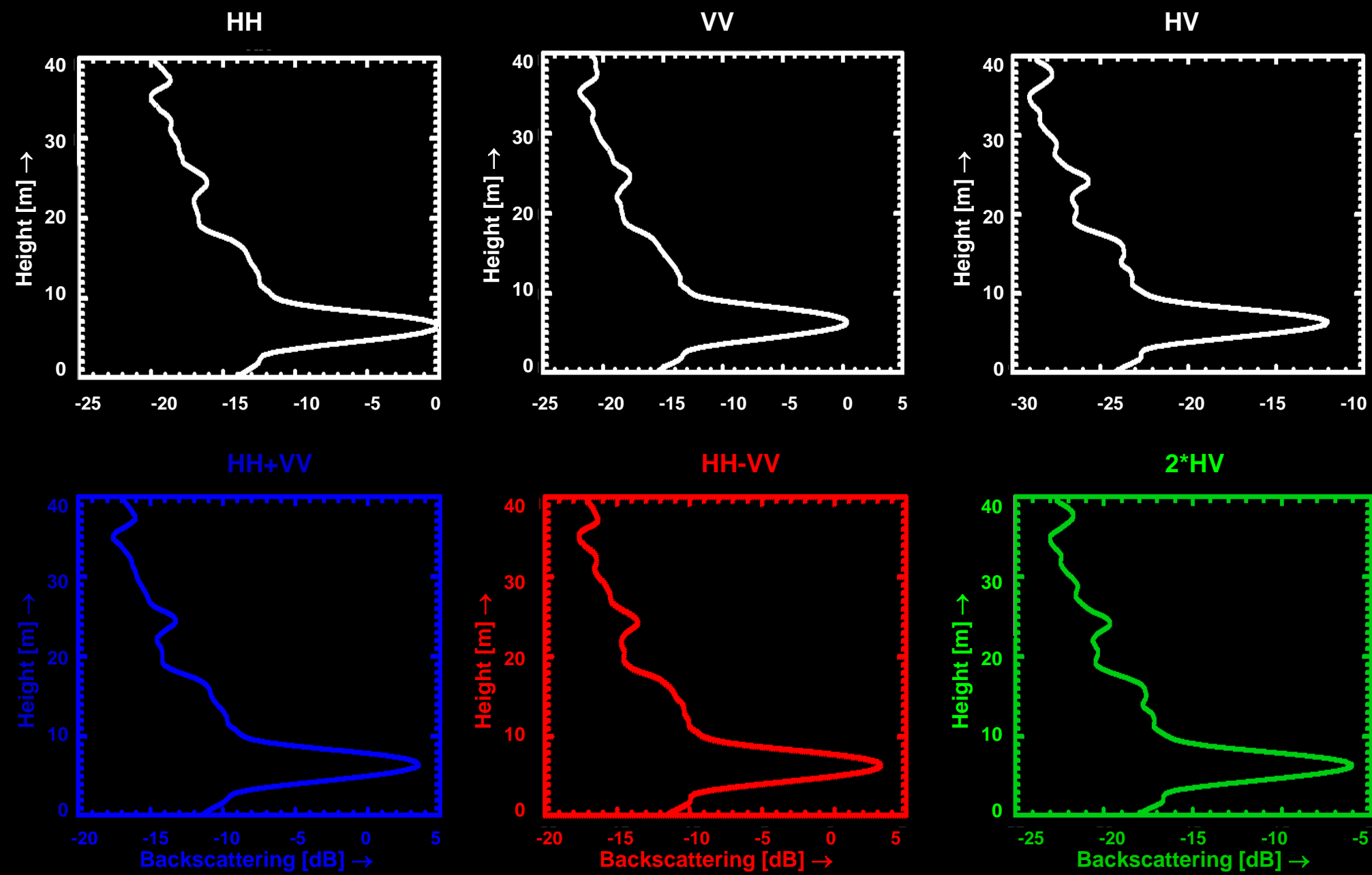
corner reflector



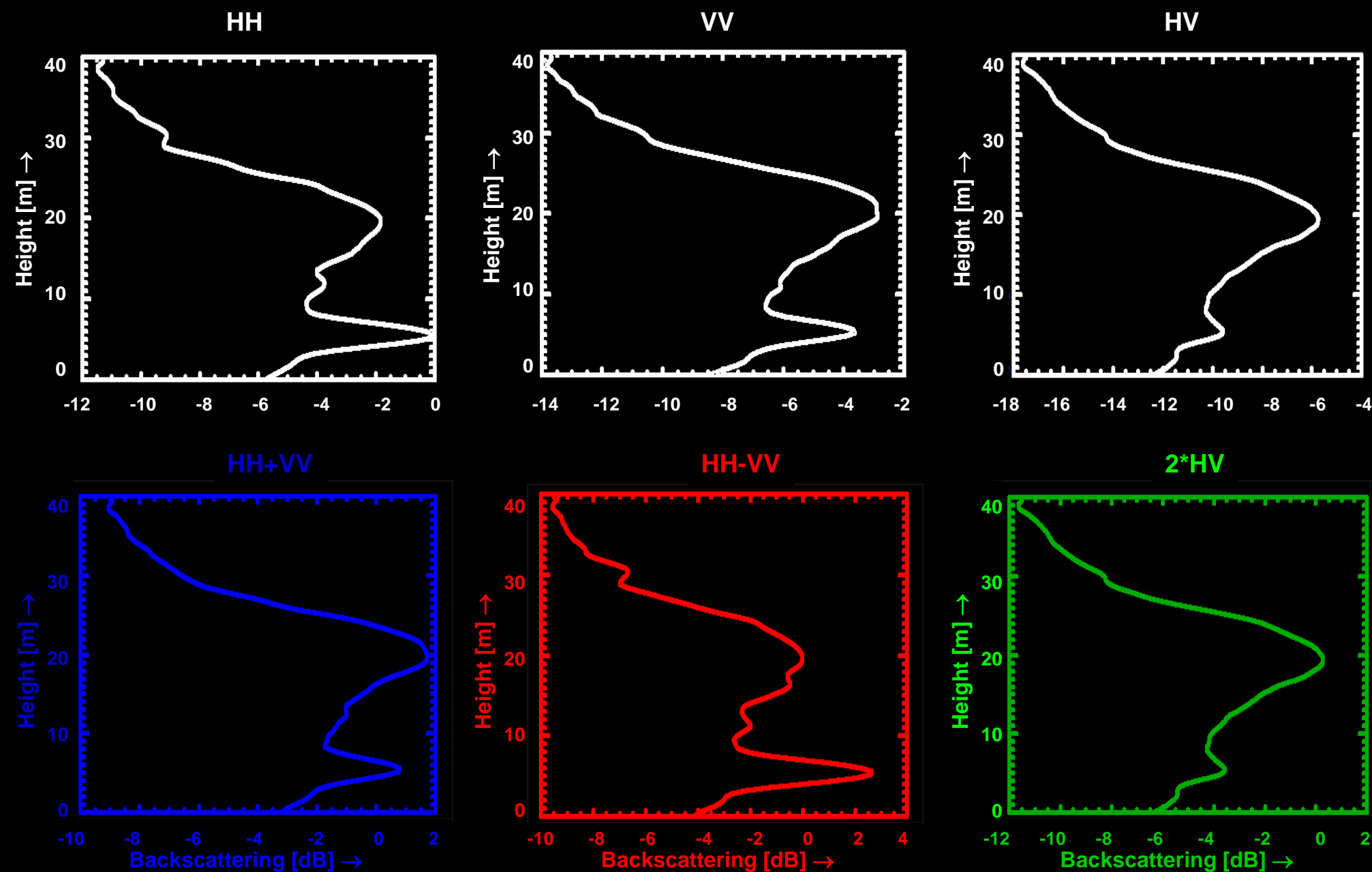
## Airborne Polarimetric SAR Tomography

Upper image: Polarimetric color composite (L-band) of a tomographic slice in the height/azimuth-direction  
■ HH+VV, ■ HH-VV, ■ 2\*HV

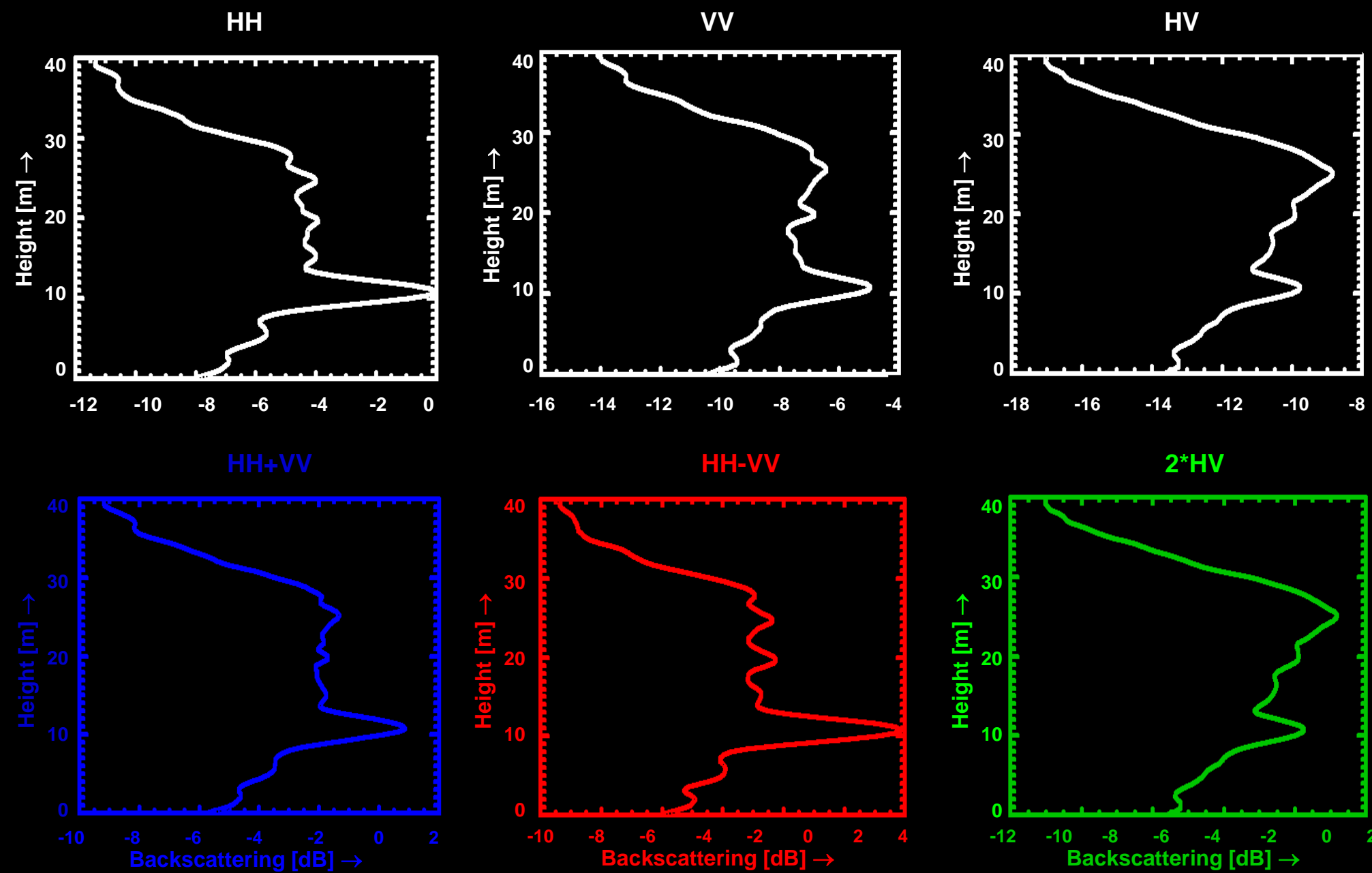
Lower image: Schematic view of the imaged area



Bare Surface Backscattering Profiles (12-20 m height)



Spruce Forest Backscattering Profiles (15-20 m height)



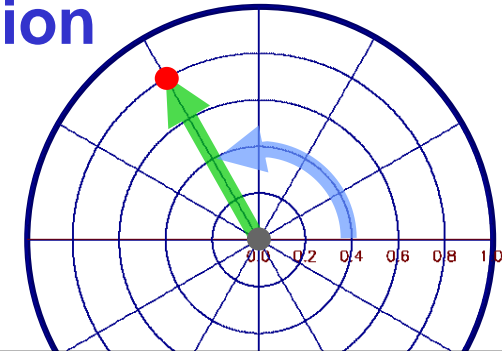
Mixed Forest Backscattering Profiles (12-20 m height)

# Geometrical Representation: The Coherence Region

Interferometric Coherence:  $\tilde{\gamma}(\vec{w}_i, \vec{w}_i) = |\tilde{\gamma}(\vec{w}_i, \vec{w}_i)| \cdot \exp(i \operatorname{Arg}\{\tilde{\gamma}(\vec{w}_i, \vec{w}_i)\})$

Radius                          Angle

► can be represented by a single point on the unit circle (UC)

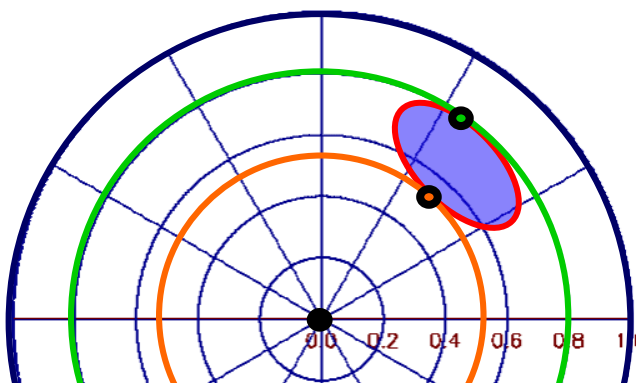
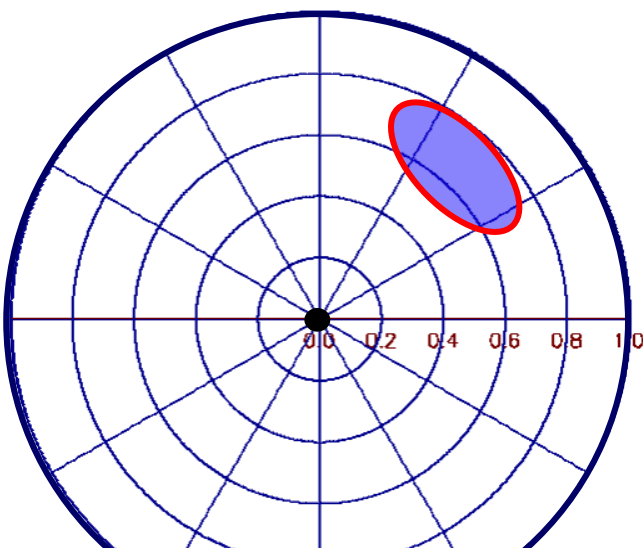


**Coherence Region:**

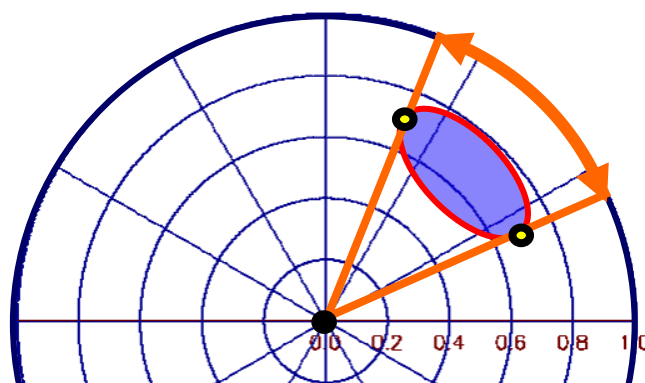
$$\tilde{\gamma}(\vec{w}_i, \vec{w}_i) \quad \forall \quad \vec{w}_i = \begin{bmatrix} \cos \alpha \exp(i\varphi_1) \\ \sin \alpha \cos \beta \exp(i\varphi_2) \\ \sin \alpha \sin \beta \exp(i\varphi_3) \end{bmatrix} \text{ with } 0 \leq \alpha \leq \frac{\pi}{2} \text{ and } -\pi \leq \beta \leq \pi$$

The set of interferometric coherences obtained for all the possible polarizations  $\vec{w}_i$  plotted on the unit circle (UC) defines the so-called **coherence region**.

Its shape & size depend on the structure of the underlying scatterer and on acquisition parameters.

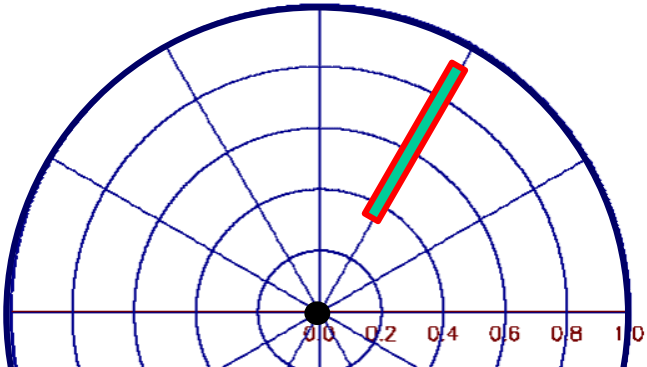


Max./ Min. Interferometric Coherence  
as function of  $\vec{w}_i$



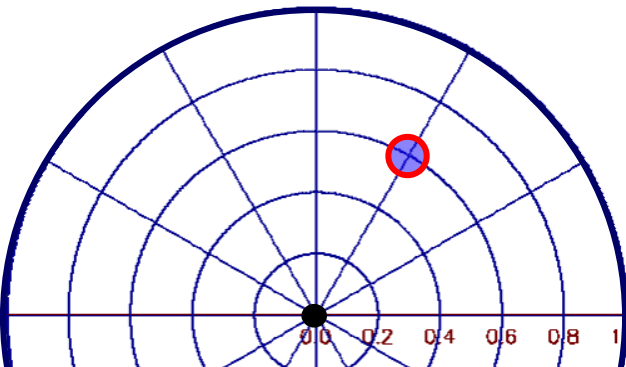
Max. Phase Difference between  
interferograms formed with  $\vec{w}_i$  and  $\vec{w}_j$

# Coherence Region Interpretation



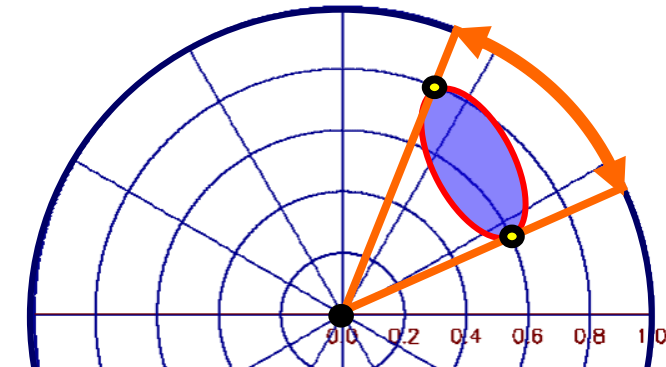
## Radial Shaped CR

i.e. InSAR coherence amplitude changes with polarisation but not the location of the phase center.



## Point Like Coherence Region

i.e. InSAR Coherence and Phase are independent of polarisation.

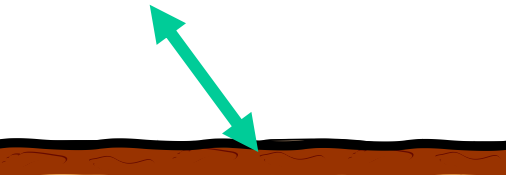


## Elliptical Shaped CR

i.e. InSAR coherence magnitude and phase center location changes with polarisation.

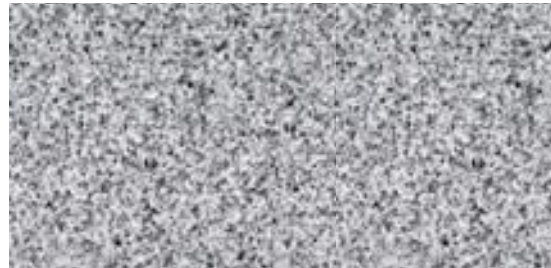
## Surface Scattering

$$\bar{\gamma}(\vec{w}) = \gamma_{\text{SNR}}(\vec{w}) \quad \bar{\gamma}_{\text{Vol}} := 1 \quad \bar{\gamma}_{\text{Vol}} = \gamma_{\text{SNR}}(\vec{w})$$

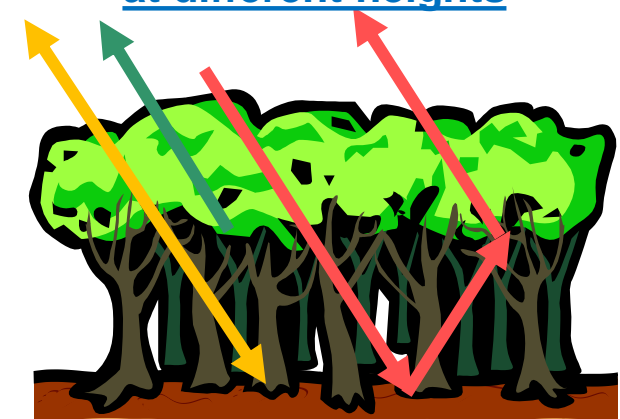


Pol-InSAR does not provide any additional information compared to InSAR !!!

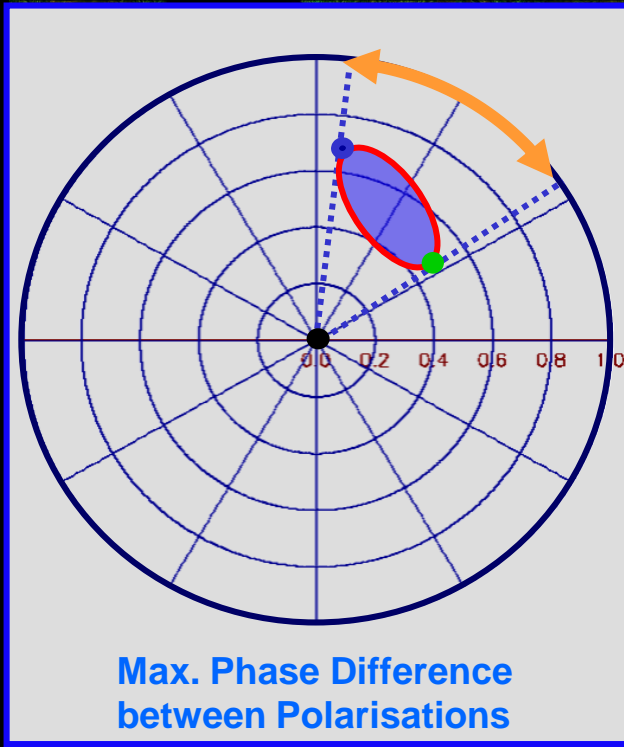
## (Random) Volume scattering



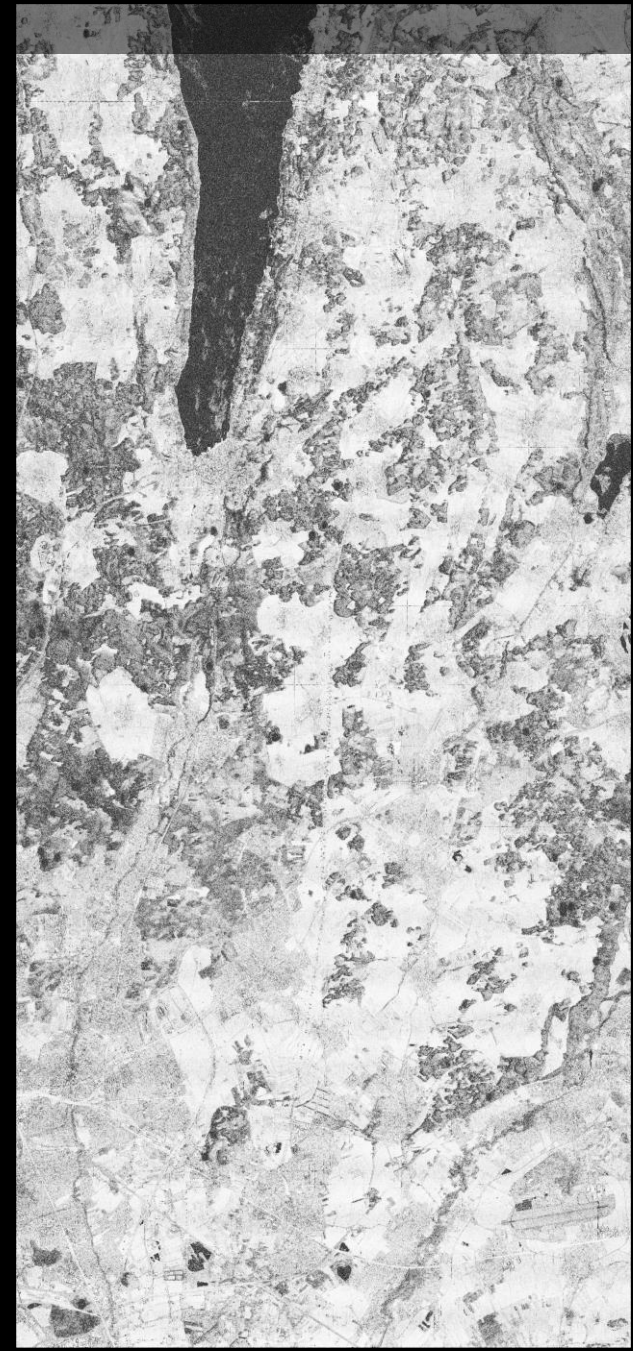
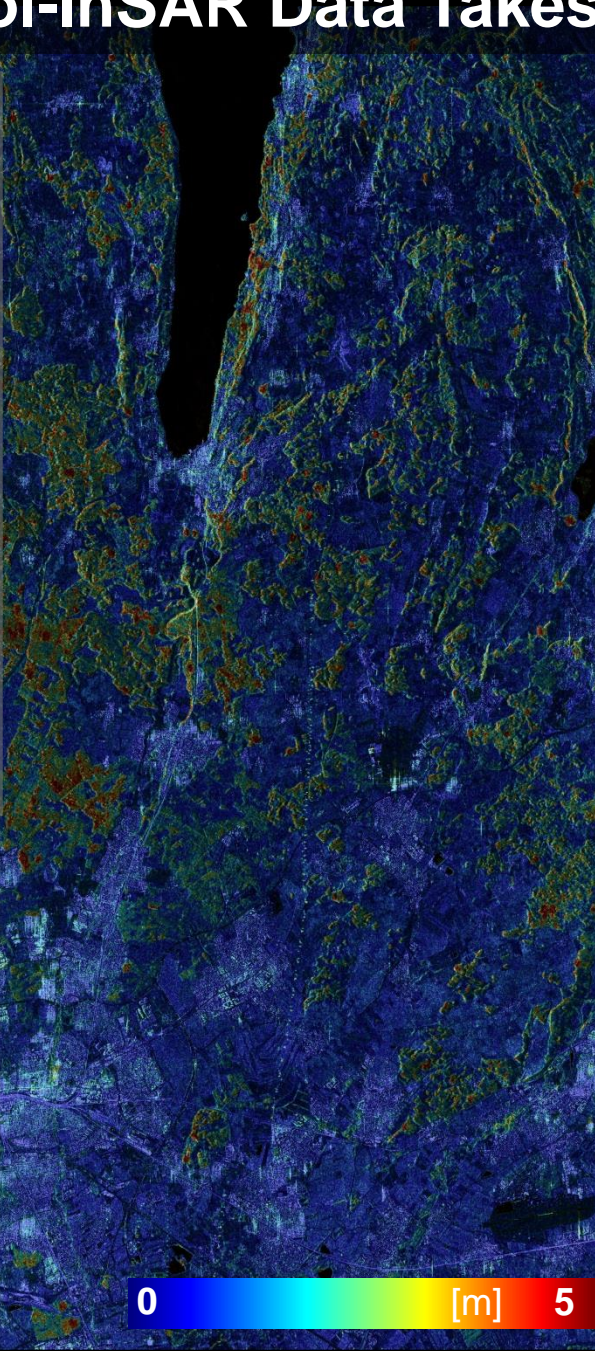
## (Depolarising) Scatterers at different heights



# First Bistatic Dual Pol-InSAR Data Takes



Dual-Pol HH-VV Stripmap  
Test Site Location: OP  
InSAR Mode: Bistatic  
Vertical Wavenumber: 0.1m



# Structure Parameters & Applications

## Forest

- Forest Height
- Forest (Vertical) Structure
- Forest Biomass
- Underlying Topography



- Forest Ecology
- Forest Management
- Ecosystem Modeling
- Climate Change

## Agriculture

- Underlying Soil Moisture
- Moisture of Vegetation Layer
- Height of Vegetation Layer
- Soil Roughness



- Farming Management
- Ecosystem Modeling
- Water Cycle / CC
- Desertification

## Snow & Ice

- Ice Layer Structure
- Penetration Depth (Ice)
- Snow Layer Thickness
- Snow Water Equivalent



- Ecosystem Change
- Water Cycle
- Water Management

# Pol-InSAR In Orbit

**ALOS-2 (4)**



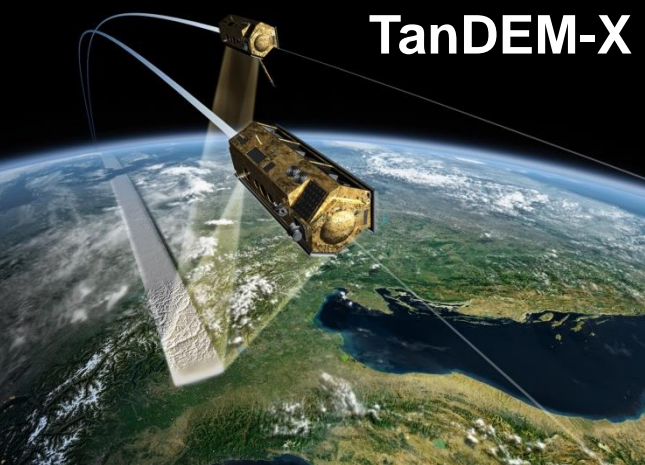
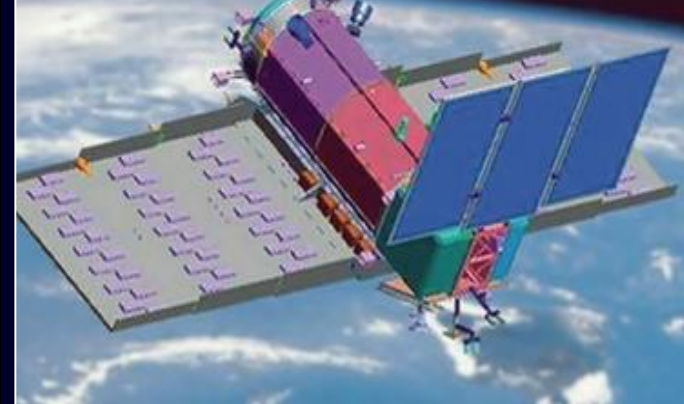
**RadarSAT 2**



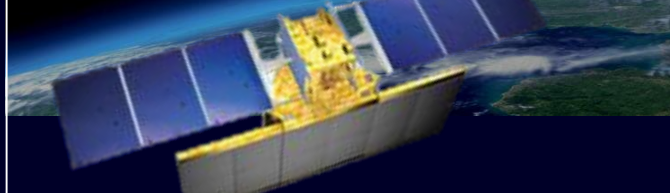
**Sentinel 1a+1b (1c + 1d)**



**SAOCOM 1A+1B**

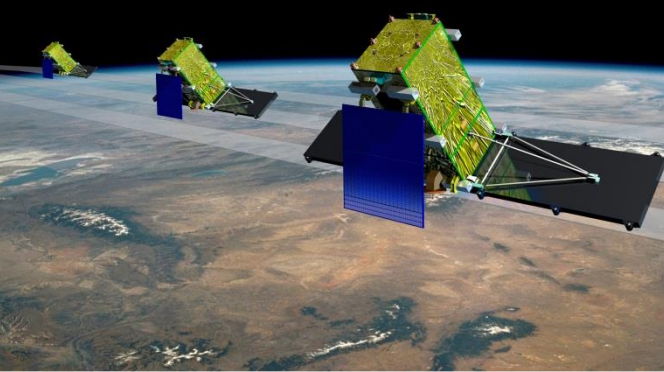


**RISAT-1**

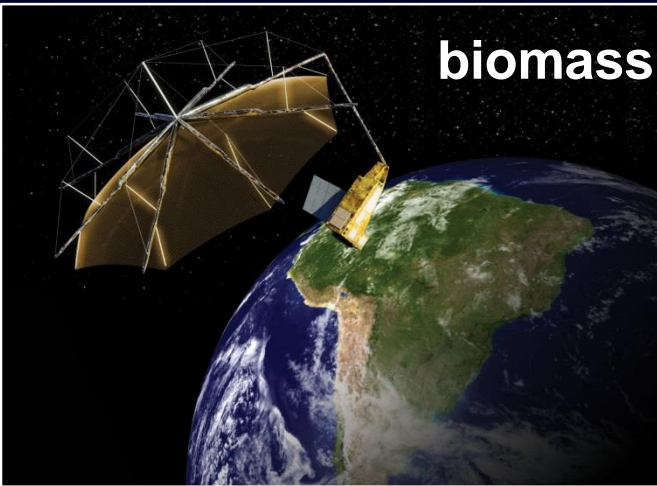


# Pol-InSAR In Orbit

RadarSAT Constellation



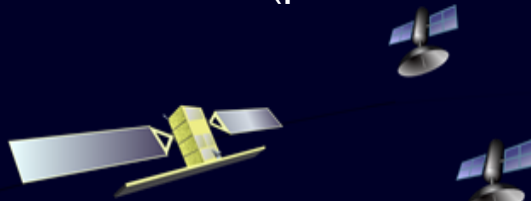
biomass



NISAR



Missions with (passive or



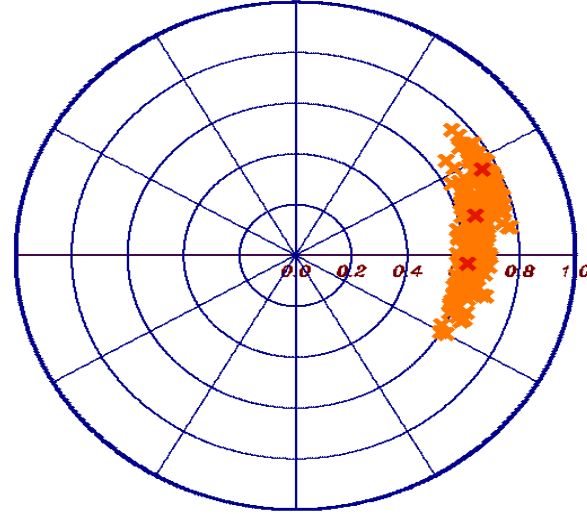
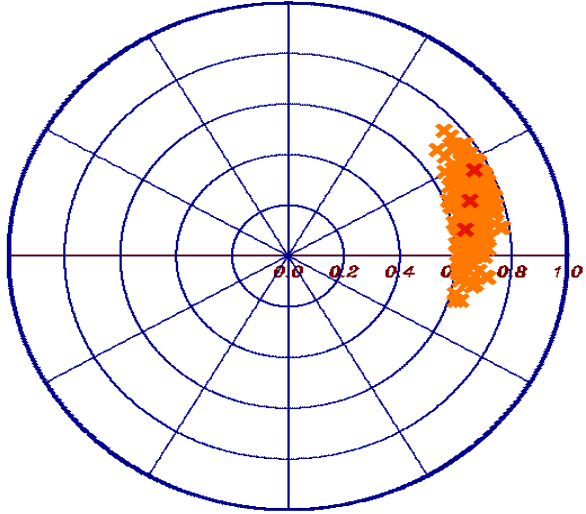
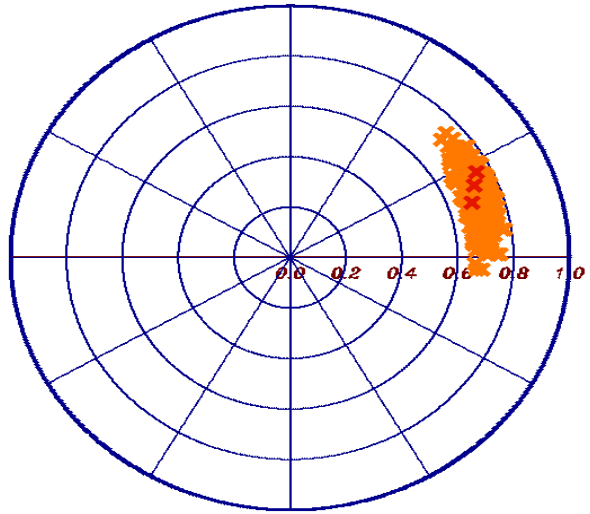
active) Pol. Companions:  
Harmony

Rose-L (+)

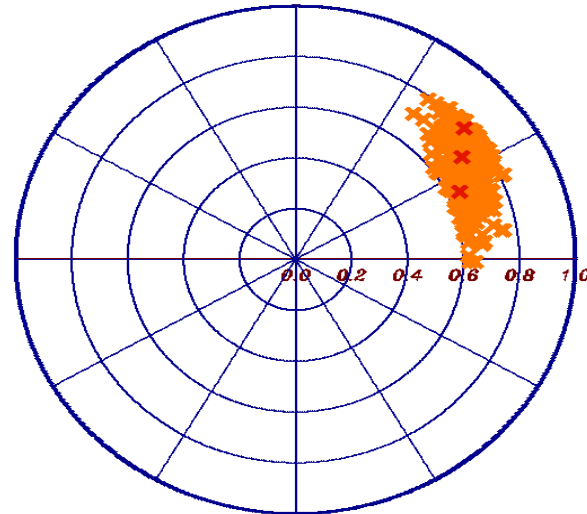
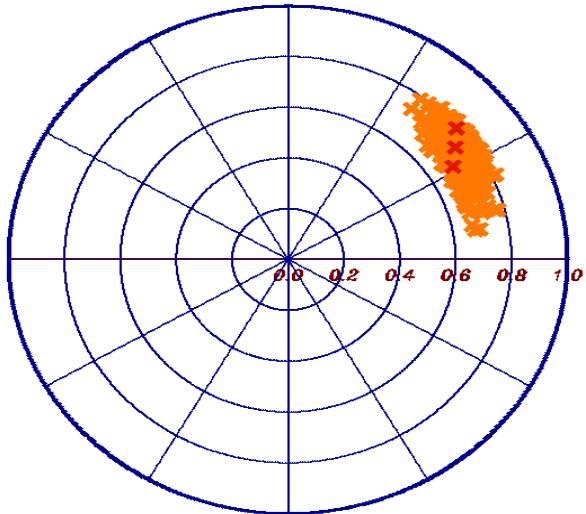
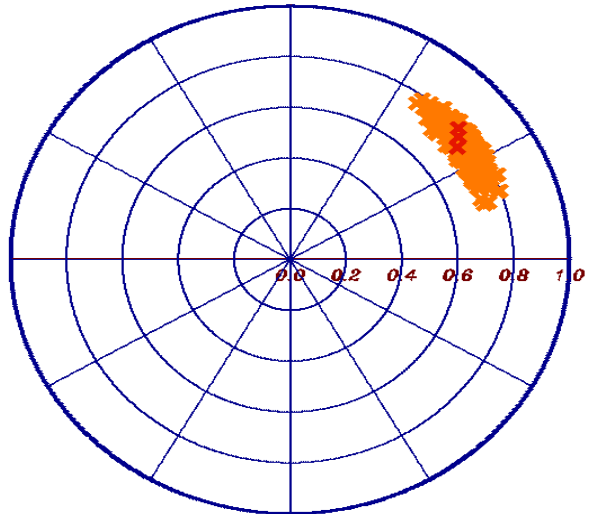


Tandem-L





## Pol-InSAR: Modelling and Inversion



# Forest Height inversion from InSAR Data



$$\tilde{\gamma}(s_1 s_2) = \frac{< s_1 s_2^* >}{\sqrt{< s_1 s_1^* > < s_2 s_2^* >}}$$

Interferometric Coherence (complex)

$$\tilde{\gamma}(s_1 s_2) = \gamma_{\text{sys}} \gamma_{\text{Tmp}} \tilde{\gamma}_{\text{Vol}}$$

$\tilde{\gamma}_{\text{Vol}}$  ... volume decorrelation     $\tilde{\gamma}_{\text{Tmp}}$  ... temporal decorrelation

$$\tilde{\gamma}_{\text{Vol}}(\vec{w}, \kappa_z) = e^{ik_z z_o} \frac{\int_{z_o}^{h_v} f(z, \vec{w}) e^{ik_z z} dz}{\int_{z_o}^{h_v} f(z, \vec{w}) dz}$$

$f(z, \vec{w})$  ... vertical reflectivity function     $\kappa_z$  ... vertical wavenumber

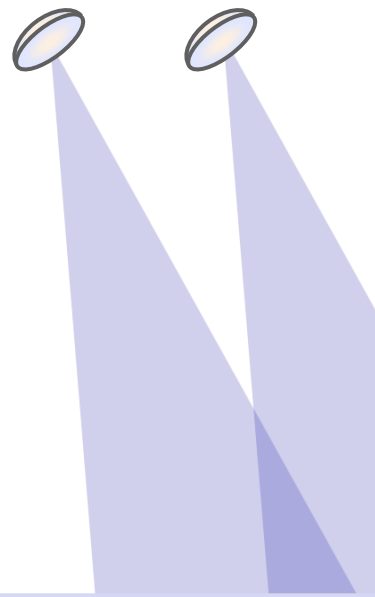
Interferometric (volume) decorrelation is sensitive to the „visible“ (forest) **height** and to the **vertical reflectivity function**  $f(z, \vec{w})$  within the interferometric resolution cell.



## Forest Height inversion challenges:

- The parameterisation / description of  $f(z, \vec{w})$
- The presence of  $\tilde{\gamma}_{\text{Tmp}}$

# 2 Layer Inversion Model: (Random) Volume over Ground (RVoG)



Volume Layer    Ground Layer

$$f(z, \vec{w}) = m_V f_V(z) + m_G(\vec{w}) \delta(z - z_0)$$

Volume Layer Coherence

$$\tilde{\gamma}_V = \frac{I}{I_0} \begin{cases} I = \int_0^{h_V} \exp(i\kappa_z z') f_V(z') dz' \\ I_0 = \int_0^{h_V} f_V(z') dz' \end{cases}$$

$m(\vec{w}) = \frac{m_G(\vec{w})}{m_V(\vec{w}) I_0}$     $\kappa_z = \frac{\kappa \Delta \theta}{\sin(\theta_0)}$

$f_V(z)$  ... volume reflectivity function

$\varphi_0 = \kappa_z z_0$  ... underlying topography

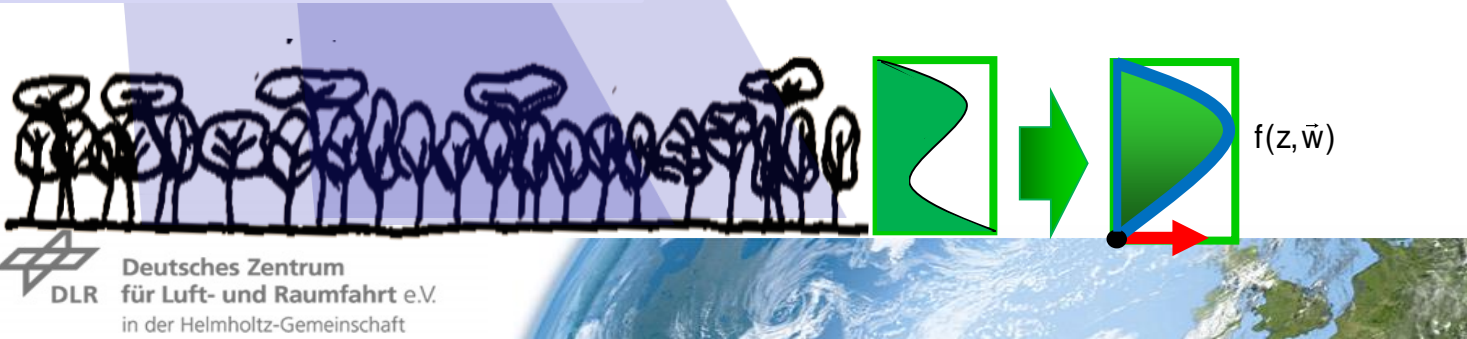
$\tilde{\gamma}_{Vol}(\vec{w}, \kappa_z) = \exp(i\varphi_0) \frac{\tilde{\gamma}_V(\kappa_z) + m(\vec{w})}{1 + m(\vec{w})}$

## Single Baseline Observations

single- / dual- / quad-pol

$$\tilde{\gamma}_{Vol}(\vec{w}_1, \kappa_z) \quad \tilde{\gamma}_{Vol}(\vec{w}_2, \kappa_z) \quad \tilde{\gamma}_{Vol}(\vec{w}_3, \kappa_z)$$

1, 2, or 3 complex coherences



Total Coherence

$$\tilde{\gamma}(\vec{w}, \kappa_z) = \gamma_{Temp}(\kappa_z) \tilde{\gamma}_{Vol}(\vec{w}, \kappa_z)$$

For a Single Baseline

3+N unknown parameters

Volume Height  $h_V$

Topography  $\varphi_0$

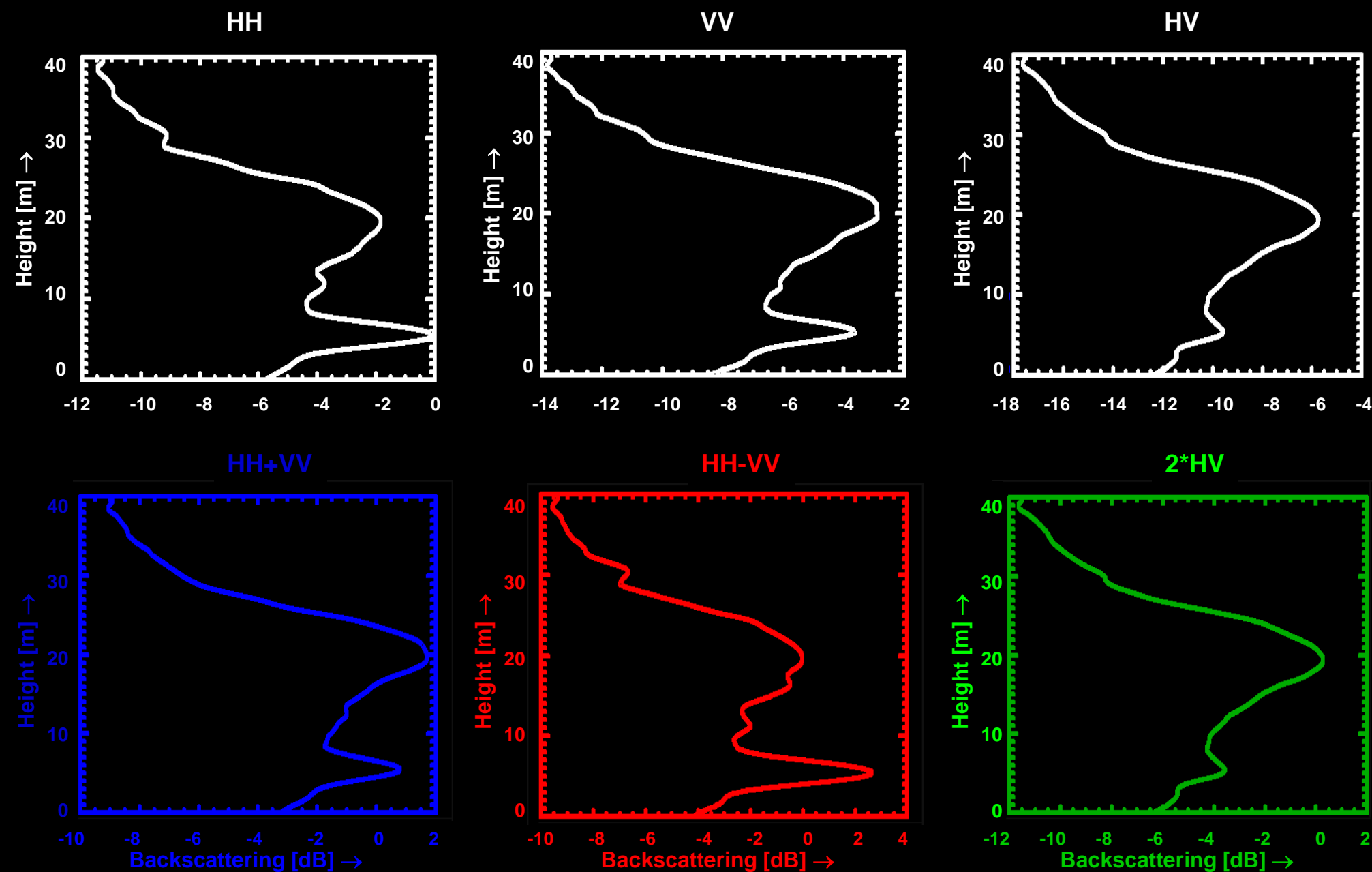
G/V Ratio  $m(\vec{w}) = f(\text{pol})$

$f_V(z)$  ... N parameters

plus one more

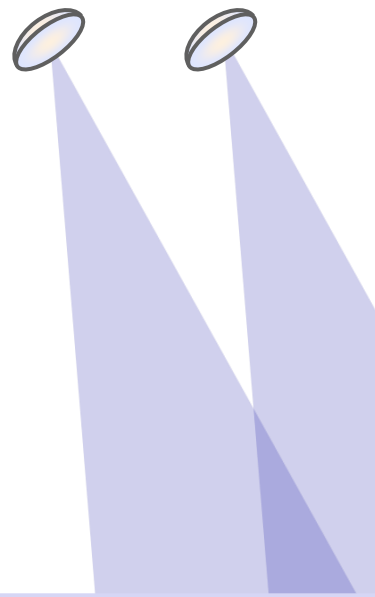
Temporal Deco  $\gamma_{Temp}$

for repeat-pass implementations



Spruce Forest Backscattering Profiles (15-20 m height)

# 2 Layer Inversion Model: (Random) Volume over Ground (RVoG)



Volume Layer    Ground Layer

$$f(z, \vec{w}) = m_V f_V(z) + m_G(\vec{w}) \delta(z - z_0)$$

Volume Layer Coherence

$$\tilde{\gamma}_V = \frac{I}{I_0} \left\{ \begin{array}{l} I = \int_0^{h_V} \exp(i\kappa_z z') f_V(z') dz' \\ I_0 = \int_0^{h_V} f_V(z') dz' \end{array} \right. \quad m(\vec{w}) = \frac{m_G(\vec{w})}{m_V(\vec{w}) I_0} \quad \kappa_z = \frac{\kappa \Delta \theta}{\sin(\theta_0)}$$

$f_V(z)$  ... volume reflectivity function  
 $\varphi_0 = \kappa_z z_0$  ... underlying topography

$\tilde{\gamma}_{Vol}(\vec{w}, \kappa_z) = \exp(i\varphi_0) \frac{\tilde{\gamma}_V(\kappa_z) + m(\vec{w})}{1 + m(\vec{w})}$

## Single Baseline Observations

single- / dual- / quad-pol

$$\tilde{\gamma}_{Vol}(\vec{w}_1, \kappa_z) \quad \tilde{\gamma}_{Vol}(\vec{w}_2, \kappa_z) \quad \tilde{\gamma}_{Vol}(\vec{w}_3, \kappa_z)$$

1, 2, or 3 complex coherences



Total Coherence

$$\tilde{\gamma}(\vec{w}, \kappa_z) = \gamma_{Temp}(\kappa_z) \tilde{\gamma}_{Vol}(\vec{w}, \kappa_z)$$

For a Single Baseline

3+N unknown parameters

Volume Height  $h_V$

Topography  $\varphi_0$

G/V Ratio  $m(\vec{w}) = f(\text{pol})$

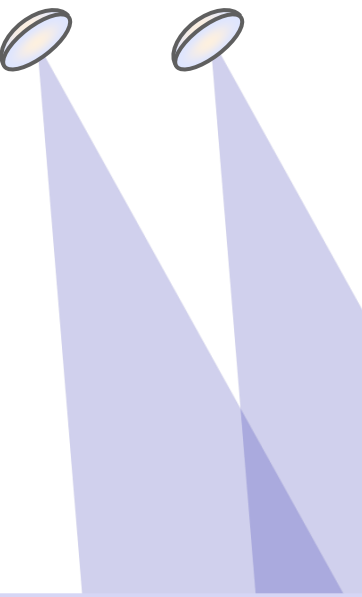
$f_V(z)$  ... N parameters

plus one more

Temporal Deco  $\gamma_{Temp}$

for repeat-pass implementations

# 2 Layer Inversion Model with exponential volume reflectivity



Volume Layer    Ground Layer

$$f(z, \vec{w}) = m_v f_v(z) + m_G(\vec{w}) \delta(z - z_0)$$

$\tilde{\gamma}_{\text{Vol}}(\vec{w}, \kappa_z) = \exp(i\varphi_0) \frac{\tilde{\gamma}_v(\kappa_z) + m(\vec{w})}{1 + m(\vec{w})}$

**Volume Layer Coherence**

$$\tilde{\gamma}_v = \frac{I}{I_0} \left\{ \begin{array}{l} I = \int_0^{h_v} \exp(i\kappa_z z') e^{\left(\frac{2 \sigma z'}{\cos \theta_0}\right)} dz' \\ I_0 = \int_0^{h_v} e^{\left(\frac{2 \sigma z'}{\cos \theta_0}\right)} dz' \end{array} \right.$$

$$m(\vec{w}) = \frac{m_G(\vec{w})}{m_v(\vec{w}) I_0} \quad \kappa_z = \frac{\kappa \Delta \theta}{\sin(\theta_0)}$$

exponential volume reflectivity

$$f_v(z) = \exp\left(\frac{2 \sigma z}{\cos \theta_0}\right)$$

## Single Baseline Observations

single- / dual- / quad-pol

$$\tilde{\gamma}_{\text{Vol}}(\vec{w}_1, \kappa_z) \quad \tilde{\gamma}_{\text{Vol}}(\vec{w}_2, \kappa_z) \quad \tilde{\gamma}_{\text{Vol}}(\vec{w}_3, \kappa_z)$$

1, 2, or 3 complex coherences



Total Coherence

$$\tilde{\gamma}(\vec{w}, \kappa_z) = \gamma_{\text{Temp}}(\kappa_z) \tilde{\gamma}_{\text{Vol}}(\vec{w}, \kappa_z)$$

## For a Single Baseline

4 unknown parameters

Volume Height  $h_v$

Topography  $\varphi_0$

G/V Ratio  $m(\vec{w}) = f(\text{pol})$

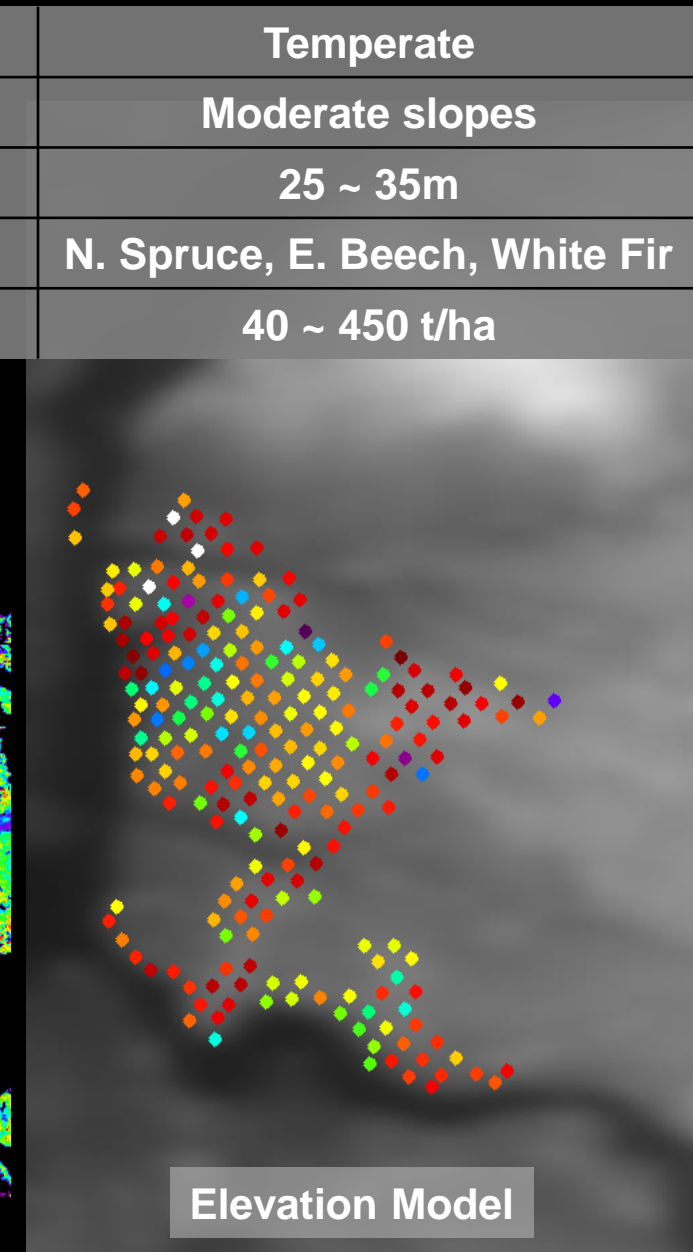
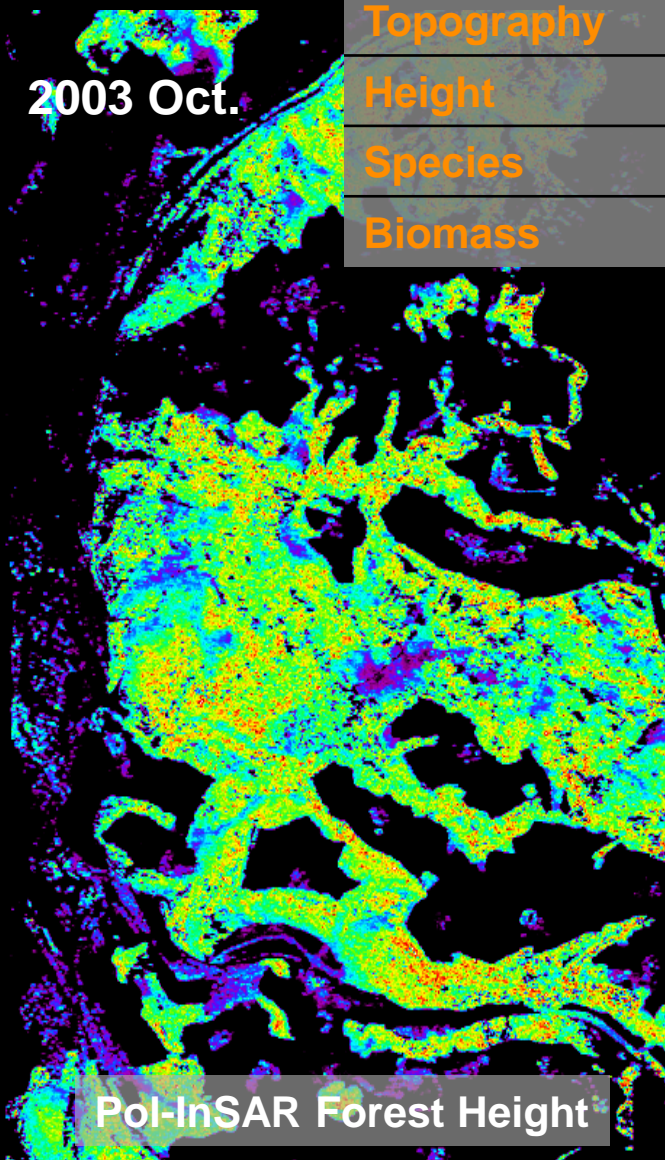
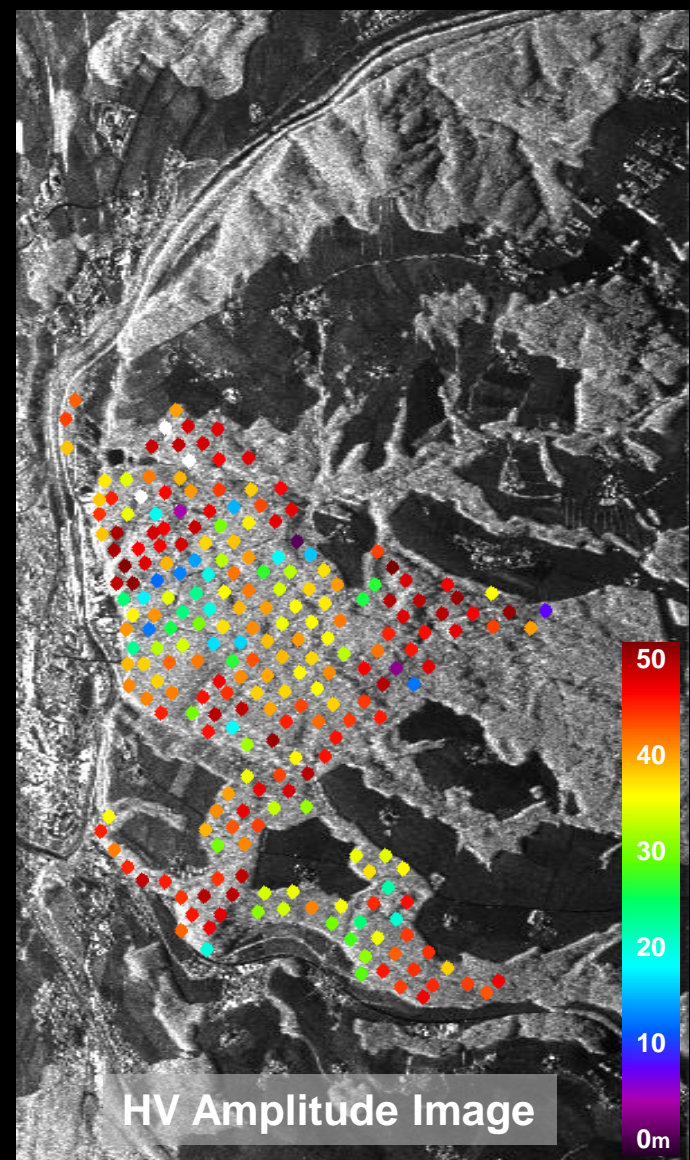
$f_v(z)$  ... 1 parameter ( $\sigma$ )

plus one more

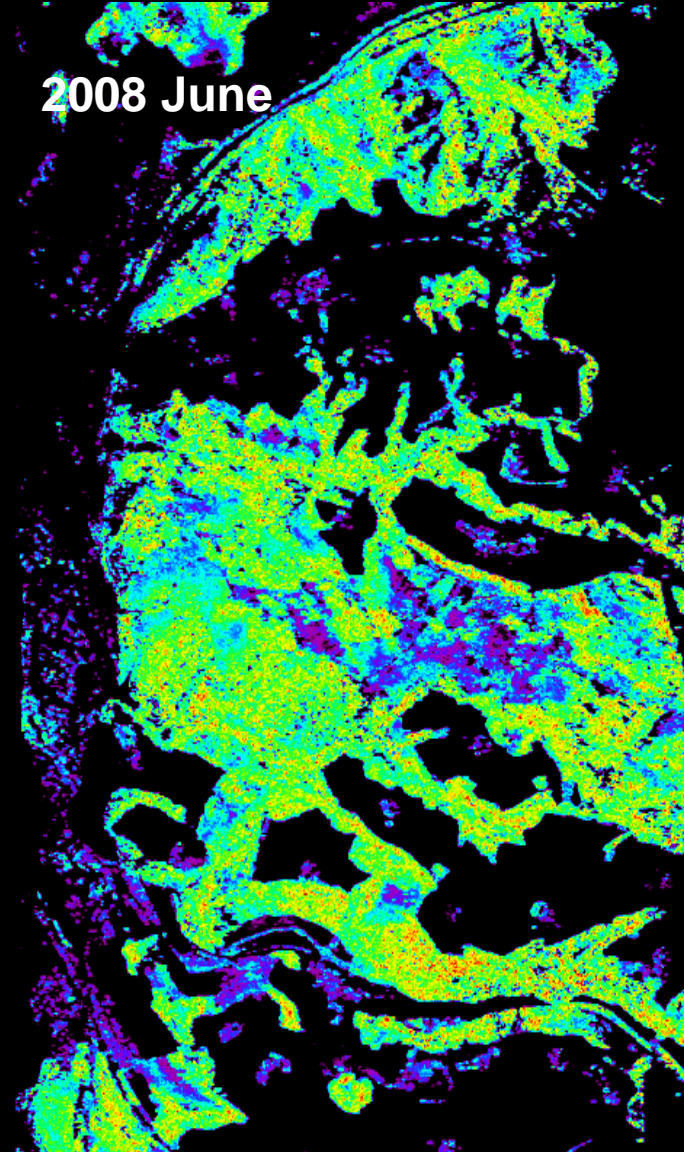
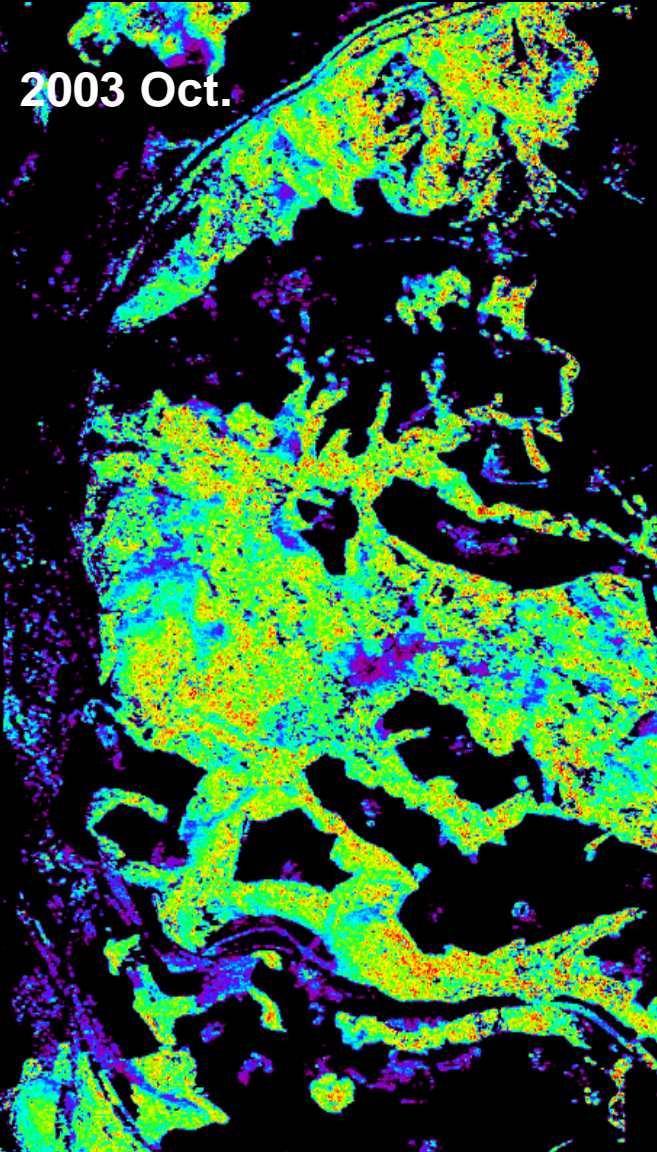
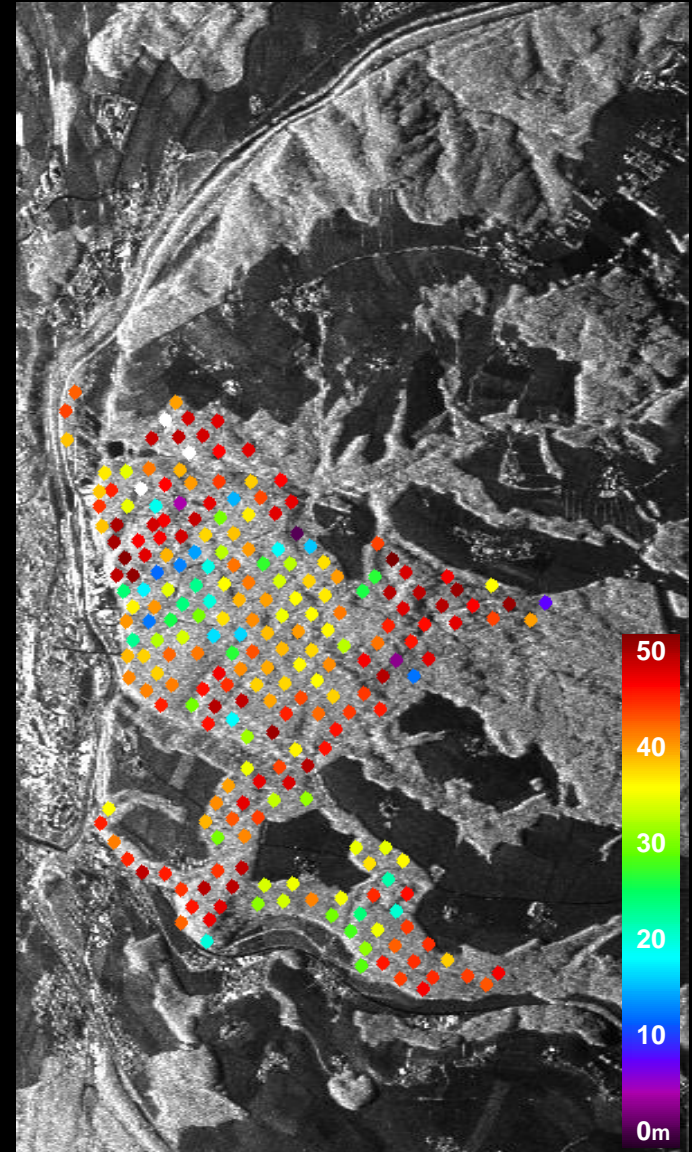
Temporal Deco  $\gamma_{\text{Temp}}$

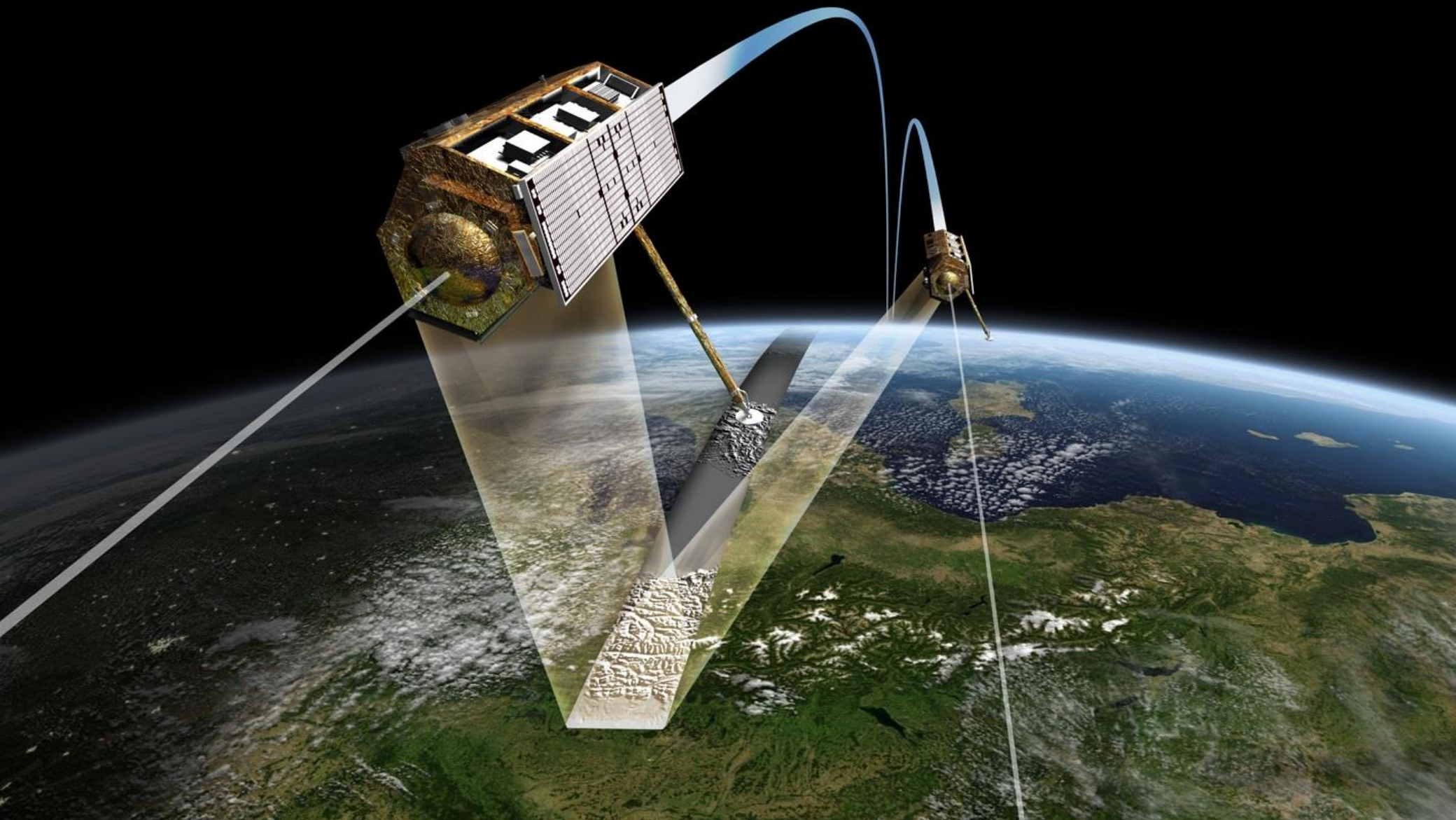
for repeat-pass implementations

# Traunstein Test Site

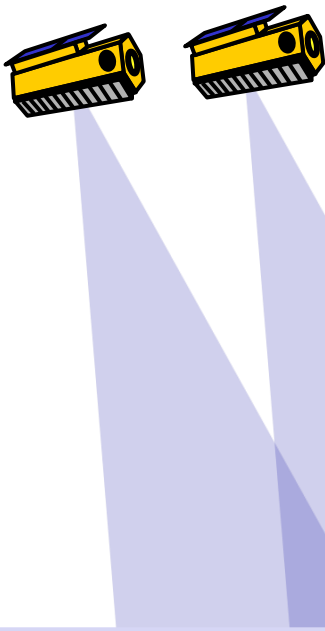


# Traunstein Test Site





# TanDEM-X: 2 Layer model with exp. volume reflectivity



Volume Layer    Ground Layer

$$f(z, \vec{w}) = m_v f_v(z) + m_G(\vec{w}) \delta(z - z_0)$$

$\tilde{\gamma}_{\text{Vol}}(\vec{w}, \kappa_z) = \exp(i\varphi_0) \frac{\tilde{\gamma}_v(\kappa_z) + m(\vec{w})}{1 + m(\vec{w})}$

**Volume Layer Coherence**

$$\tilde{\gamma}_v = \frac{I}{I_0} \left\{ \begin{array}{l} I = \int_0^{h_v} \exp(i\kappa_z z') e^{\left(\frac{2\sigma z'}{\cos\theta_0}\right)} dz' \\ I_0 = \int_0^{h_v} e^{\left(\frac{2\sigma z'}{\cos\theta_0}\right)} dz' \end{array} \right. \quad m(\vec{w}) = \frac{m_G(\vec{w})}{m_v(\vec{w})I_0} \quad \kappa_z = \frac{\kappa\Delta\theta}{\sin(\theta_0)}$$

exponential volume reflectivity

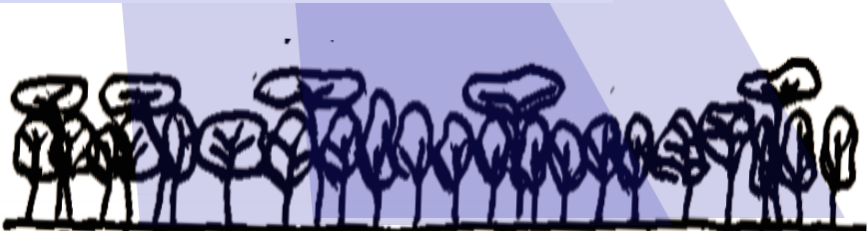
$$f_v(z) = \exp\left(\frac{2\sigma z}{\cos\theta_0}\right)$$

Single Baseline Observation(s)

single-pol

$\tilde{\gamma}_{\text{Vol}}(\vec{w}_1, \kappa_z)$

1 complex coherence



Total Coherence

$$\tilde{\gamma}(\vec{w}, \kappa_z) = \tilde{\gamma}_{\text{temp}}(\kappa_z) \tilde{\gamma}_{\text{Vol}}(\vec{w}, \kappa_z)$$

For a Single Baseline

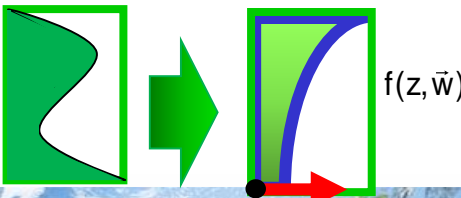
4 unknown parameters

Volume Height  $h_v$

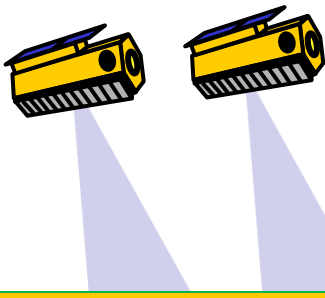
Topography  $\varphi_0$

G/V Ratio  $m(\vec{w}) = f(\text{pol})$

$f_v(z)$  ... 1 parameter ( $\sigma$ )



# TanDEM-X: 2 Layer model with exp. volume reflectivity + no ground



Invertible with single-pol data  
only if the ground topography  
 $\phi_0$  is known !!!

Volume Layer    Ground Layer

$$f(z, \vec{w}) = m_v f_v(z) + m_g(\vec{w}) \Sigma(z - z_0)$$

$\tilde{\gamma}_{vol}(\vec{w}, \kappa_z) = \exp(i\phi_0) \frac{\tilde{\gamma}_v(\kappa_z) + m_g(\vec{w})}{m_v(\vec{w})}$

Volume Layer Coherence

$$\tilde{\gamma}_v = \frac{I}{I_0} \left\{ \begin{array}{l} I = \int_0^{h_v} \exp(i\kappa_z z') e^{\left(\frac{2\sigma z'}{\cos\theta_0}\right)} dz' \\ I_0 = \int_0^{h_v} e^{\left(\frac{2\sigma z'}{\cos\theta_0}\right)} dz' \end{array} \right.$$

$m_g(\vec{w}) = \frac{m_v(\vec{w}) I_0}{m_v(\vec{w}) I_0 + \kappa \Delta \theta}$

$\kappa_z = \frac{\kappa \Delta \theta}{\sin(\theta_0)}$

$f_v(z) = \exp\left(\frac{2\sigma z}{\cos\theta_0}\right)$

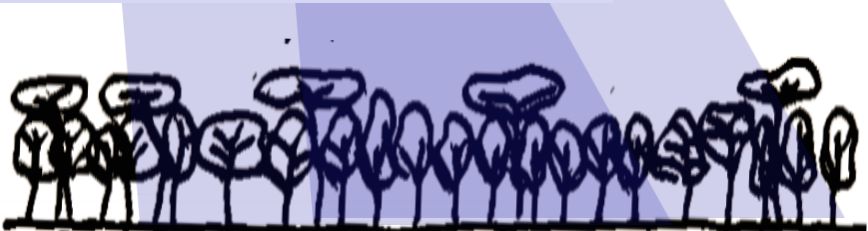
exponential volume reflectivity

Single Baseline Observation(s)

single-pol

$\tilde{\gamma}_{vol}(\vec{w}_1, \kappa_z)$

1 complex coherence



Total Coherence

$\tilde{\gamma}(\vec{w}, \kappa_z) = \gamma_{temp}(\kappa_z) \tilde{\gamma}_{vol}(\vec{w}, \kappa_z)$

For a Single Baseline

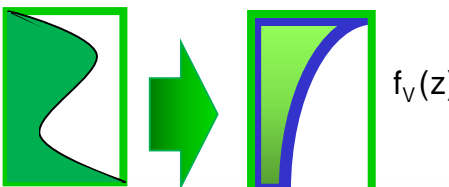
3 unknown parameters

Volume Height  $h_v$

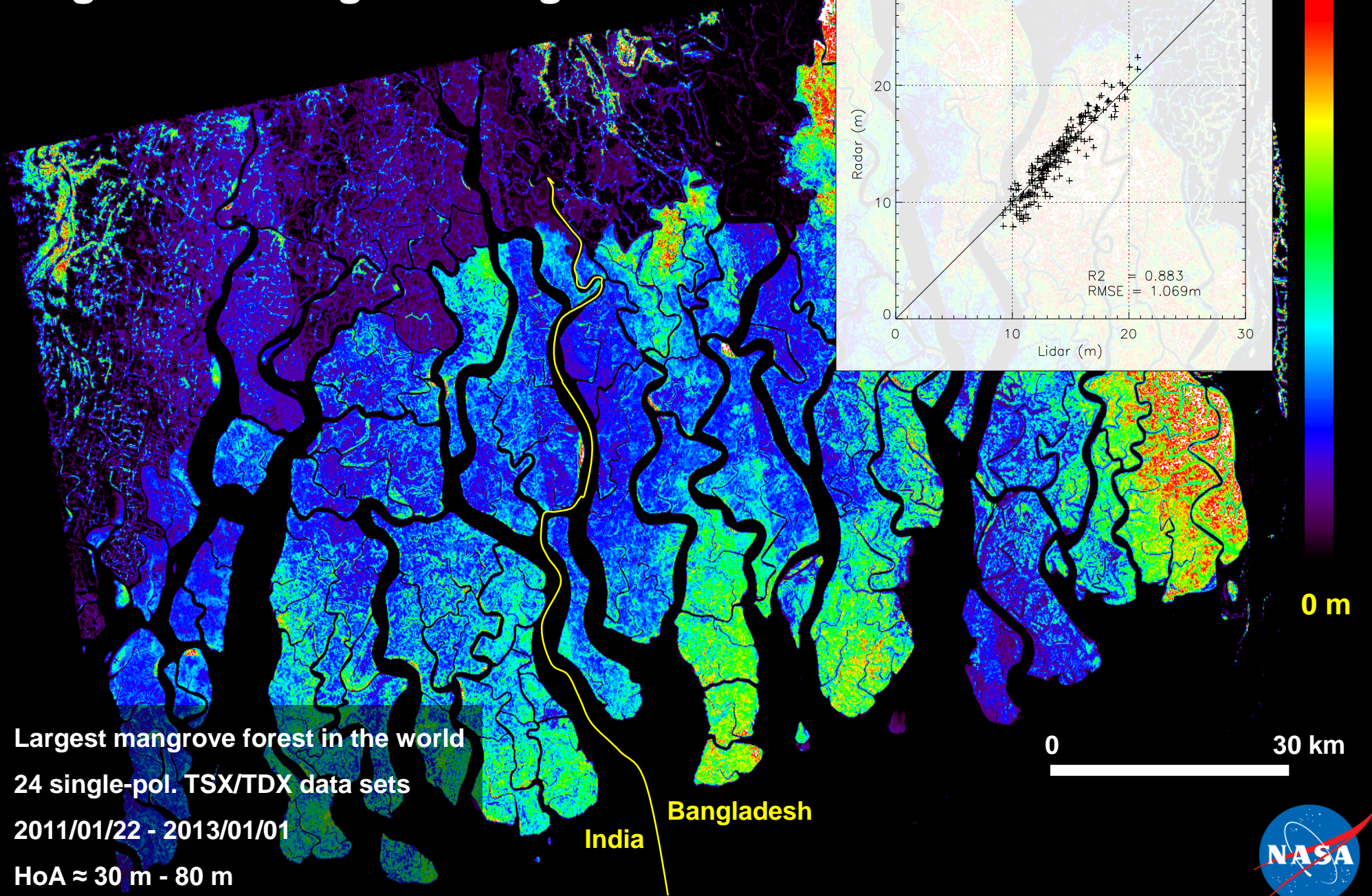
Topography  $\phi_0$

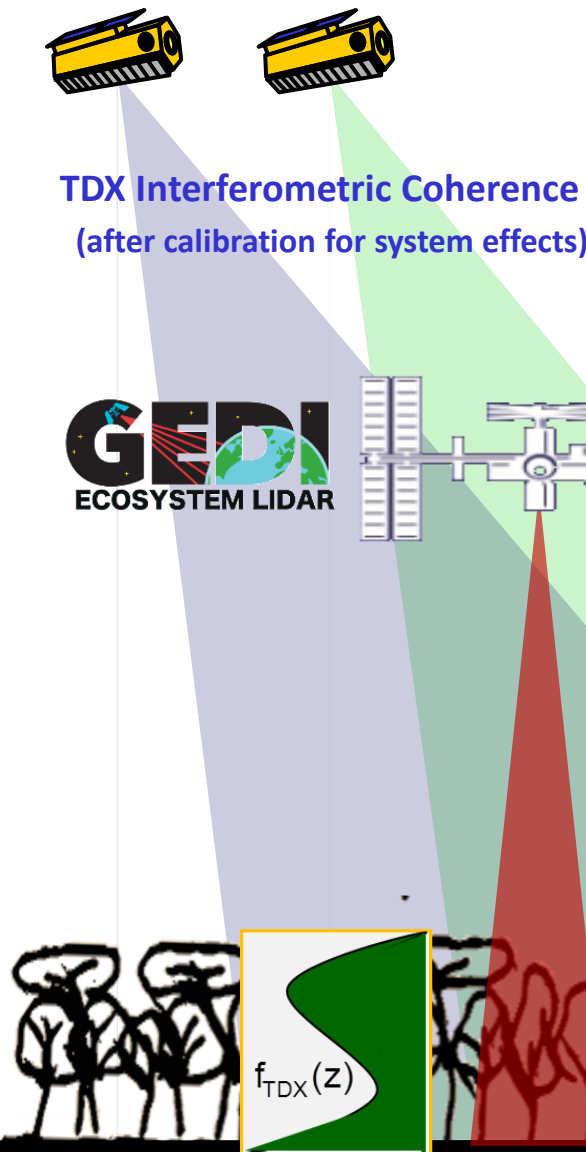
C/V Ratio  $\gamma_{temp}(\kappa_z)$  (pol.)

$f_v(z)$  ... 1 parameter ( $\sigma$ )



# Bangladesh Mangrove Height



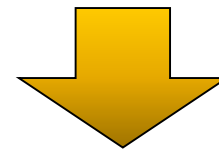


$$\tilde{\gamma}_{\text{Vol}}(k_z) = e^{ik_z z_0} \frac{\int_0^{h_v} f_{\text{TDX}}(z) e^{ik_z z} dz}{\int_0^{h_v} f_{\text{TDX}}(z) dz}$$

The TanDEM-X forest height inversion problem is underdetermined (**1 complex measurement** for at least **3 real unknowns**) and thus not solvable !

GEDI waveforms can be used to approximate the X-band (vertical) reflectivity profiles

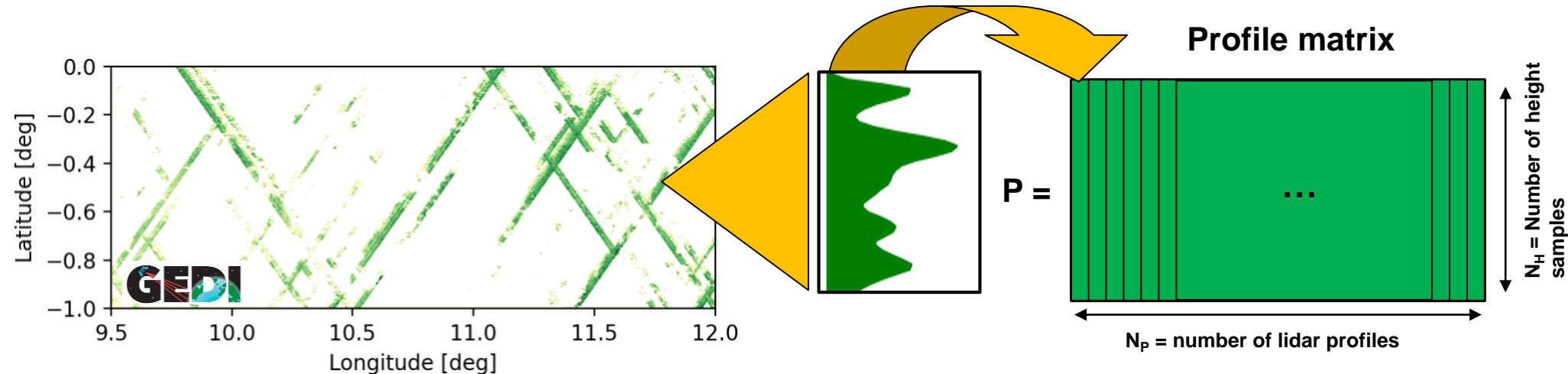
$$f_{\text{TDX}}(z) \approx P_{\text{GEDI}}(z)$$



$$\tilde{\gamma}_{\text{Vol}}(k_z) = e^{ik_z z_0} \frac{\int_0^{h_v} P_{\text{GEDI}}(z) e^{ik_z z} dz}{\int_0^{h_v} P_{\text{GEDI}}(z) dz}$$

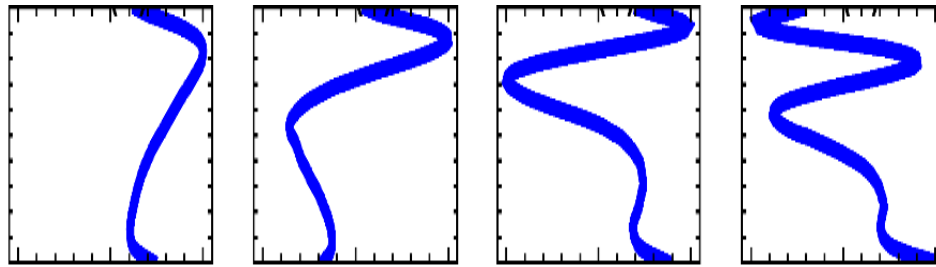
The TanDEM-X/GEDI forest height inversion problem is balanced (with **1 complex measurement** for **2 real unknowns**) and becomes solvable !

# TanDEM-X GEDI Fusion: Common Reflectivity Profile Estimation

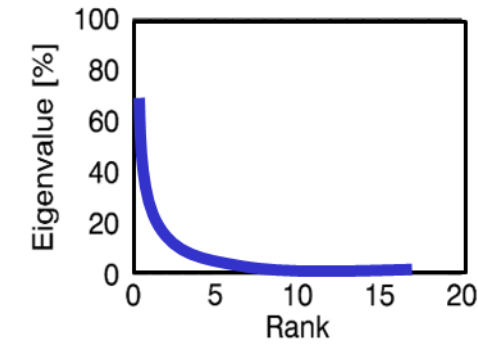


Profile covariance matrix:  $R = P P^T = U \Lambda U^T$  Eigen-decomposition of  $R$

Eigen-Vectors (e.g. Eigen-Functions)

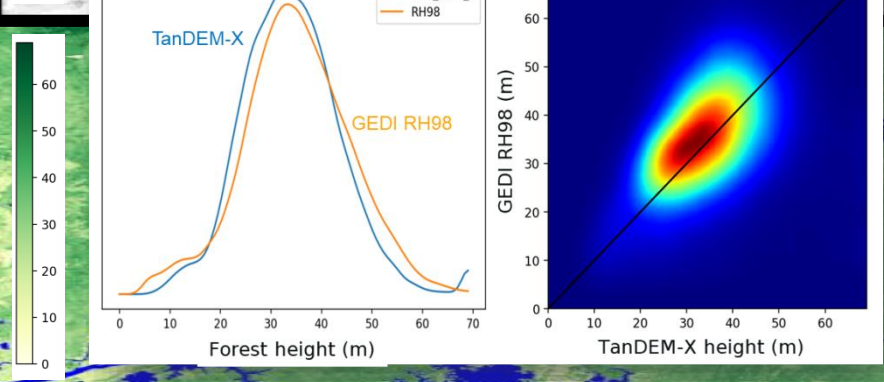
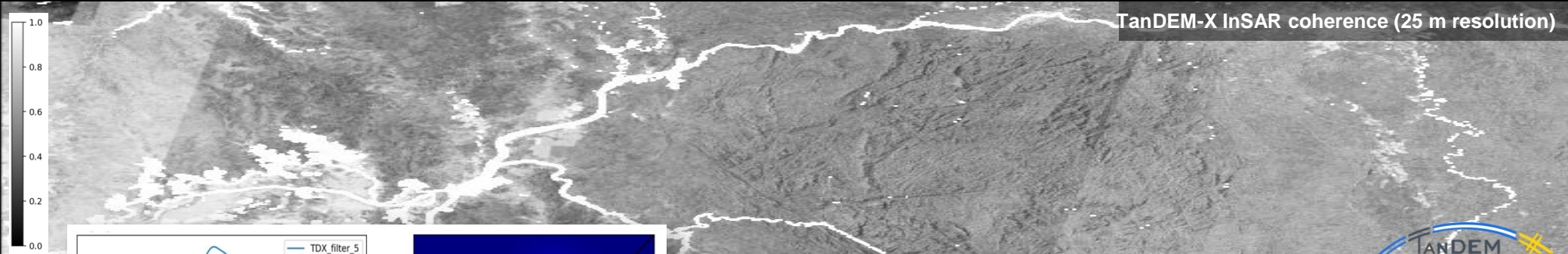
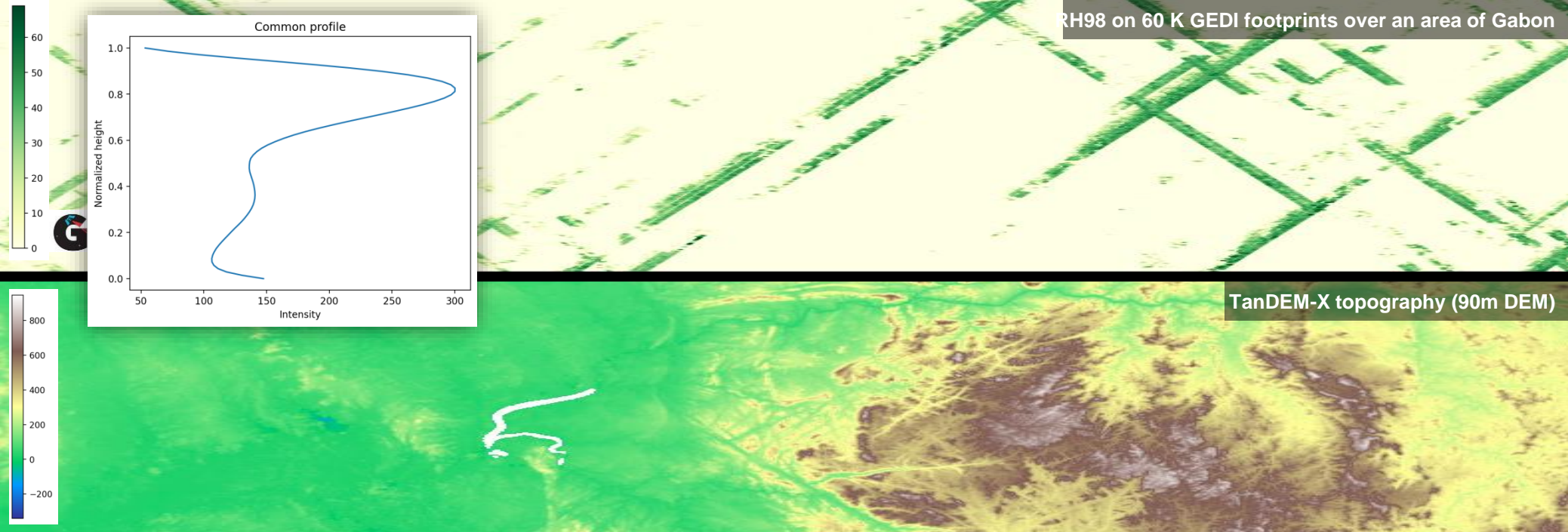


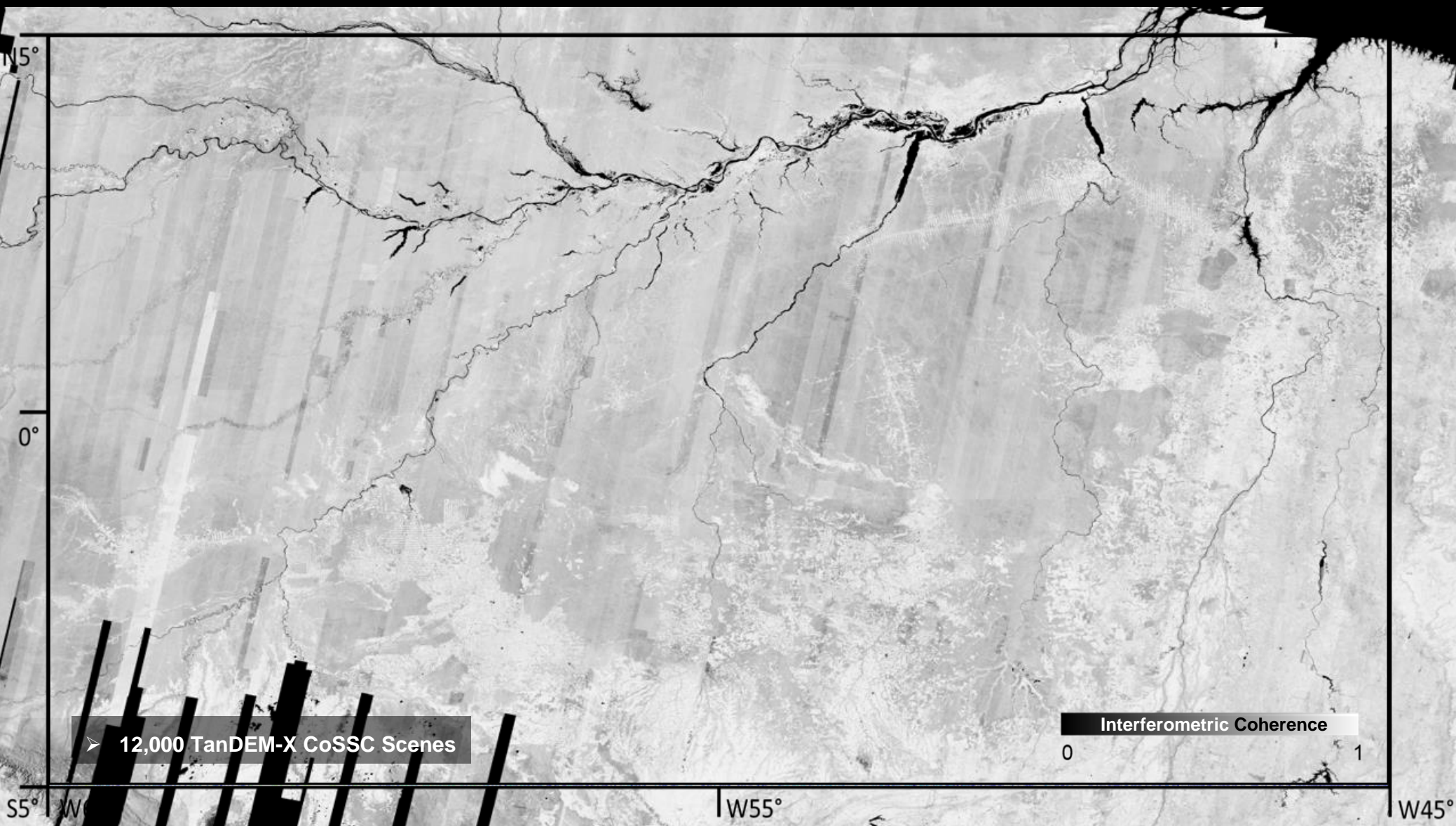
Eigen-Values

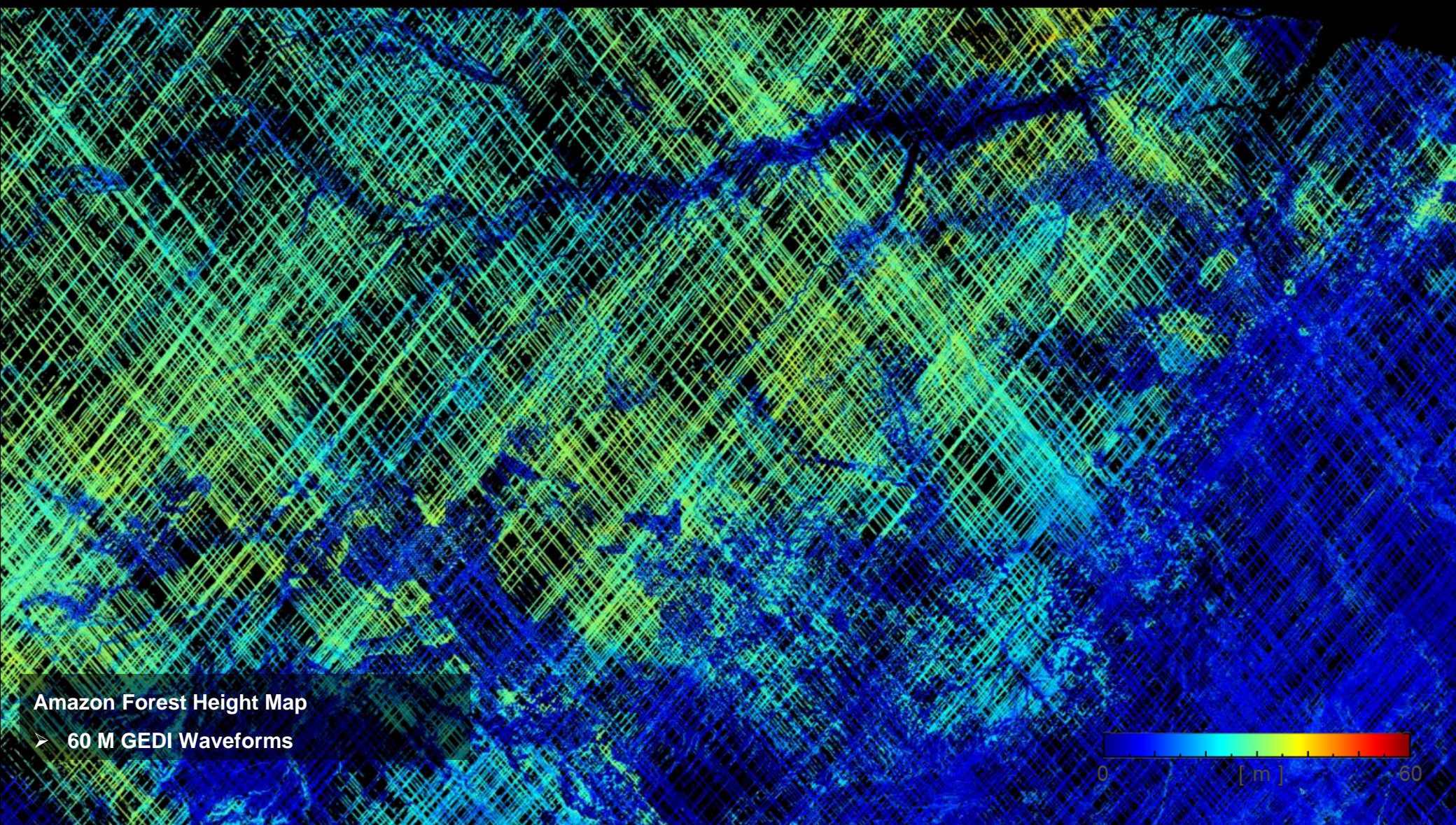


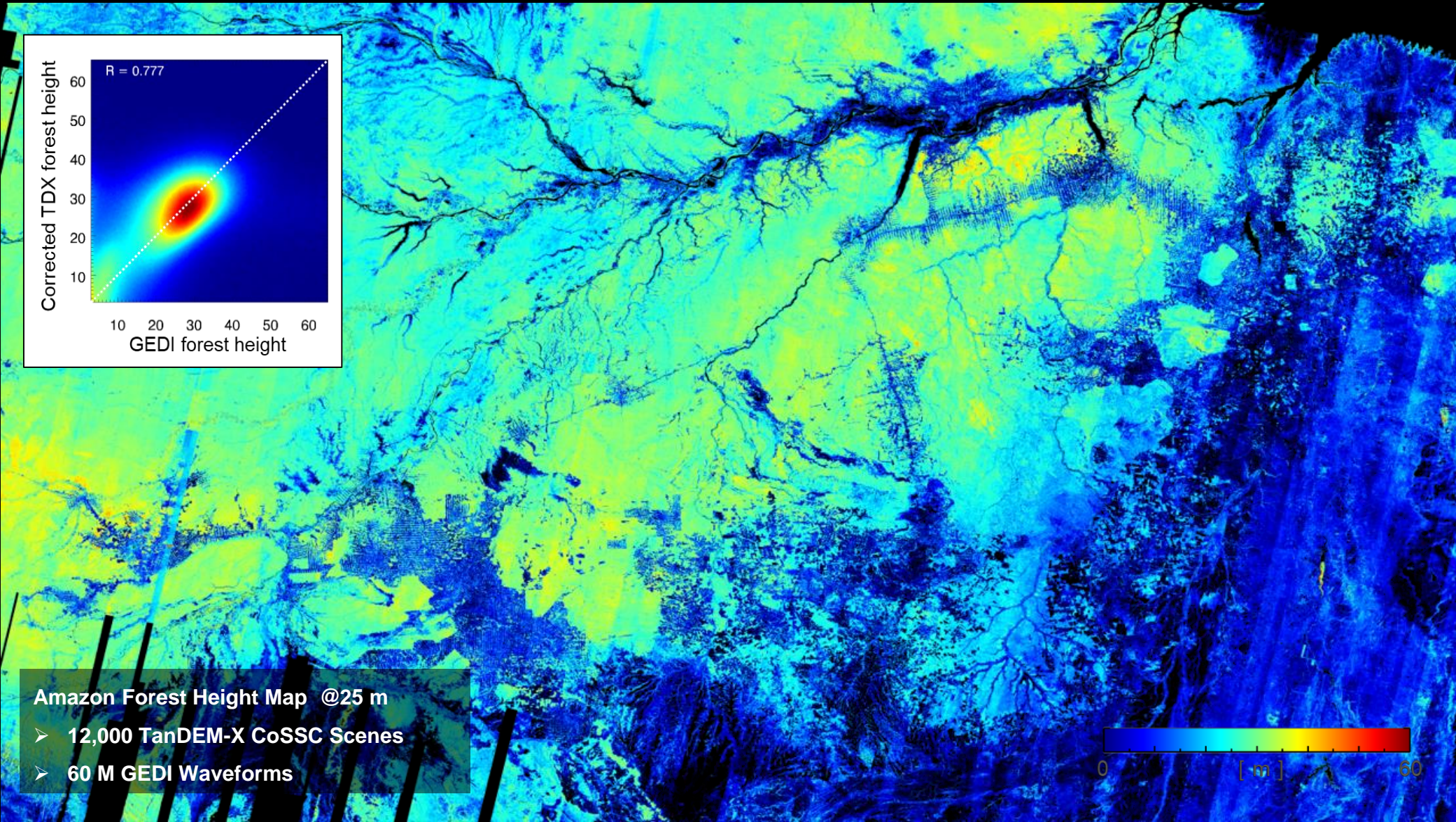
The Eigen-Vectors can be used derive a “mean” vertical profile

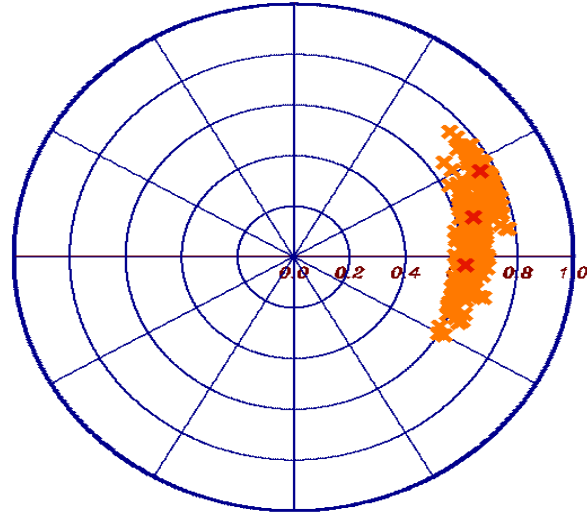
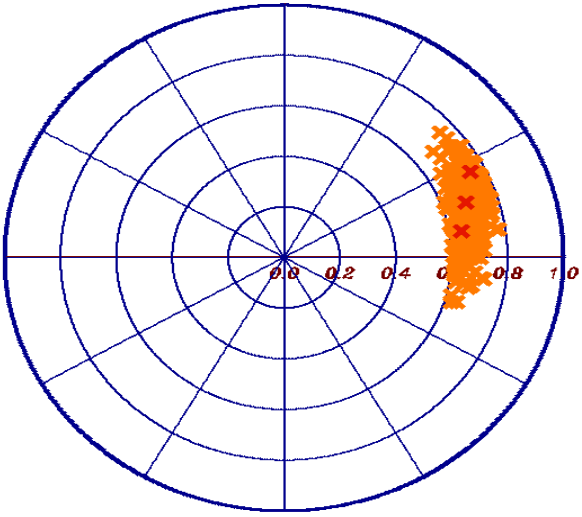
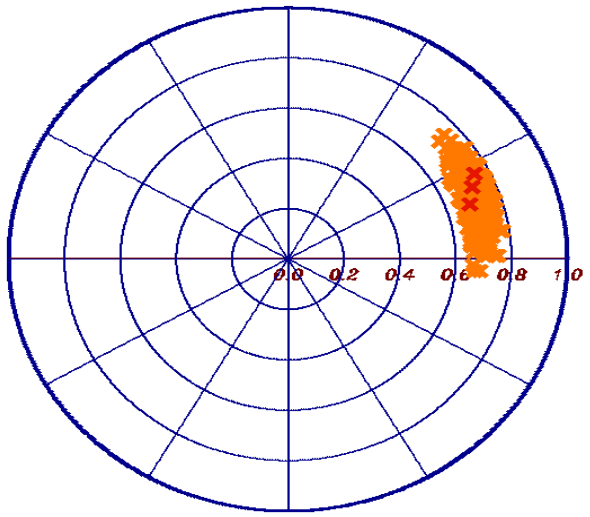
RH98 on 60 K GEDI footprints over an area of Gabon



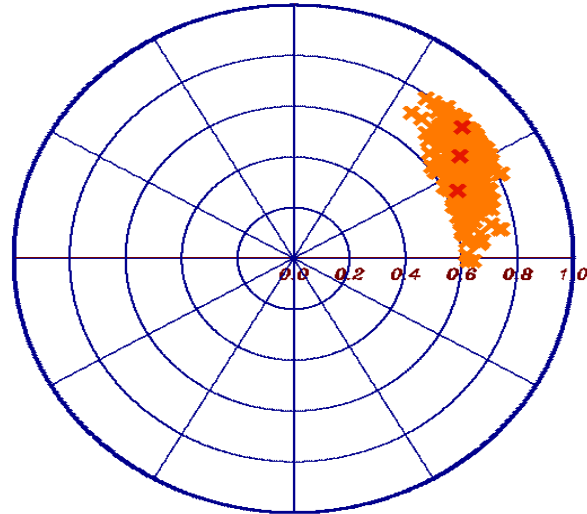
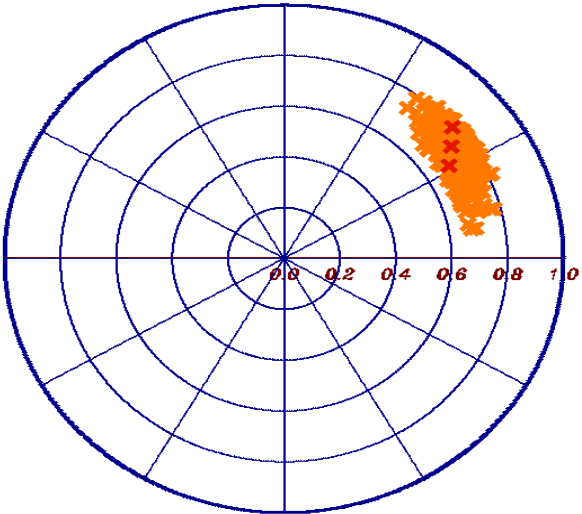
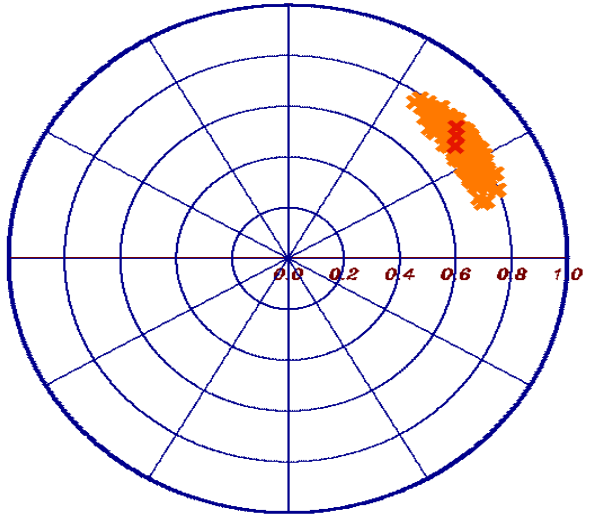








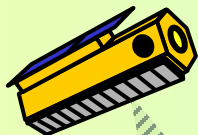
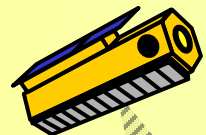
## Agriculture Vegetation



# Agriculture Pol-InSAR Applications

## Pol-SAR

$$[\mathbf{S}] = \begin{bmatrix} S_{HH} & S_{HV} \\ S_{VH} & S_{VV} \end{bmatrix}$$



## Pol-InSAR

$$[\mathbf{S}_1] = \begin{bmatrix} S_{HH}^1 & S_{HV}^1 \\ S_{VH}^1 & S_{VV}^1 \end{bmatrix}$$

$$[\mathbf{S}_2] = \begin{bmatrix} S_{HH}^2 & S_{HV}^2 \\ S_{VH}^2 & S_{VV}^2 \end{bmatrix}$$

### Bare Surfaces: Isolated Scattering Center

- Low Entropy scatterers -> High polarimetric coherence

### Vegetated Surfaces: Volume Scatterers

- High Entropy scatterers -> Low polarimetric coherence

### Agricultural vs. Forest Vegetation

Orientation effects in the vegetation layer ►

Anisotropic Propagation

Thinner / shorter vegetation layer

► Increased Importance of Ground Scattering  
Large Spatial Baselines

Short crop / plant phenological cycle

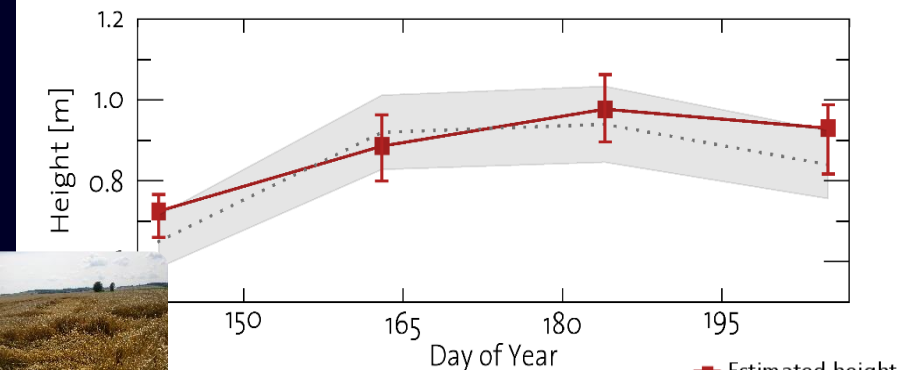
► Short Temporal Baselines

Variety of crop / plant structure

► Abstract Modelling

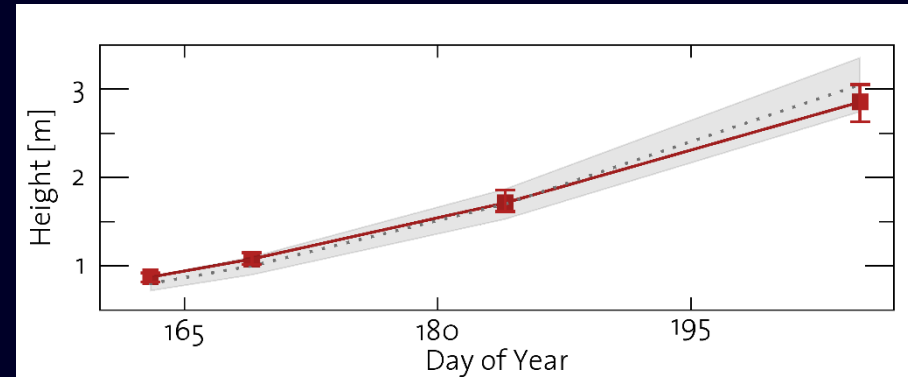


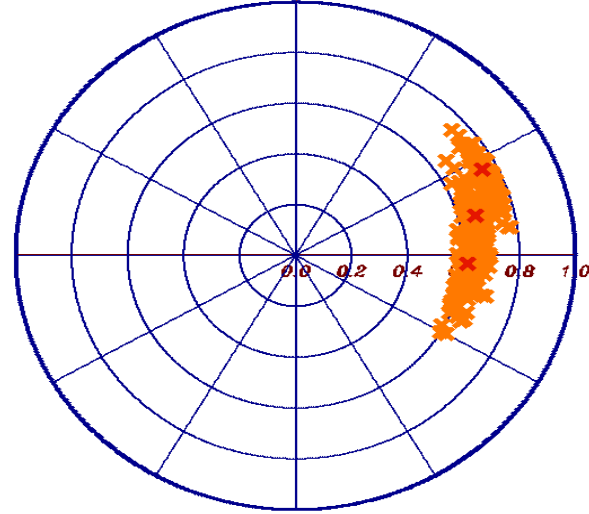
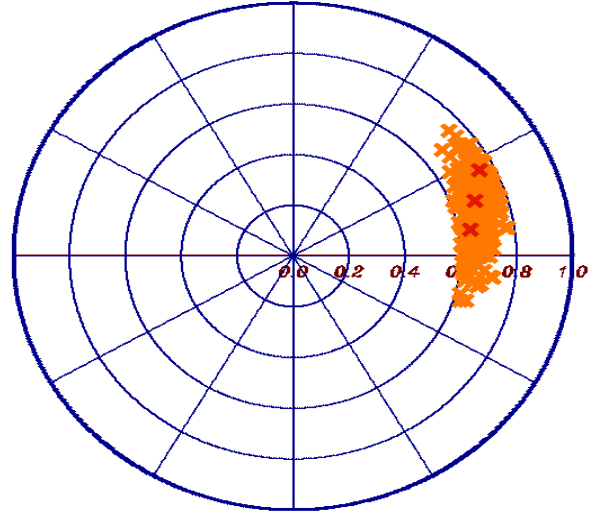
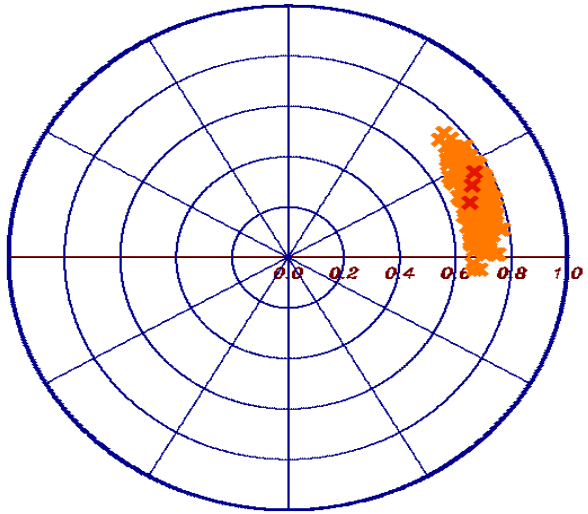
# Wheat



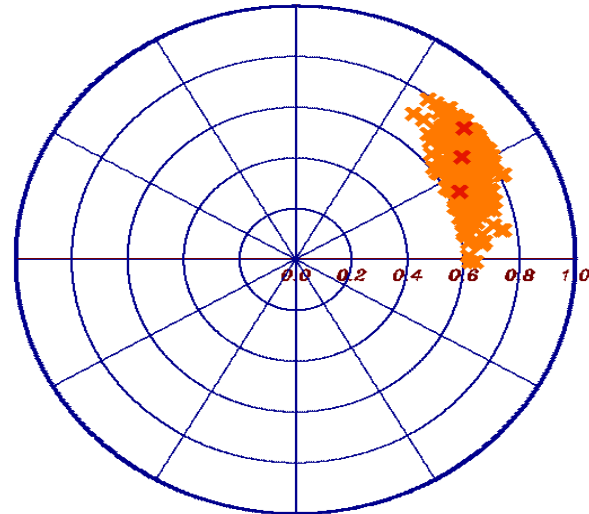
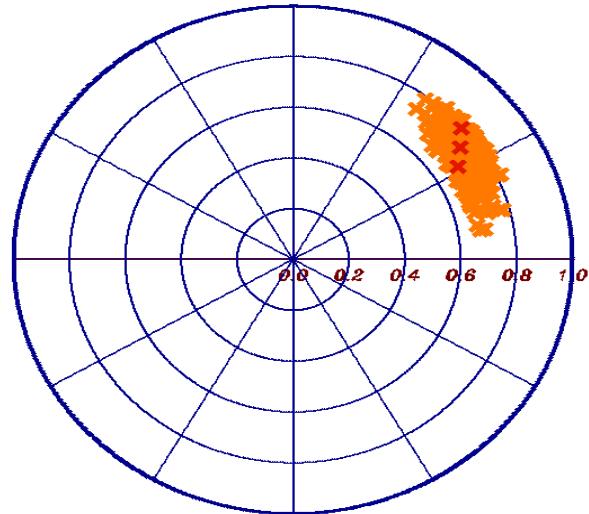
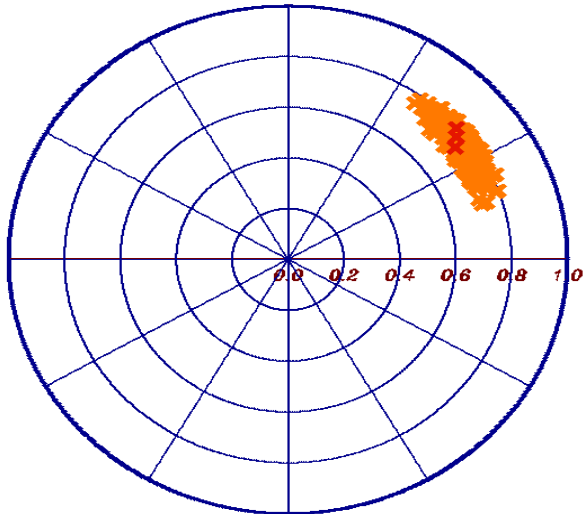
**Sensor:** DLR's F-SAR  
**Frequency:** C-Band ( $\approx$ 5 GHz)  
**Number of spatial baselines:** 2  
**Max. temporal baseline:** 90 minutes  
**Equivalent Number of Looks:** 100

# Corn (Maize)

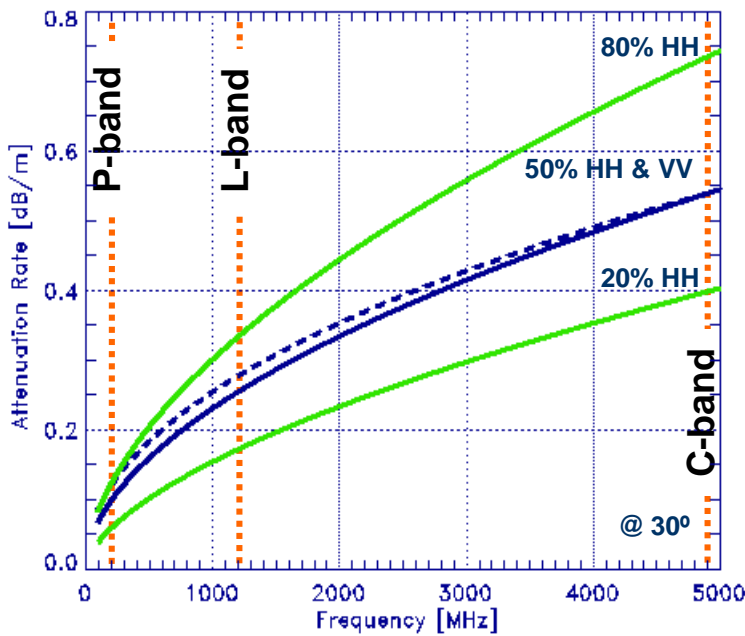




## Pol-InSAR: Frequency Effects

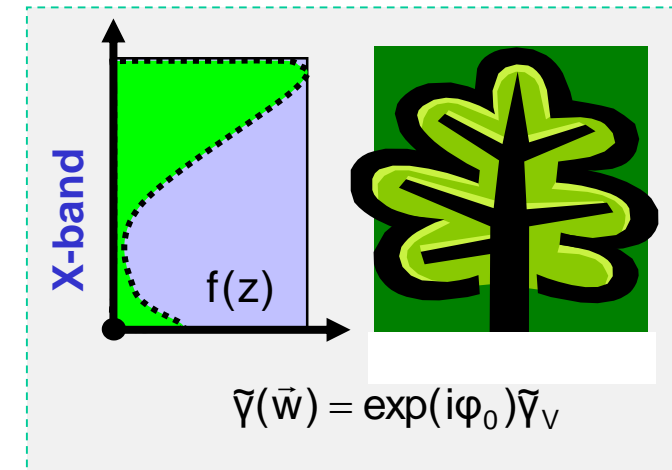
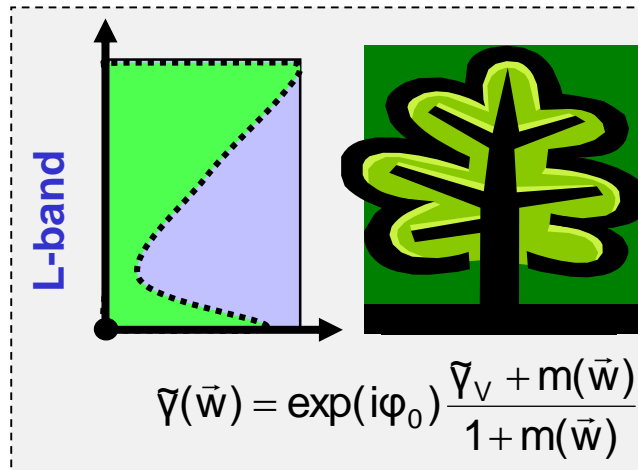
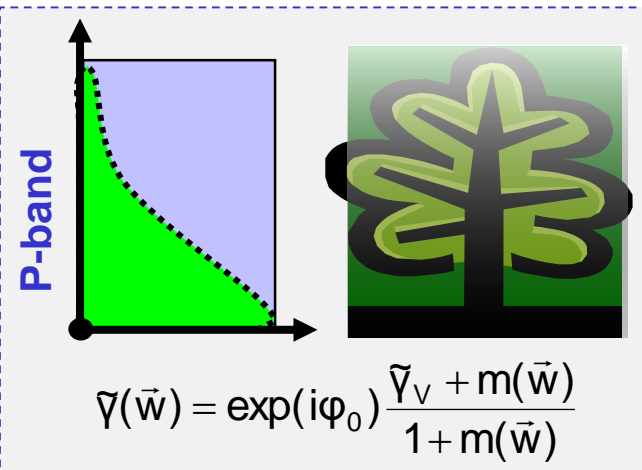


# Frequency Dependency



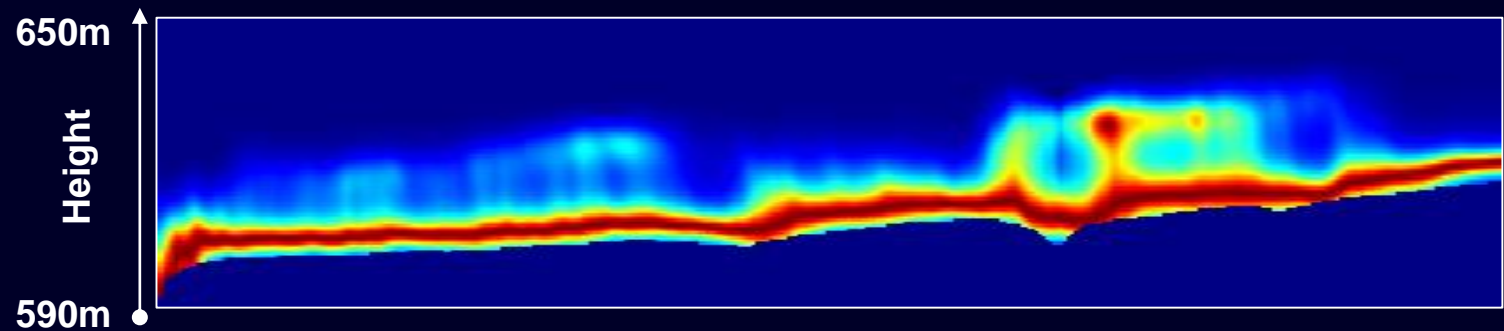
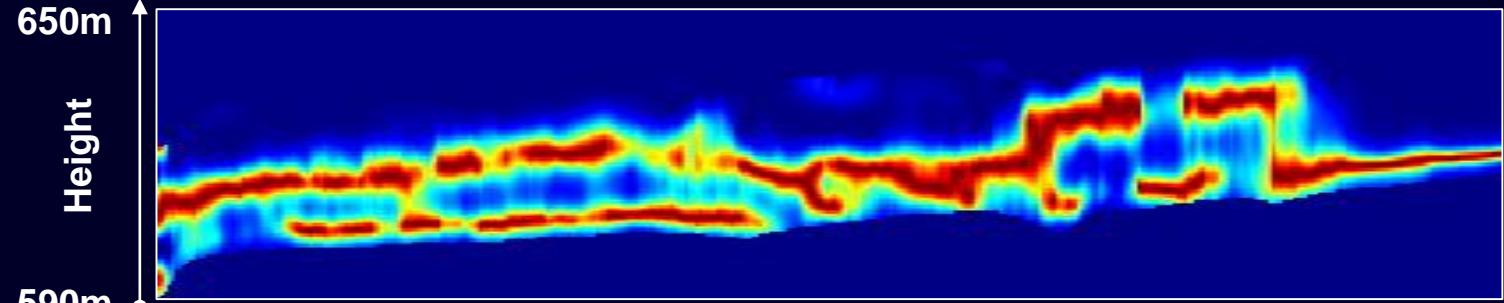
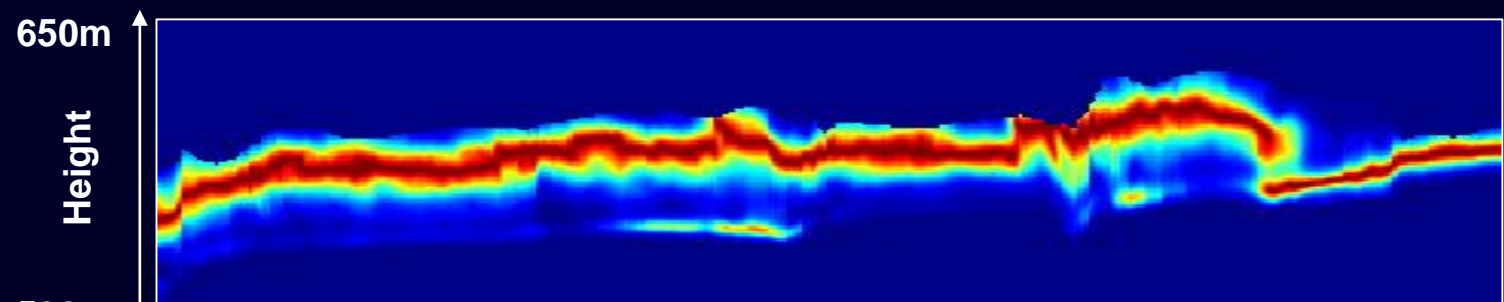
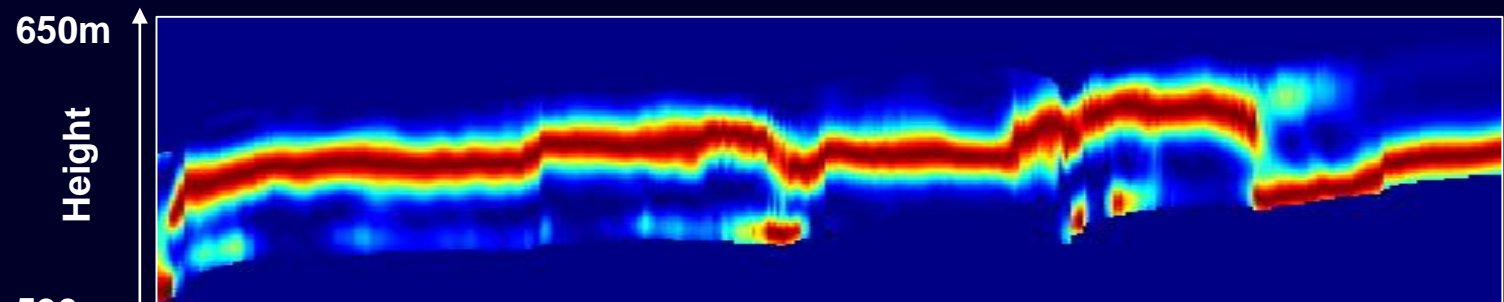
With decreasing frequency:

- The attenuation through the vegetation decreases;
- The relative importance of the volume decreases;
- The relative importance of the ground increases;
- The effective scatterers and their distribution changes.

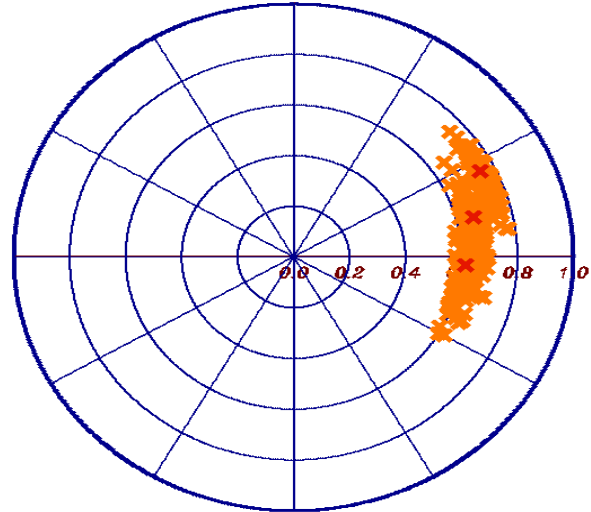
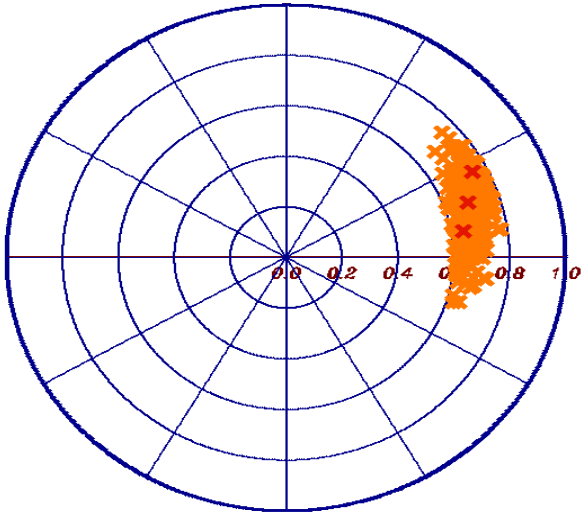
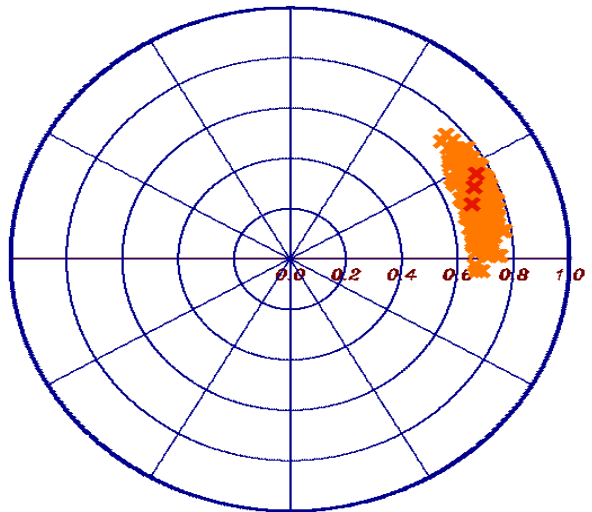


L.Bessette, S.Ayasli "Ultra Wide Band P-3 and Carabas II Foliage Attenuation and Backscatter Analysis", Proceedings of IEEE Radar Conference, 2001.

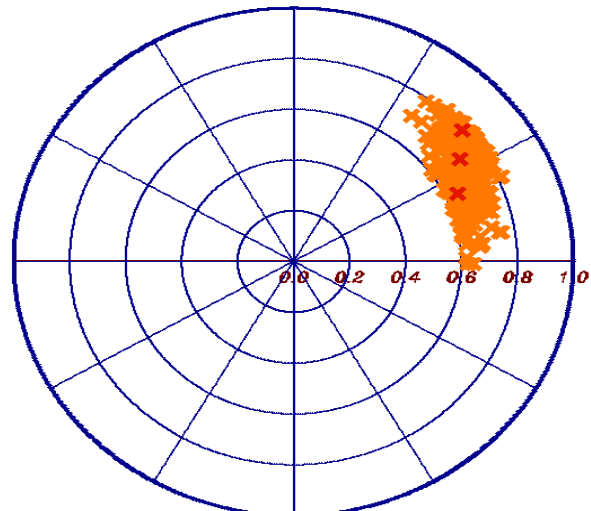
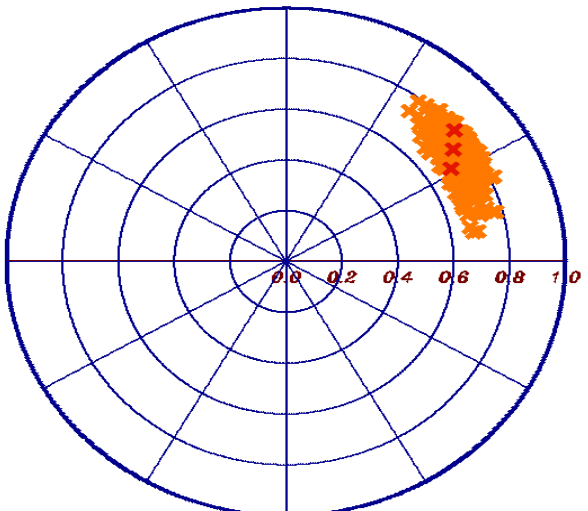
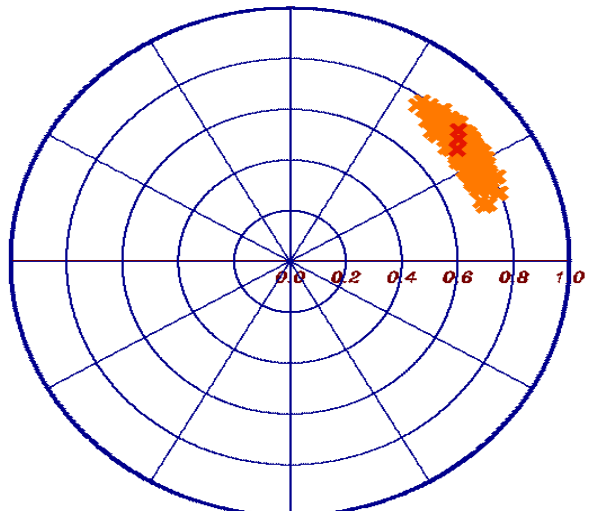


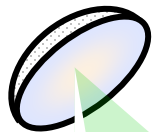
**P-band****L-band****S-band****X-band**

Slant range (0.6Km)



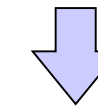
## Non-Volumetric Decorrelation Effects



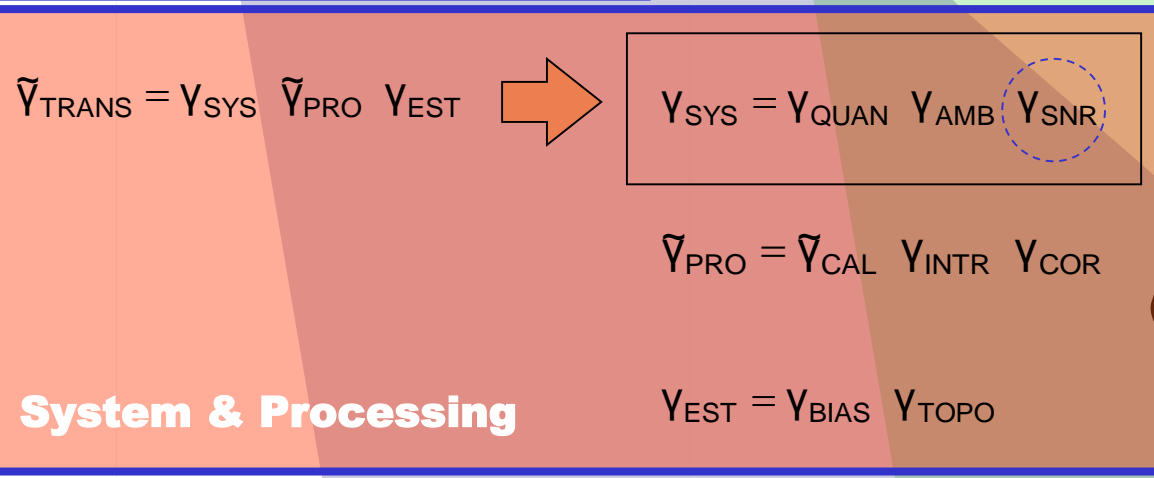
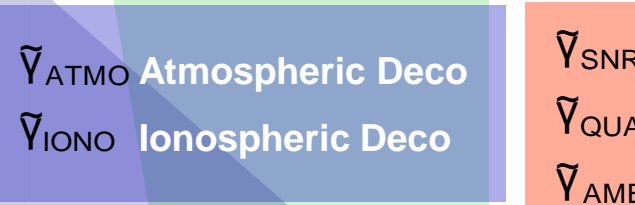
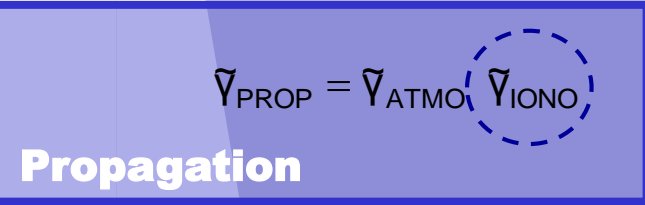
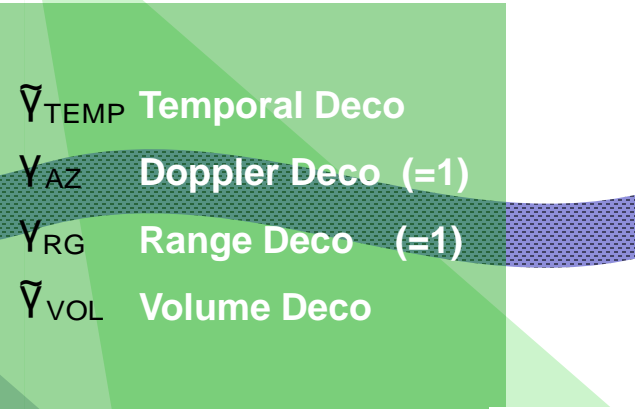
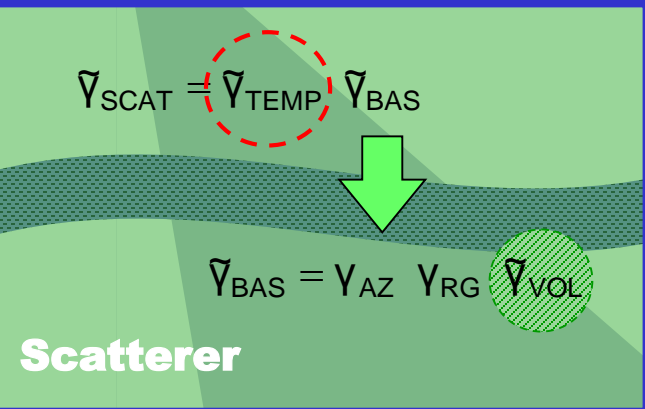
 $S_1$  $S_2$ 

## Interferometric Coherence

$$\tilde{\gamma}_{\text{OBS}} = \frac{\langle S_1 S_2^* \rangle}{\sqrt{\langle S_1 S_1^* \rangle \langle S_2 S_2^* \rangle}}$$



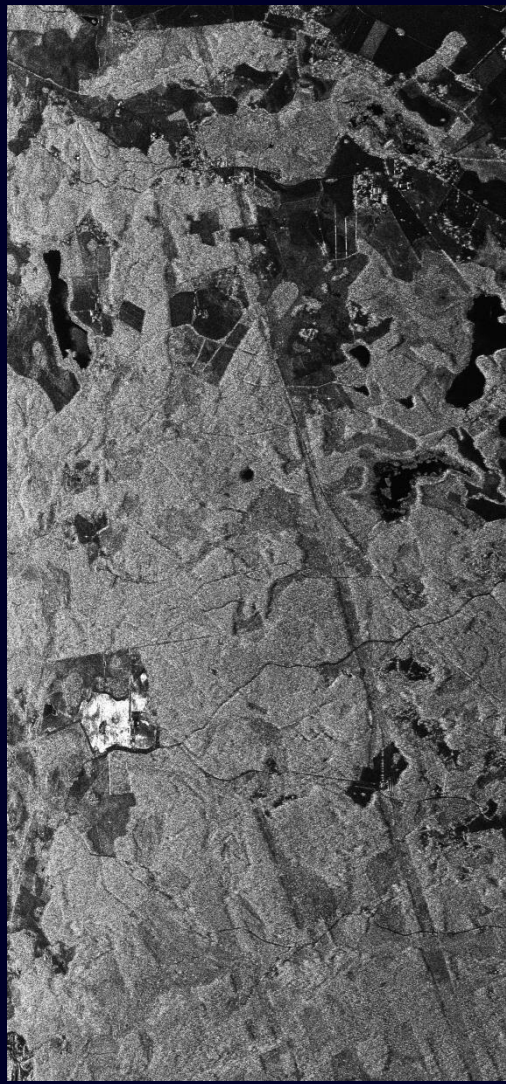
$$\tilde{\gamma}_{\text{OBS}} = \tilde{\gamma}_{\text{TRANS}} \tilde{\gamma}_{\text{PROP}} \tilde{\gamma}_{\text{SCAT}}$$



$\tilde{\gamma}_{\text{SNR}}$	<b>SNR Decorrelation</b>
$\tilde{\gamma}_{\text{QUAN}}$	<b>Quantisation Effects (0.99)</b>
$\tilde{\gamma}_{\text{AMB}}$	<b>Ambiguities</b>
$\tilde{\gamma}_{\text{CAL}}$	<b>Calibration Deccorelation</b>
$\gamma_{\text{INTR}}$	<b>Interpolation Effects</b>
$\gamma_{\text{COR}}$	<b>Corregistration Effects</b>
$\gamma_{\text{BIAS}}$	<b>Coh Estimation Bias (=1)</b>
$\gamma_{\text{TOPO}}$	<b>Topography Induced Coh Bias</b>



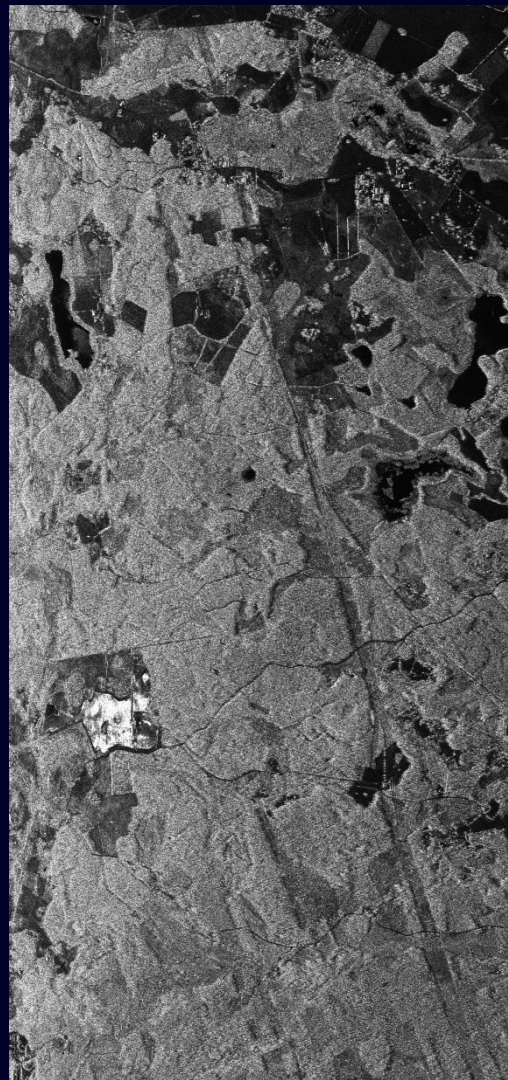
# Amplitude Image



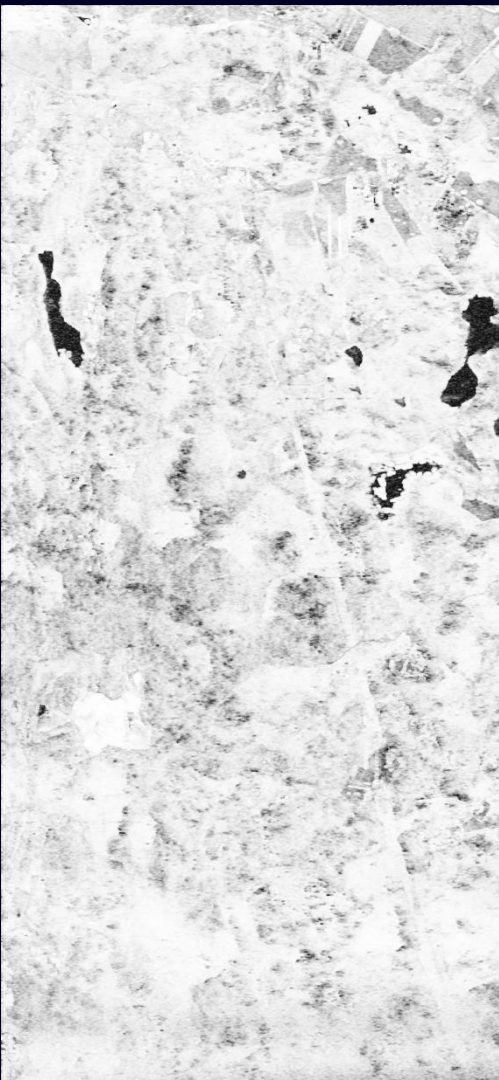
Amplitude Image HH



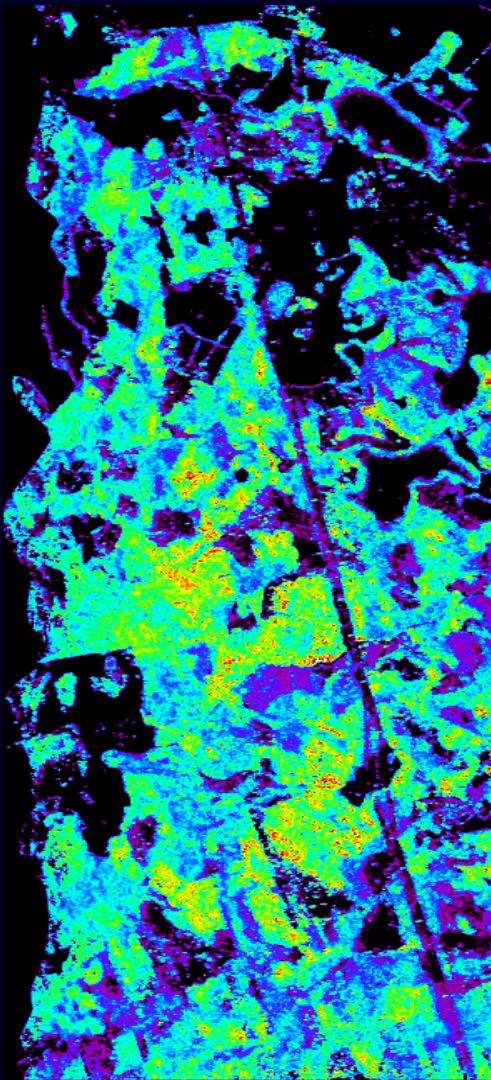
# Interferometric Coherence: Volume vs Temporal Decorrelation



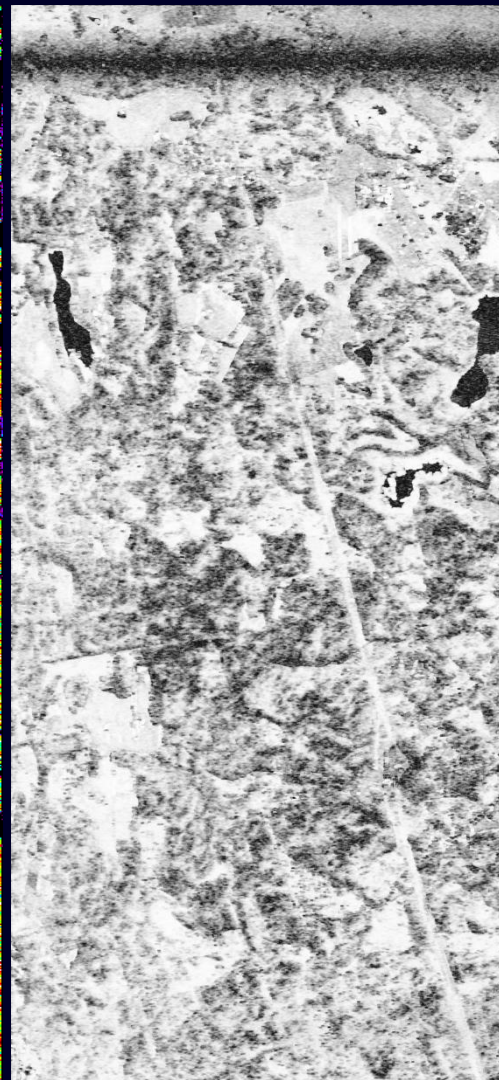
Amplitude Image HH



Volume Coherence



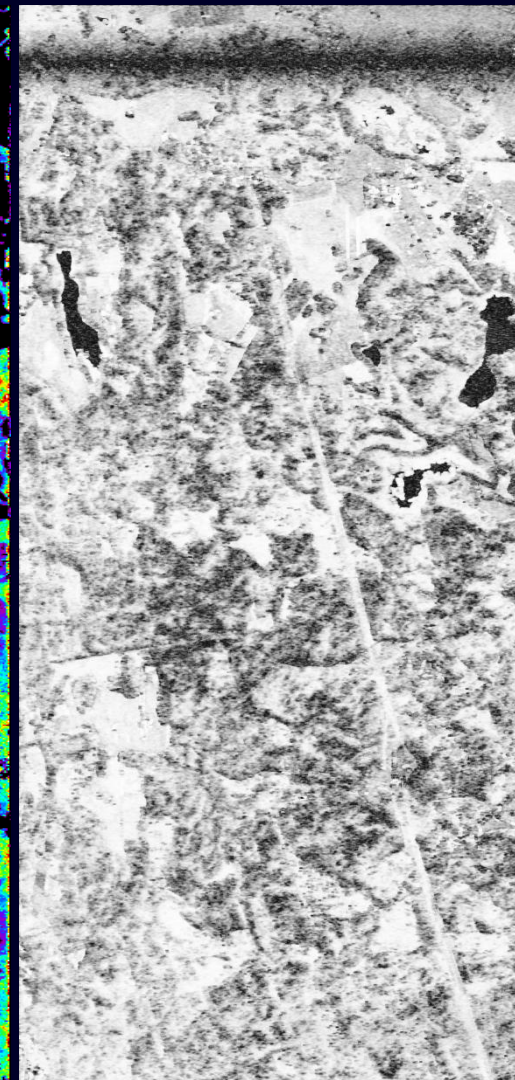
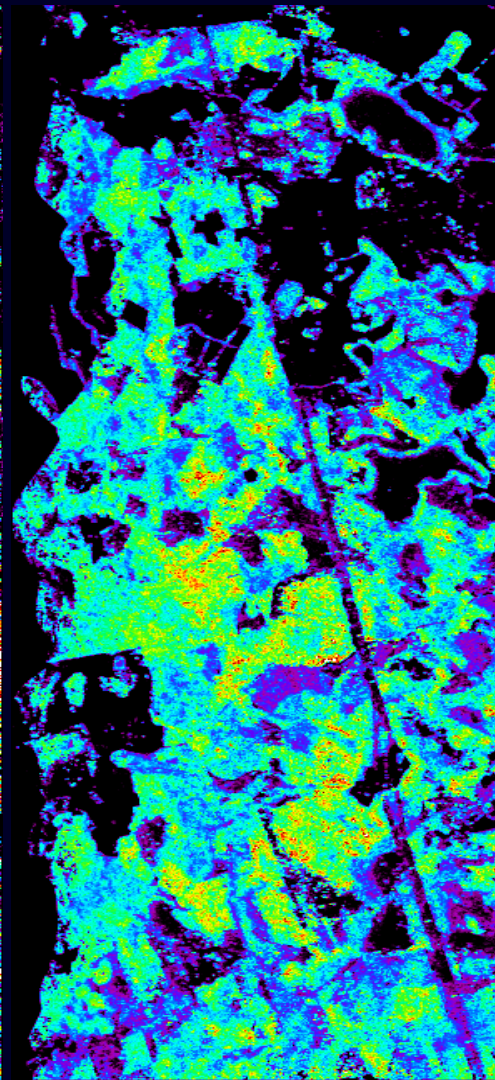
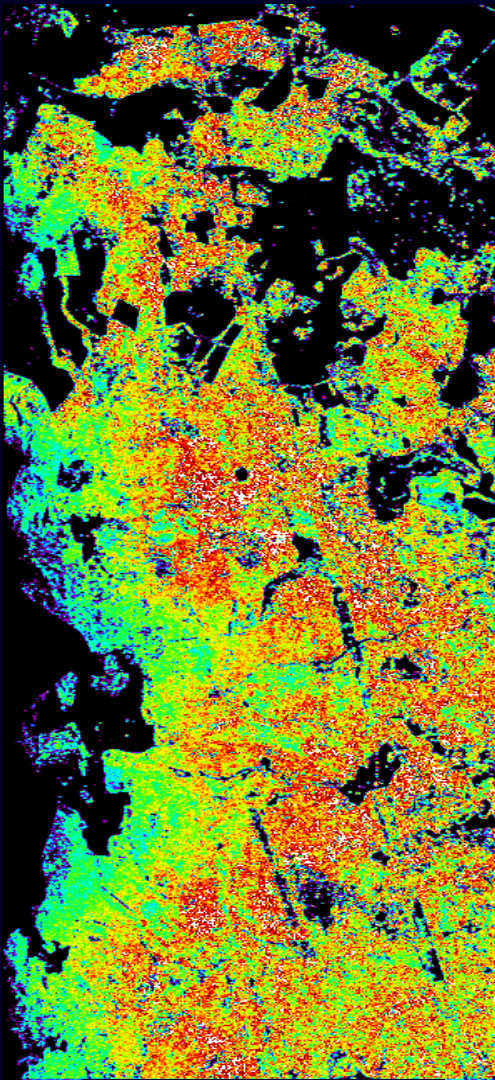
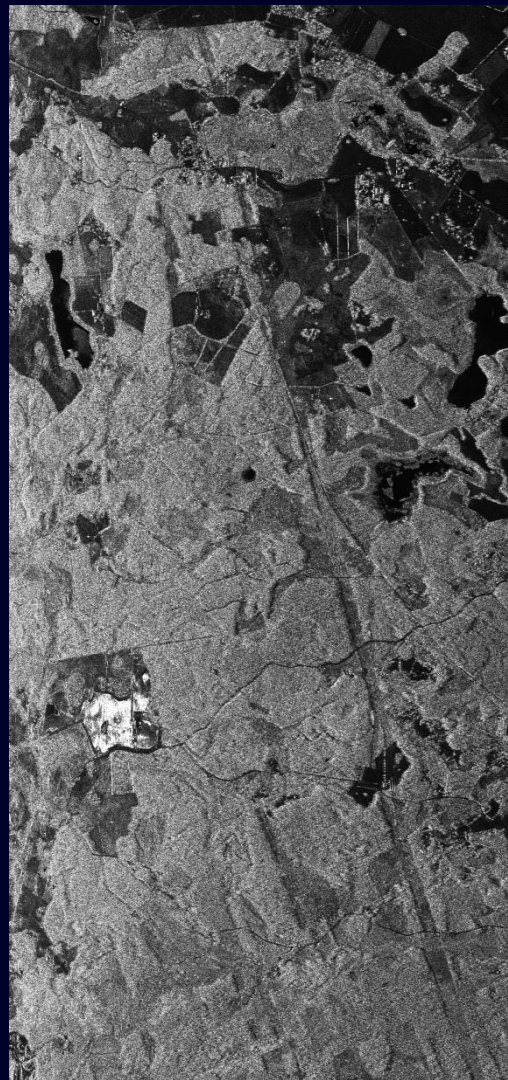
Forest Height Map



Volume + Temporal 24h



# Interferometric Coherence: Volume vs Temporal Decorrelation



Amplitude Image HH

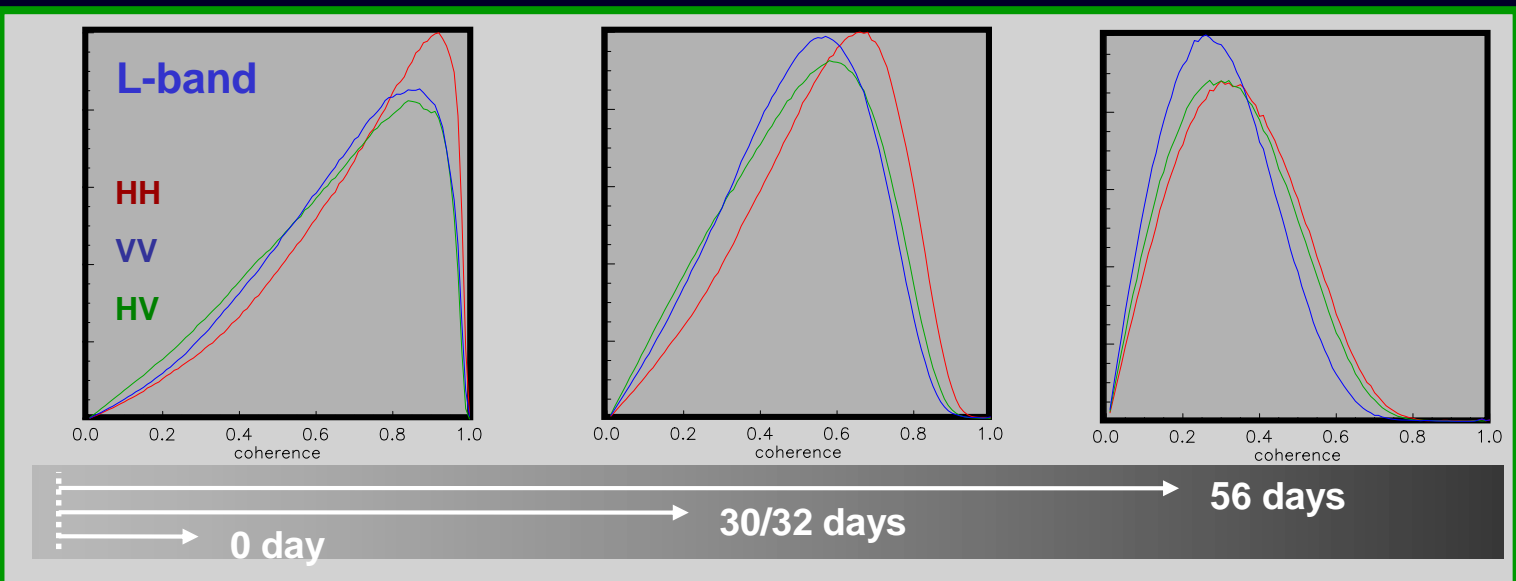
Forest Height Map

Forest Height Map

Volume + Temporal 24h



# Remningstorp Test Site: Temporal Decorrelation: L-band



HV Amplitude Image

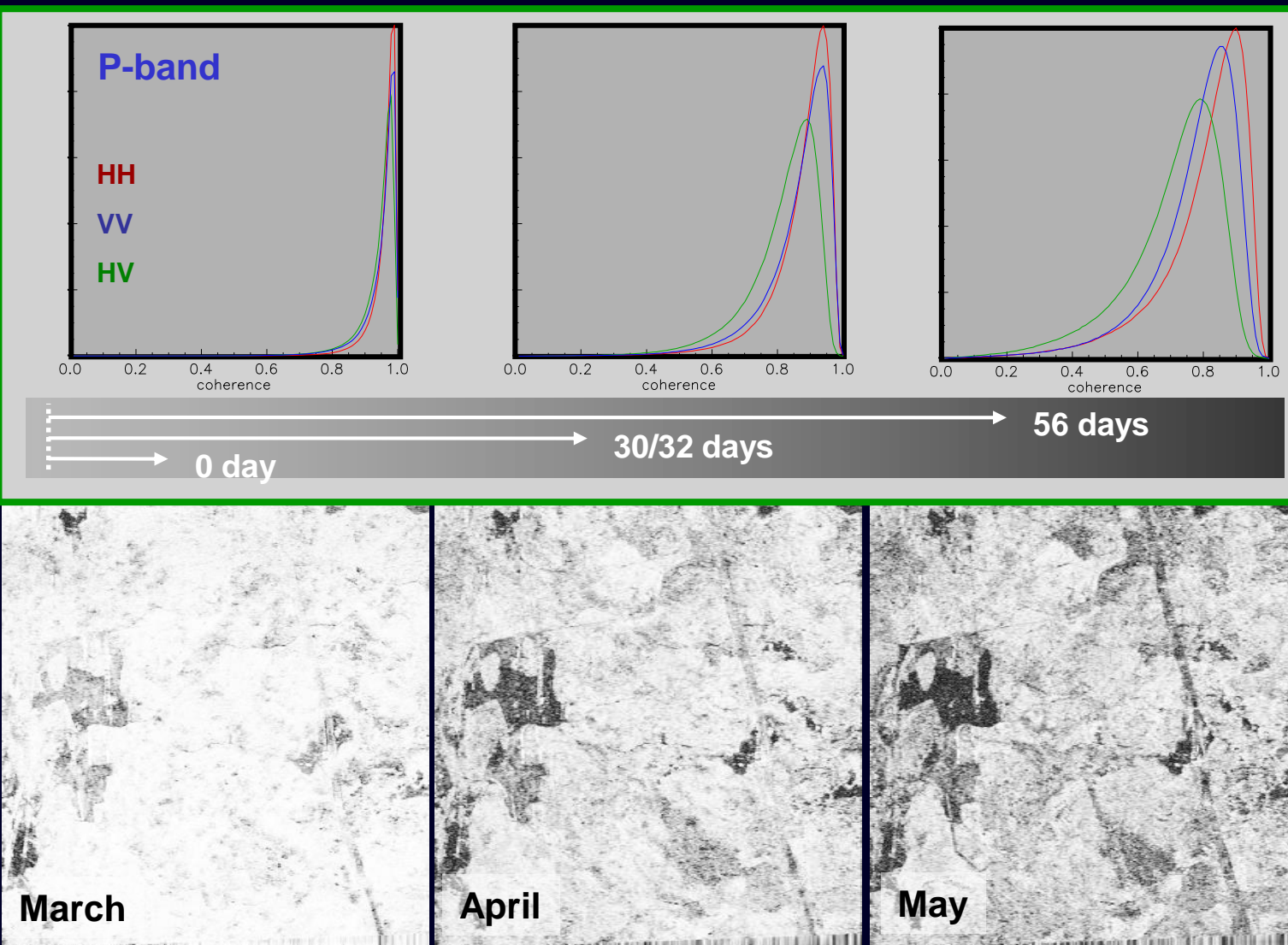
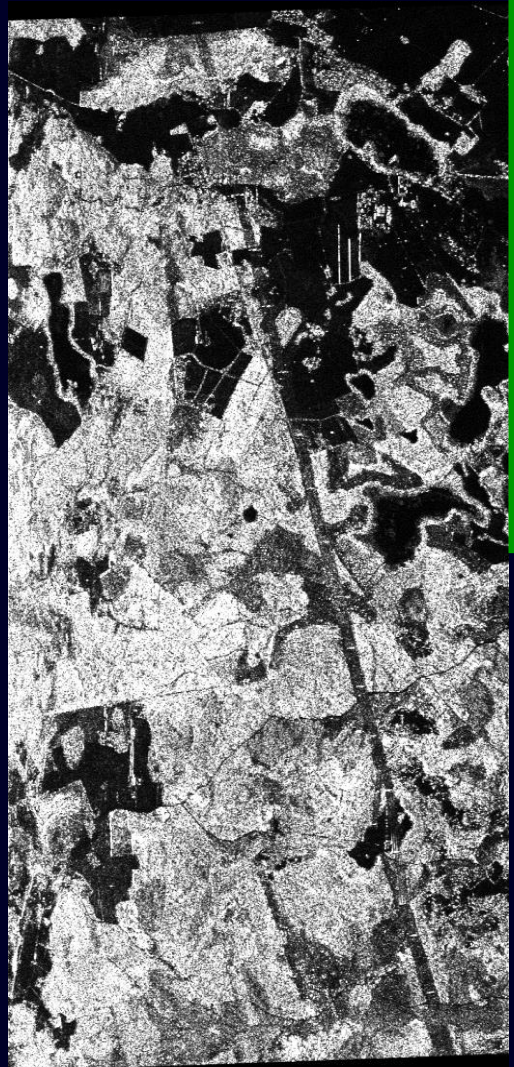
0days

30days

58days



# Remningstorp Test Site: Temporal Decorrelation: P-Band



**HV Amplitude Image**

**0days**

**30days**

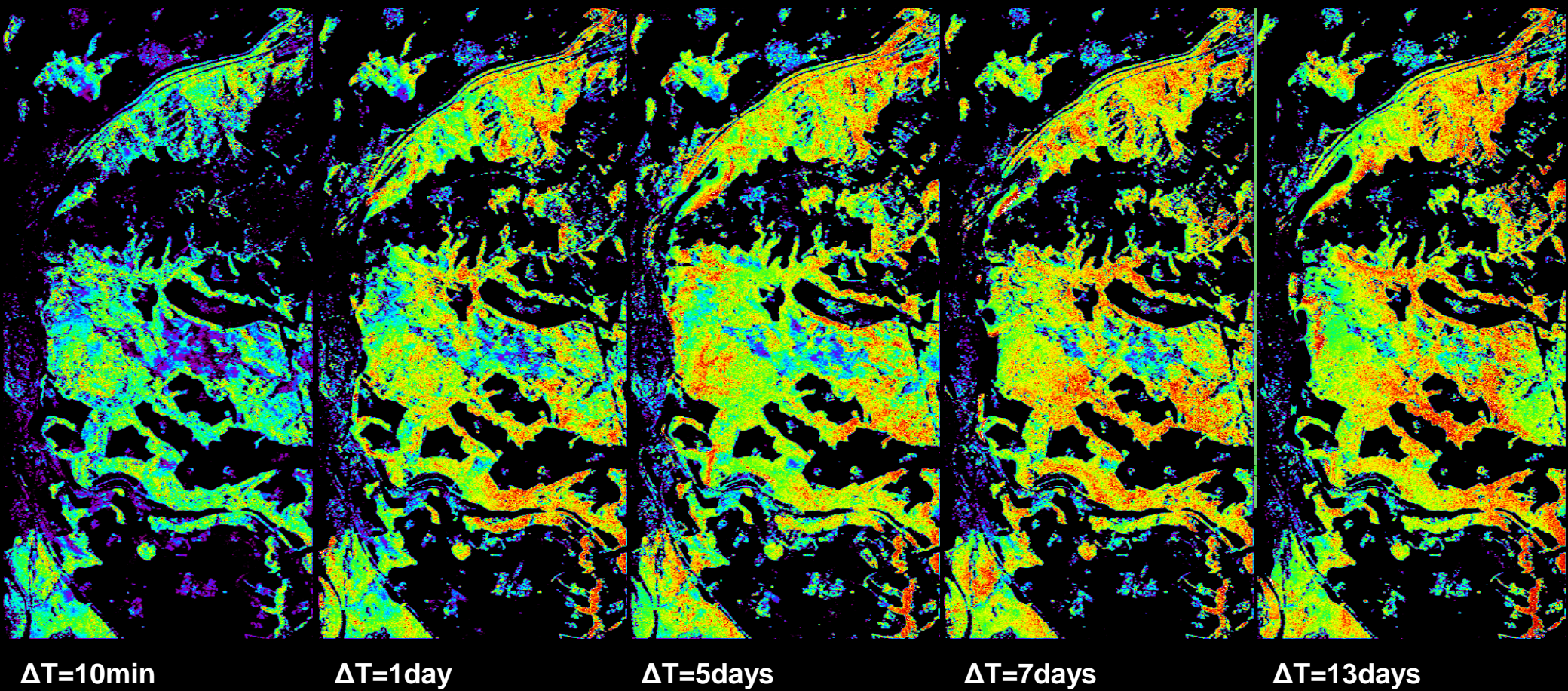
**56days**

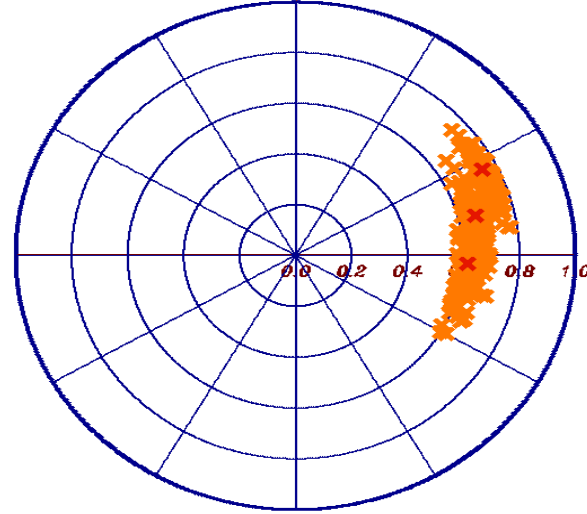
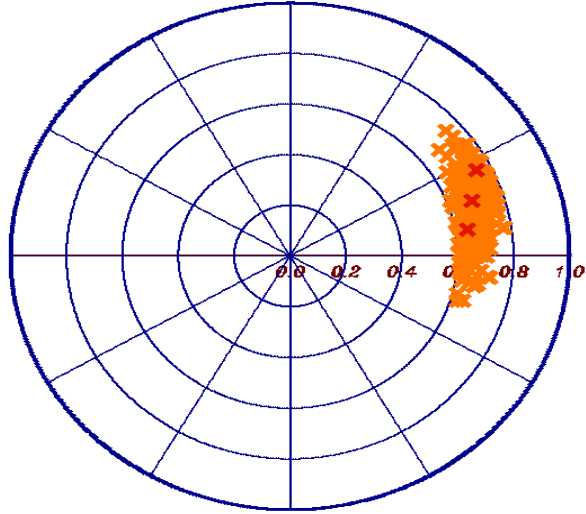
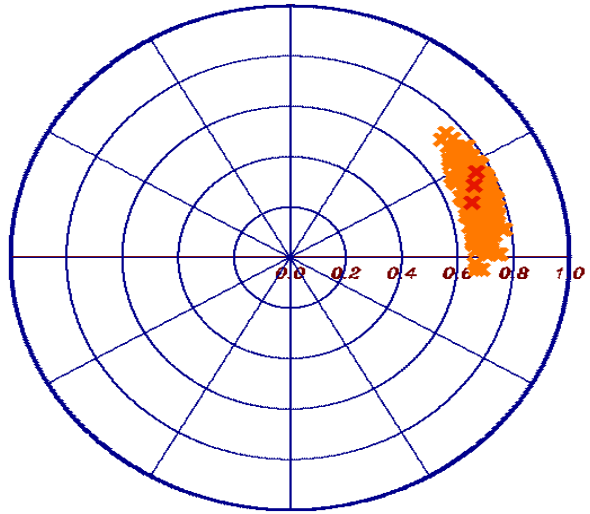


# Traunstein Test Site

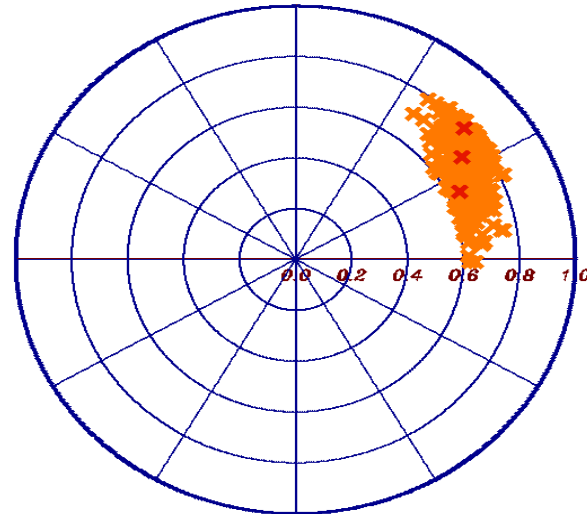
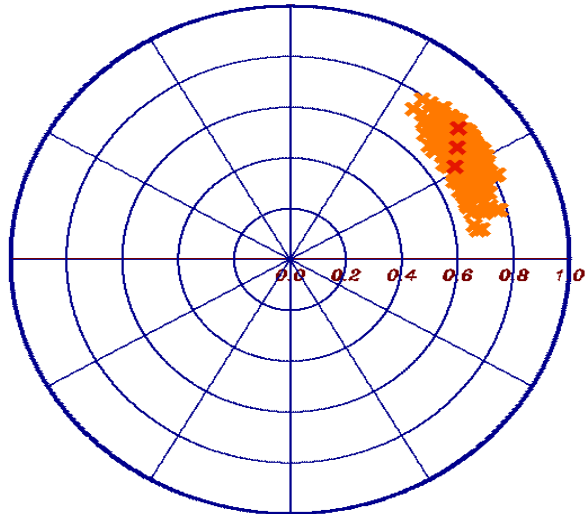
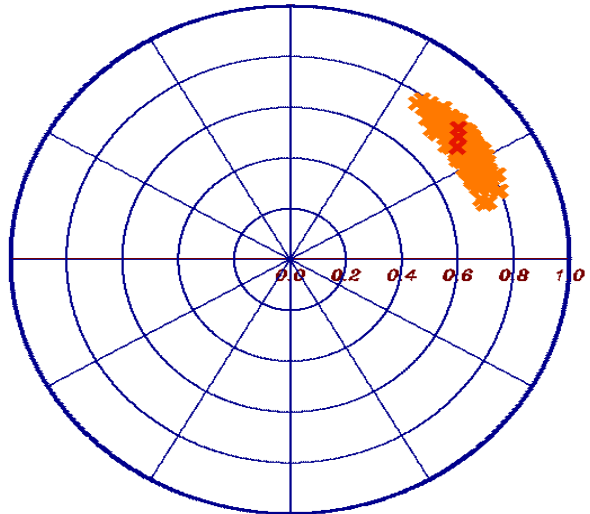
50 40 30 20 10 0m

Forest Height Maps from different Temporal Baselines: 10min-13days

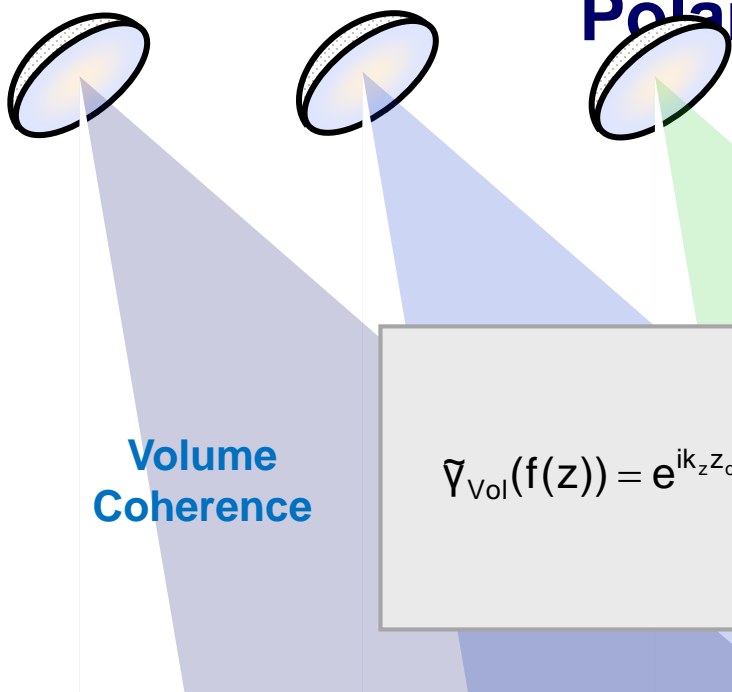




## Polarimetric Coherence Tomography (PCT)

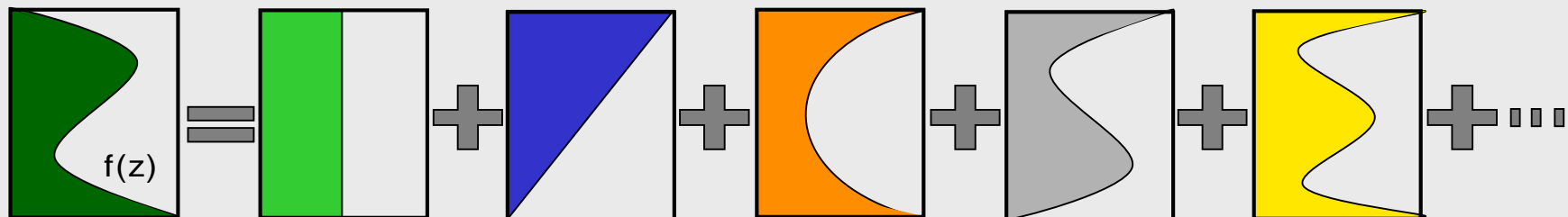
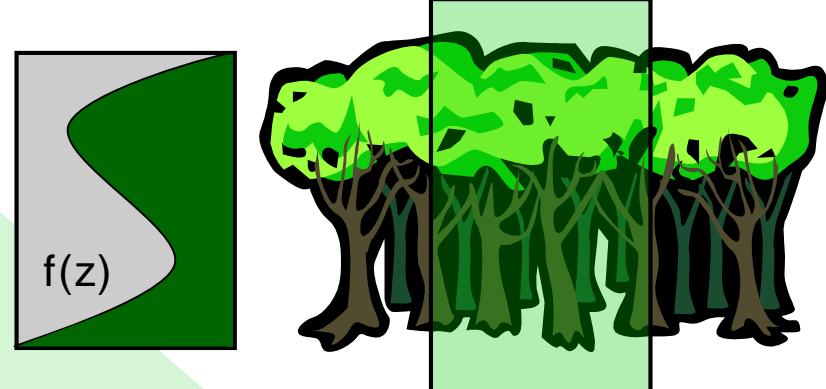


# Polarimetric Coherence Tomography (PCT)



$f(z)$  ... vertical reflectivity function

$$\tilde{\gamma}_{\text{Vol}}(f(z)) = e^{ik_z z_0} \frac{\int_0^{h_v} f(z) e^{ik_z z} dz}{\int_0^{h_v} f(z) dz}$$



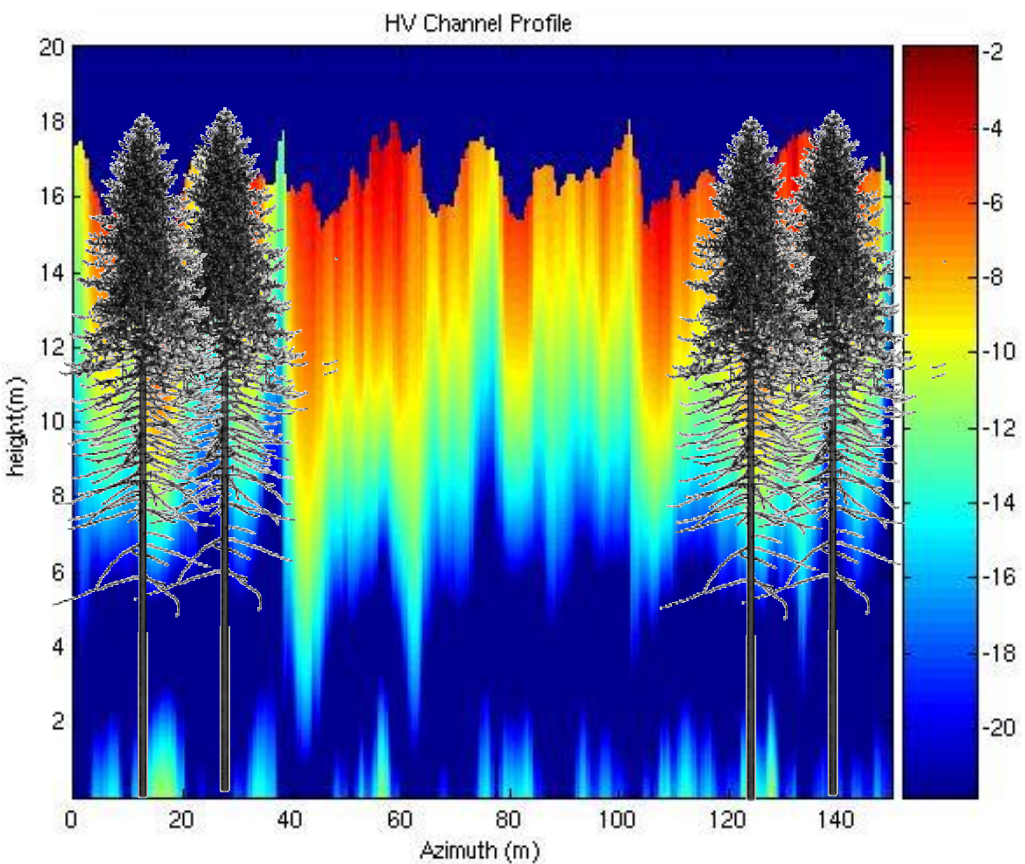
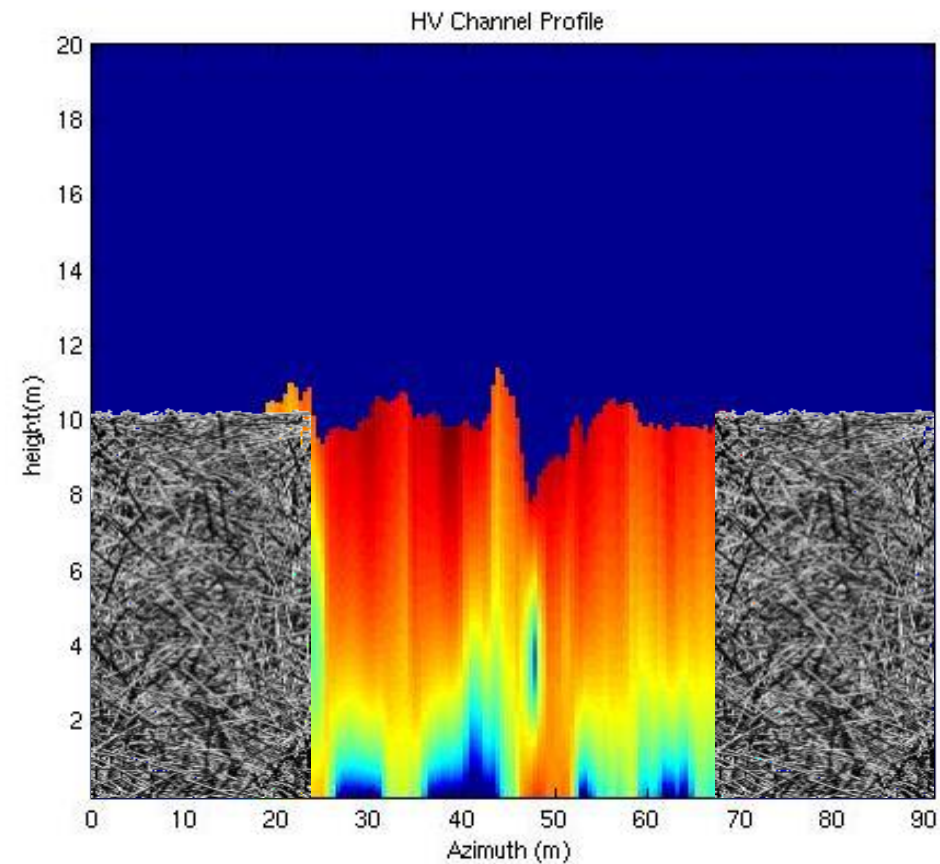
$$\tilde{\gamma}_{\text{Vol}}(f(z)) = e^{ik_z z_0} \frac{\int_0^{h_v} f(z) e^{ik_z z} dz}{\int_0^{h_v} f(z) dz}$$

$$\int_0^{h_v} f(z) e^{ik_z z} dz = \frac{h_v}{2} e^{\frac{i k_z h_v}{2}} \int_{-1}^1 (1 + f(z')) e^{\frac{i k_z h_v}{2} z'} dz'$$

$$\int_0^{h_v} f(z) dz = \frac{h_v}{2} \int_{-1}^1 (1 + f(z')) dz'$$

Fourier Legendre Series:

$$f(z') = \sum_n a_n P_n(z') \quad \text{where} \quad a_n = \frac{2n+1}{2} \int_{-1}^1 f(z') P_n(z') dz'$$



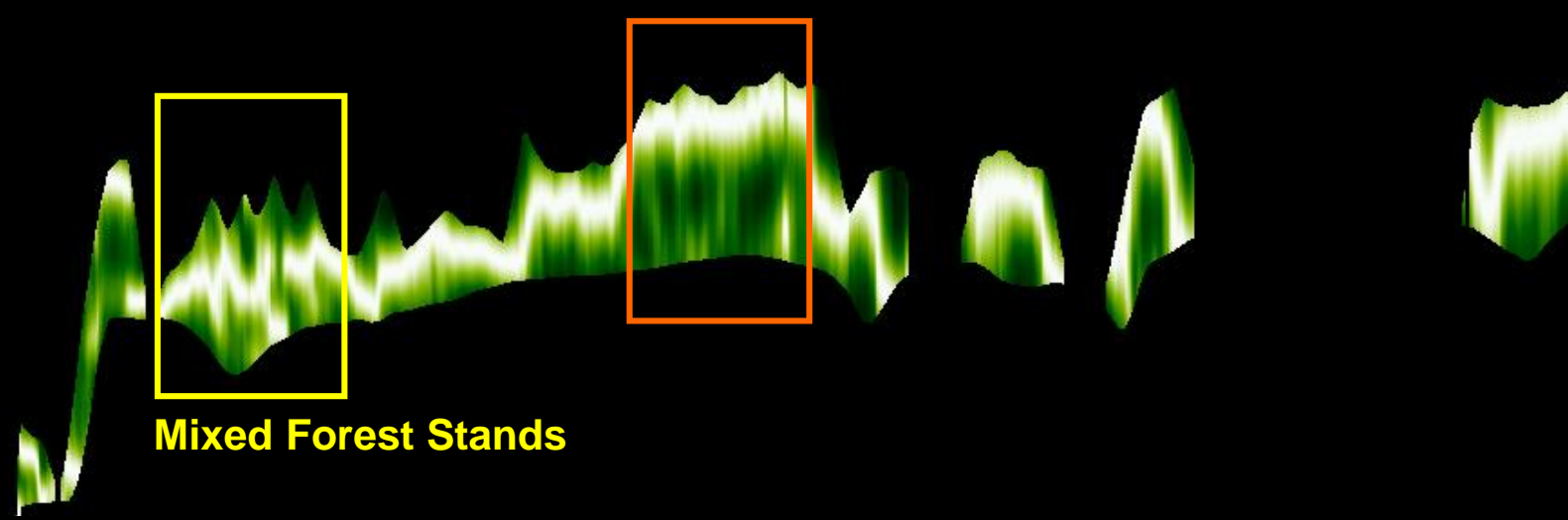
Simulations courtesy of Mark Williams:

S.R. Cloude, D.G. Corr, M.L. Williams, "Target Detection Beneath Foliage Using PolInSAR", Waves in Random Media, vol. 14, pages S393 - S414., 2004



Topo Height [m]

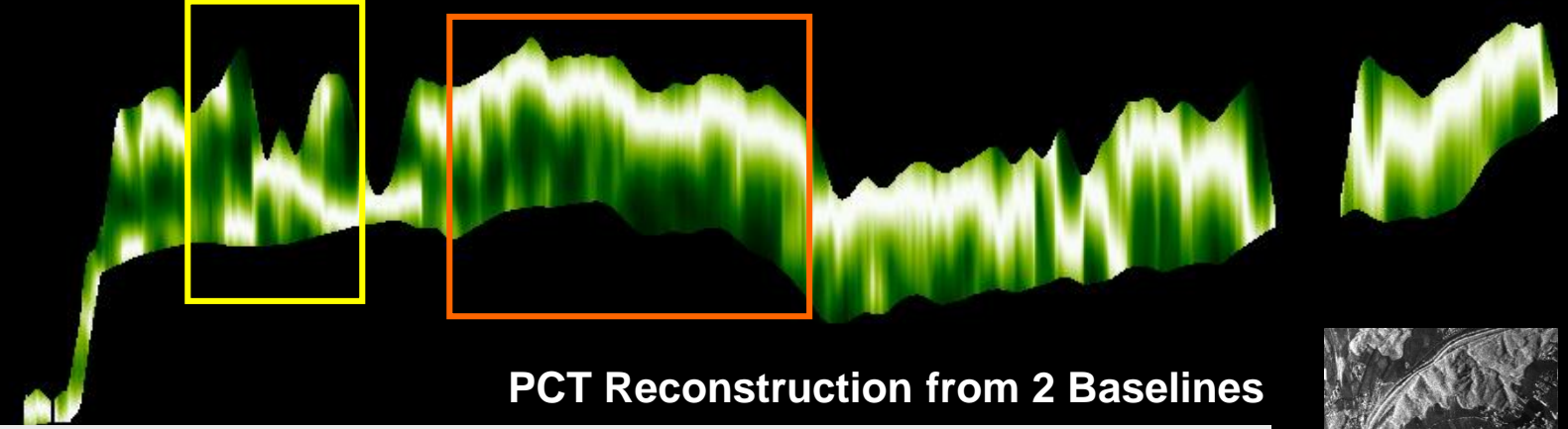
690



Mixed Forest Stands

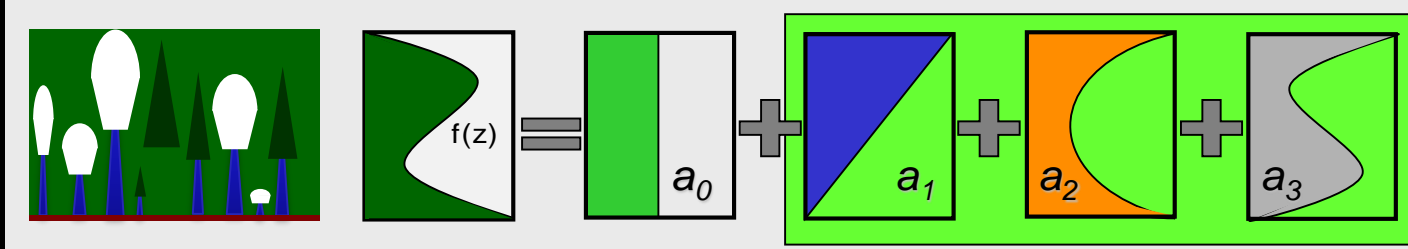
Topo Height [m]

570

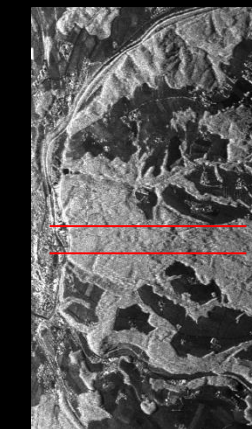


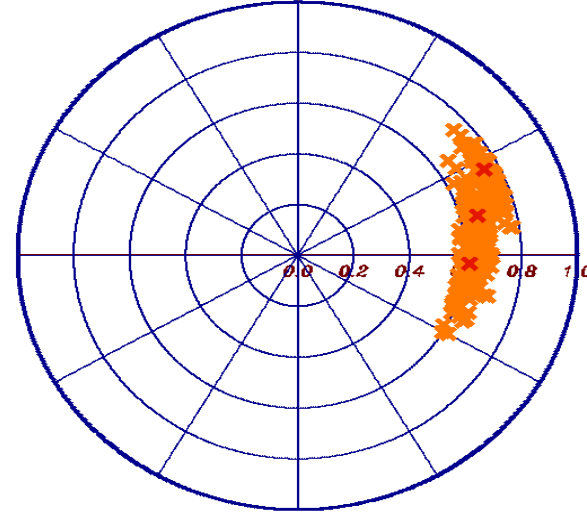
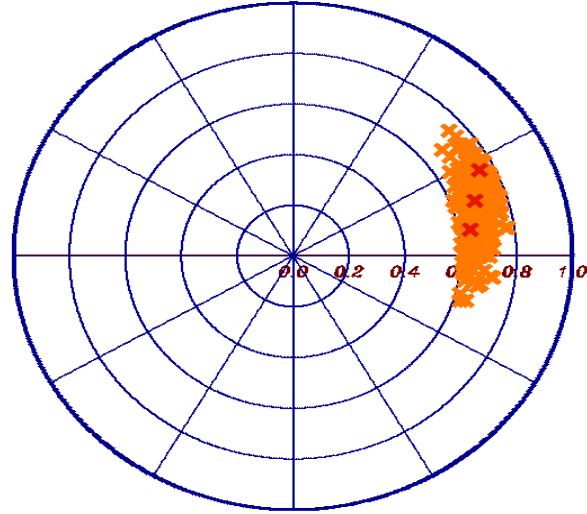
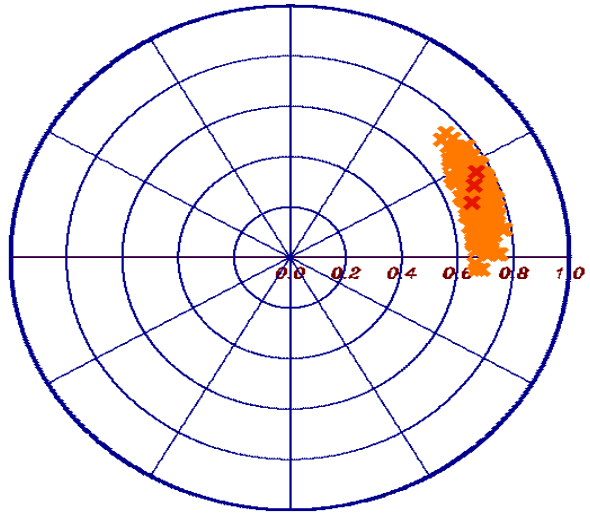
Mature Spruce Stands

PCT Reconstruction from 2 Baselines

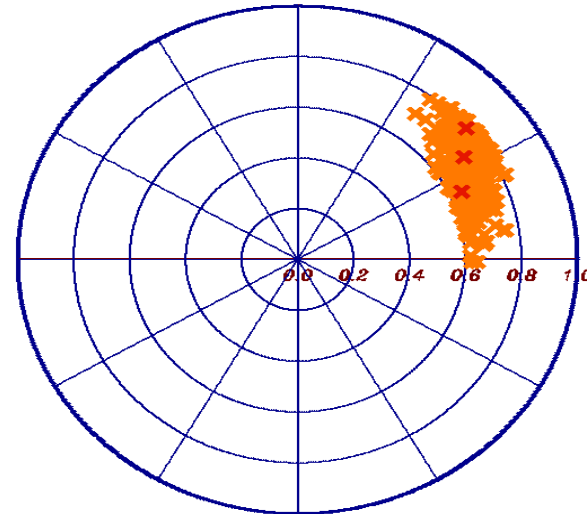
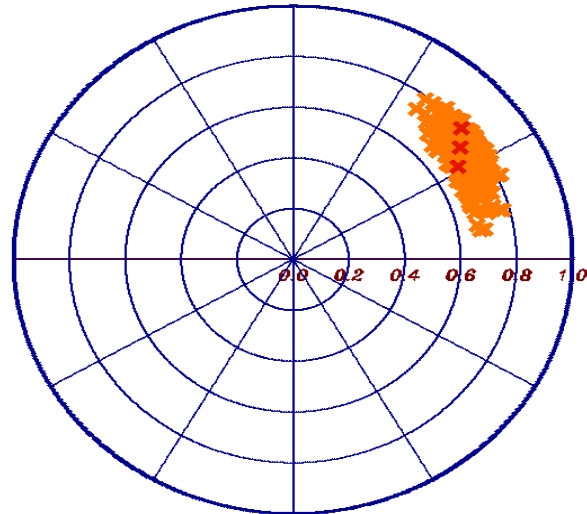
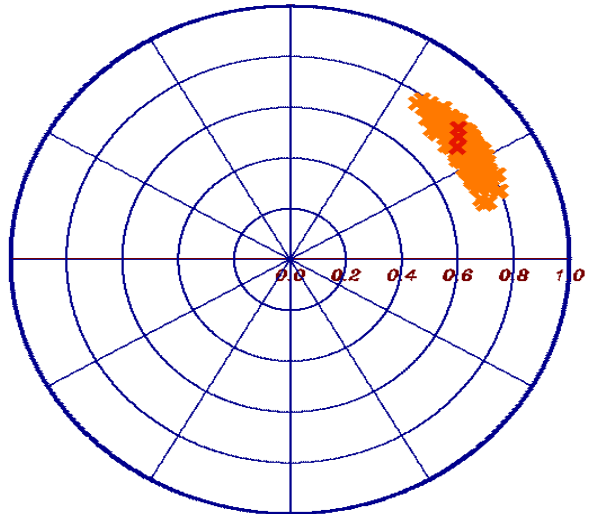


Test site: Traunstein, Germany, L-band @ HV Polarisation

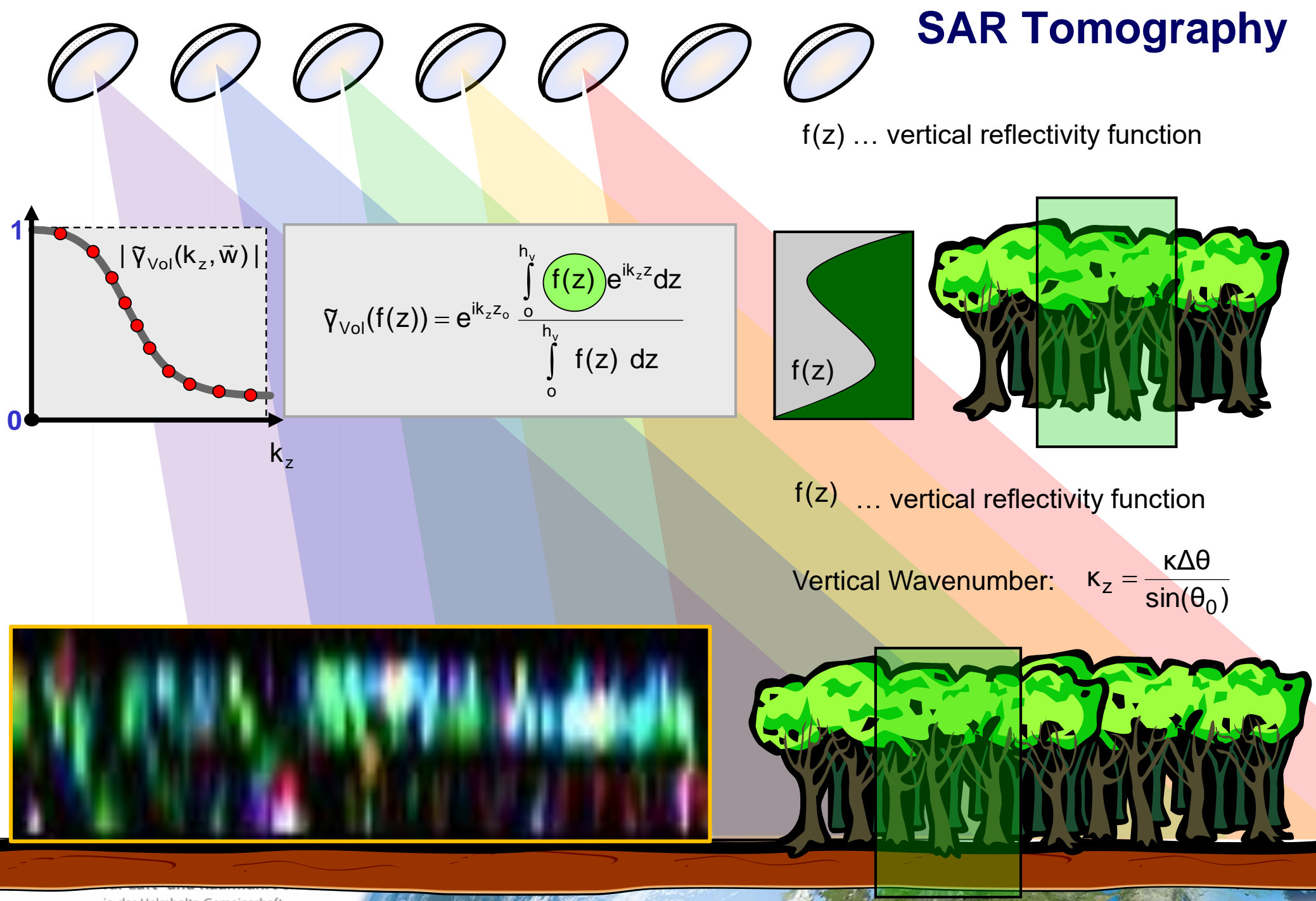


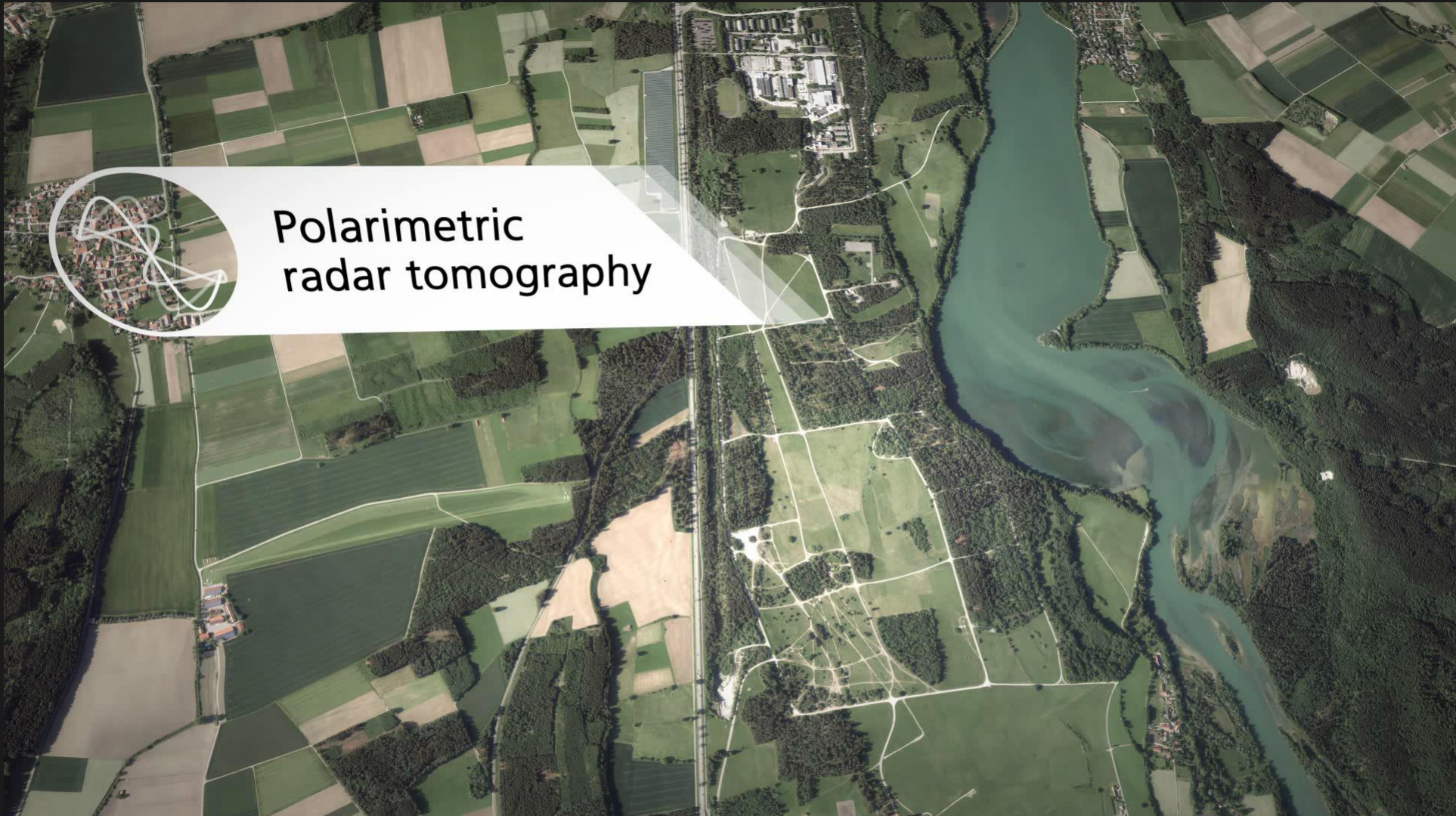


## Polarimetric SAR Tomography (TomoSAR)

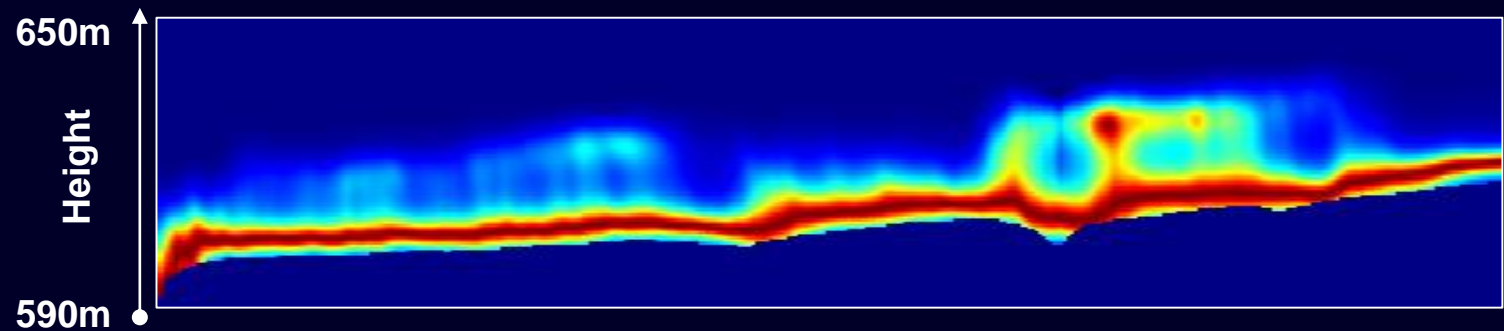
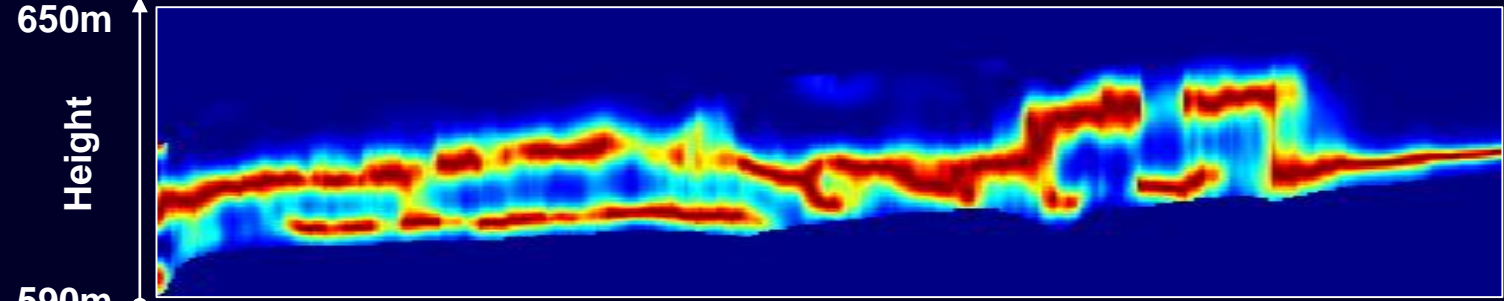
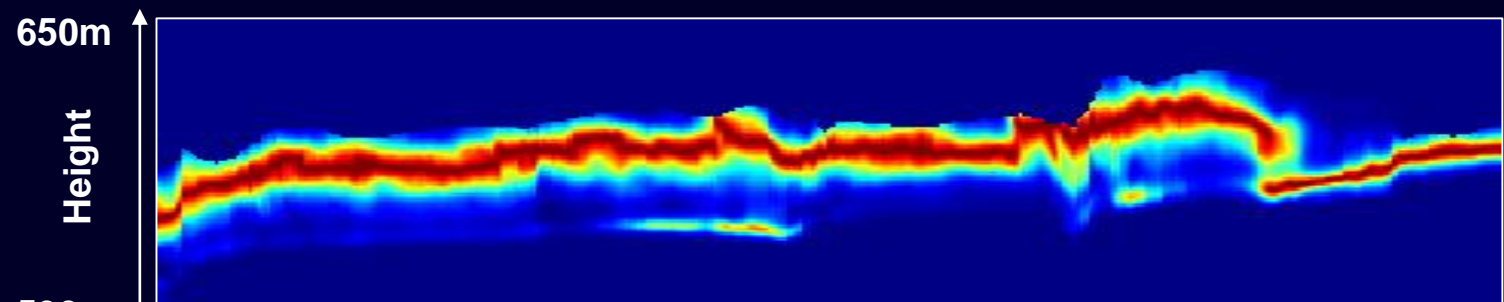
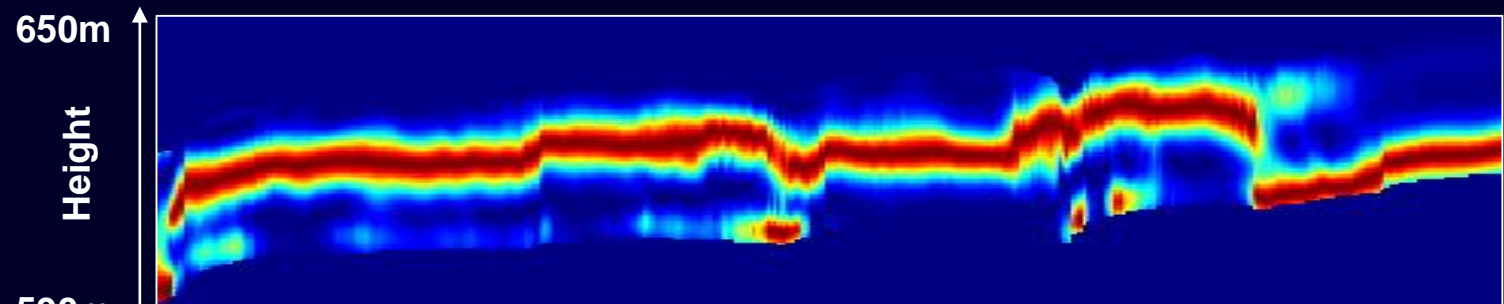


# SAR Tomography



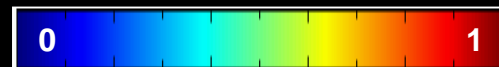


Polarimetric  
radar tomography

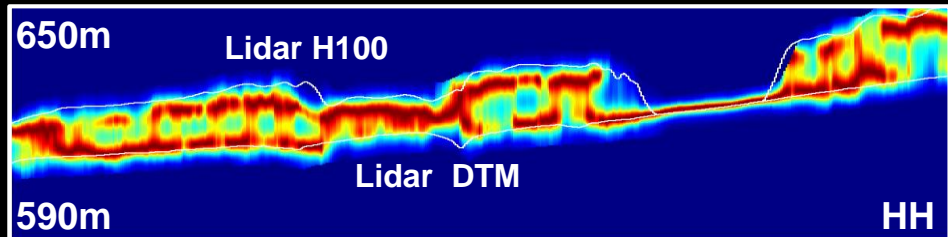
**P-band****L-band****S-band****X-band**

Slant range (0.6Km)

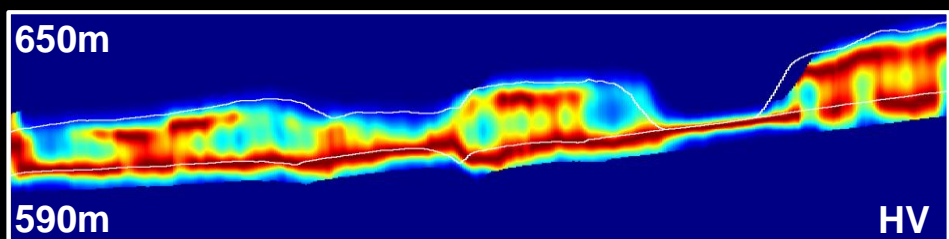
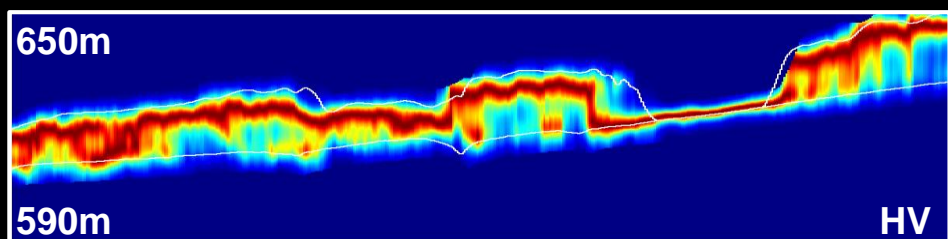
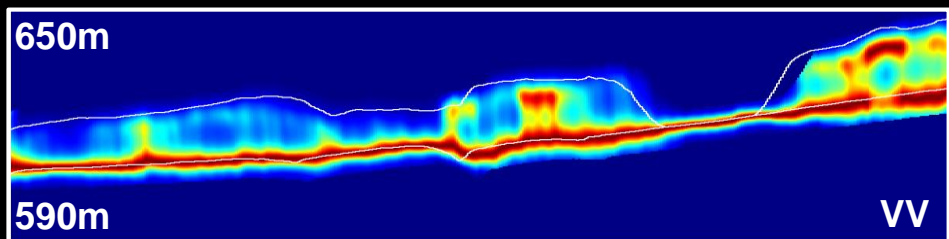
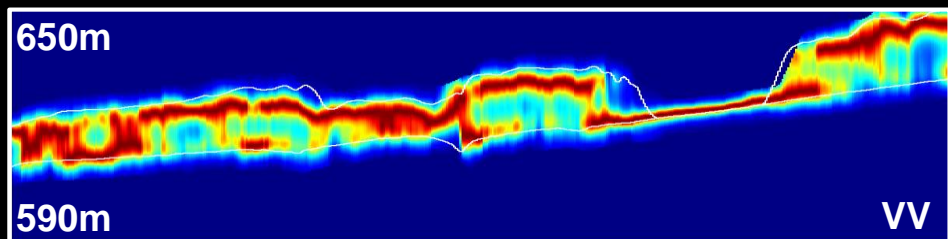
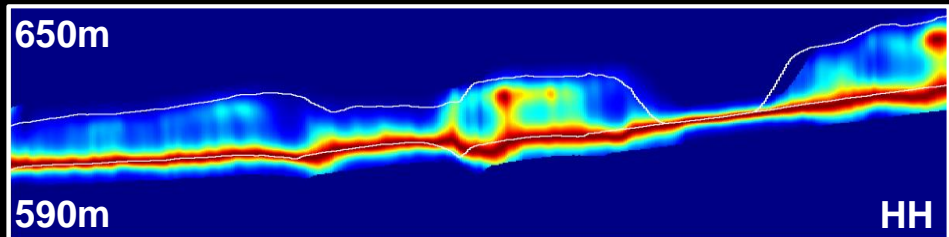
# Dependence on frequency: L- vs P-band



L-band (23cm)



P-band (80cm)



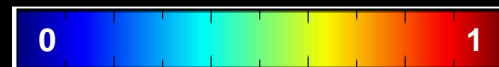
Slant range (~1Km)

Slant range (~1Km)

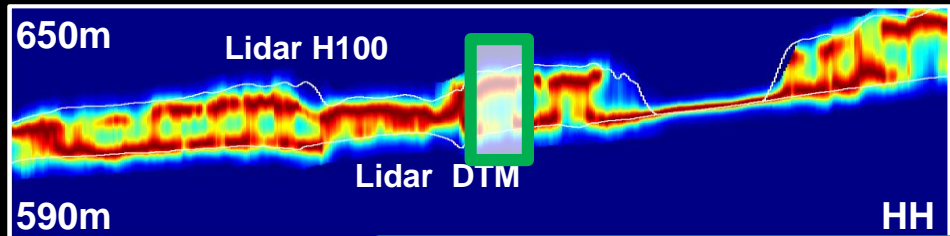


Traunstein site (Germany), 4 tracks L / 5 tracks P, E-SAR, Capon

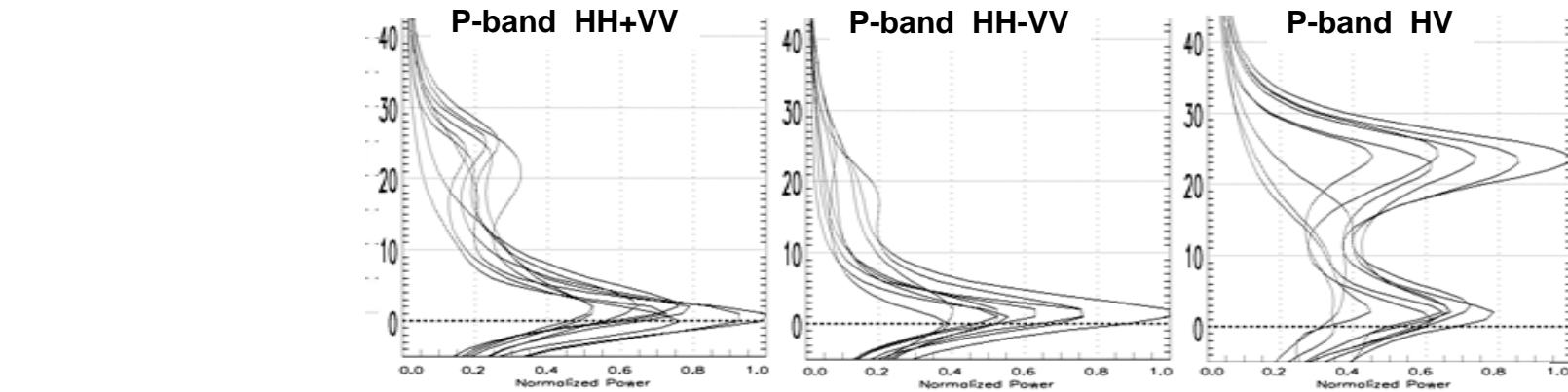
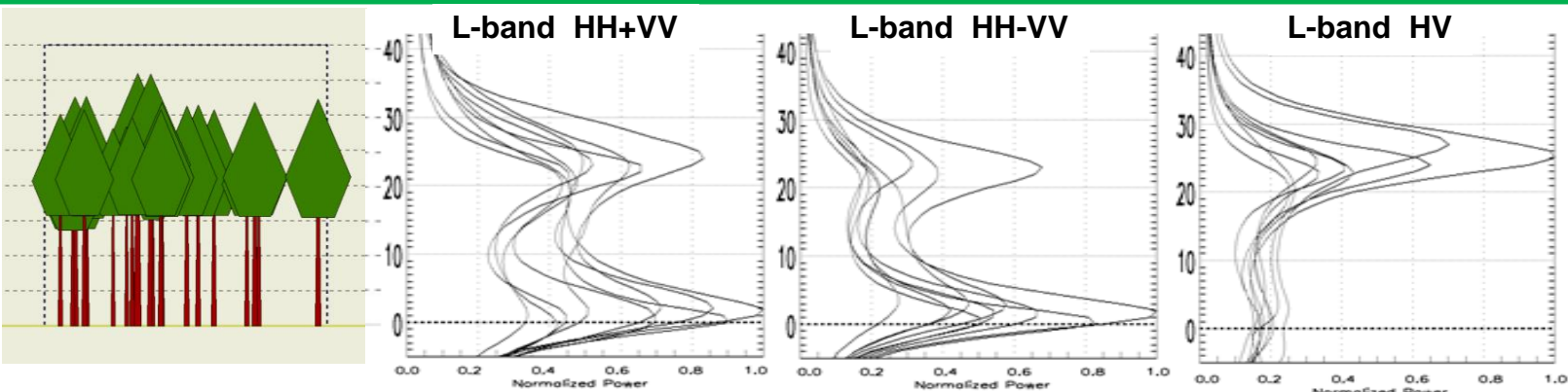
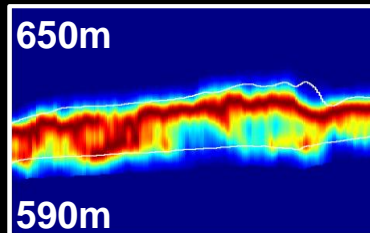
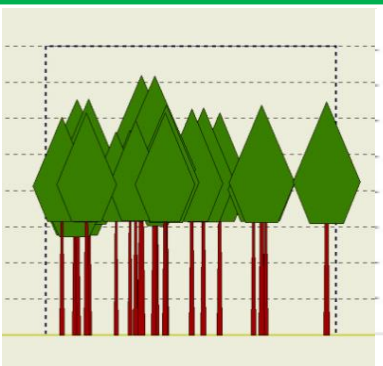
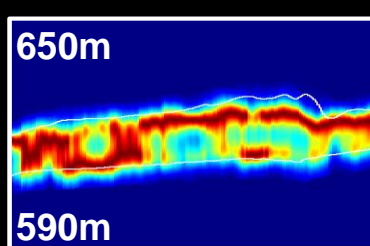
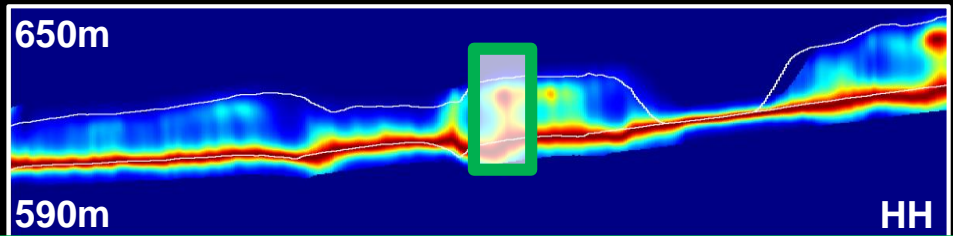
# Dependence on frequency: L- vs P-band



L-band (23cm)

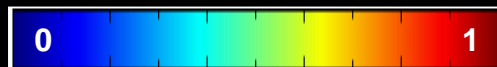


P-band (80cm)

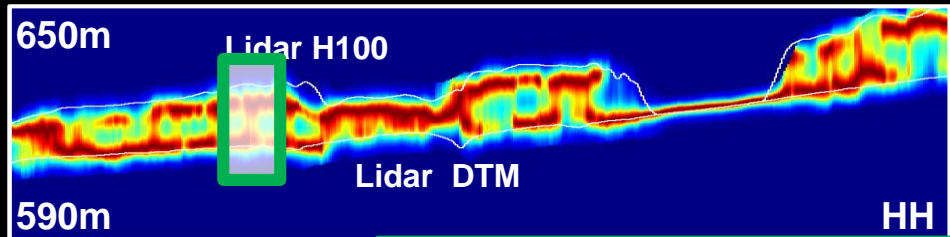


Traunstein site (Germany), 4 tracks L / 5 tracks P, E-SAR, Capon

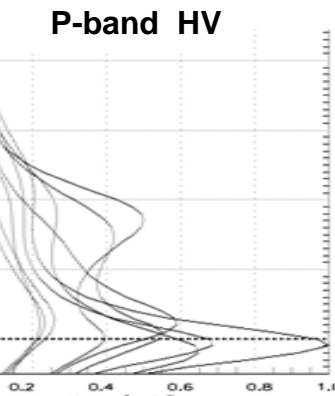
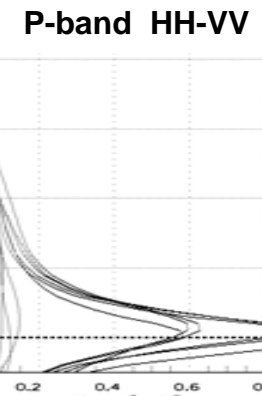
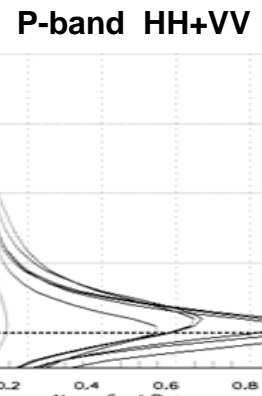
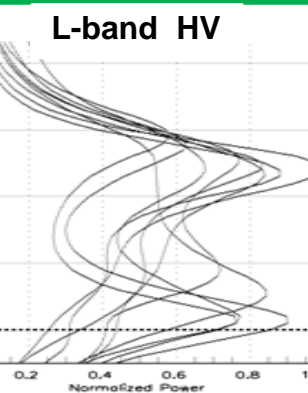
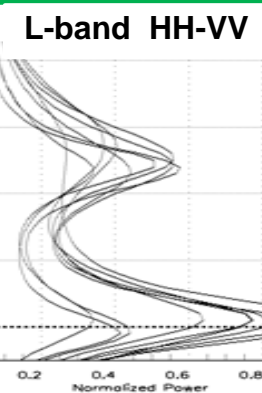
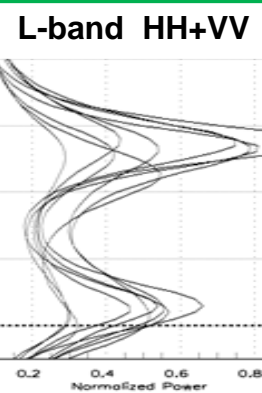
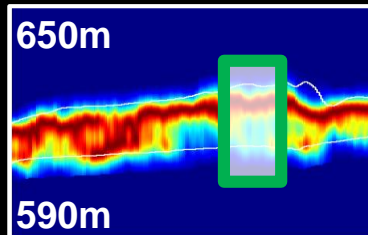
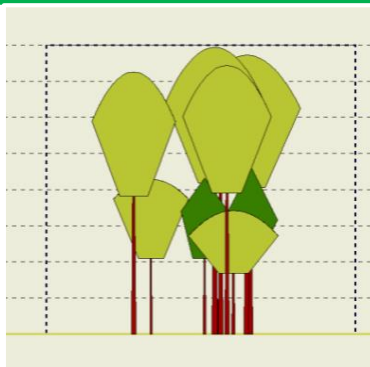
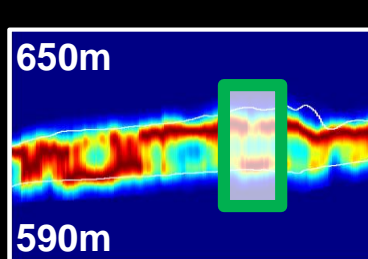
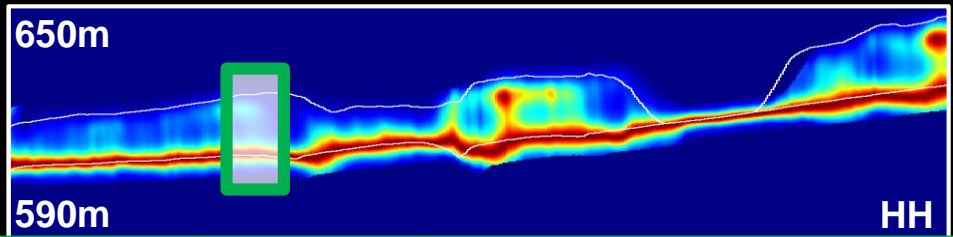
# Dependence on frequency: L- vs P-band



L-band (23cm)

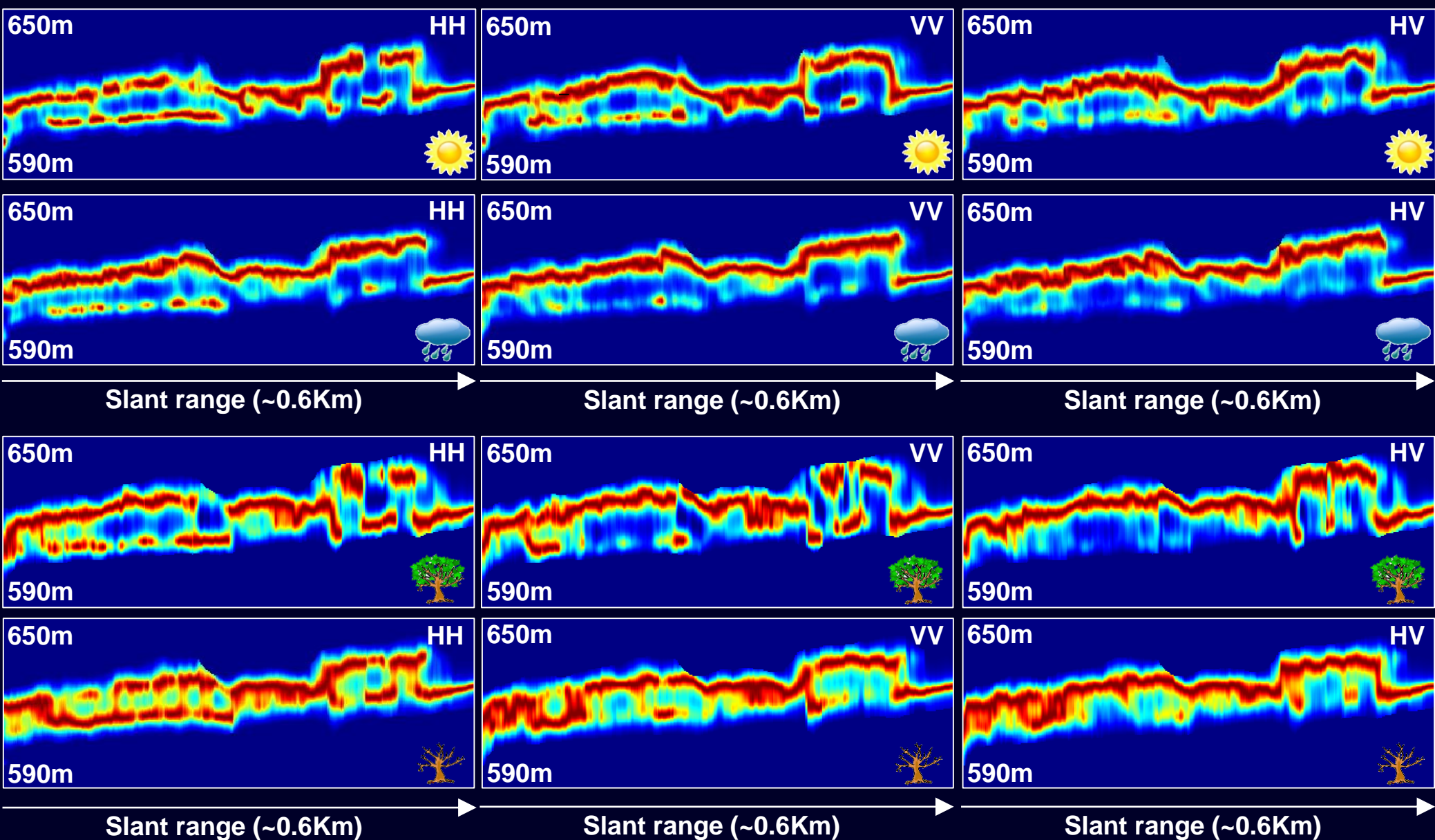


P-band (80cm)



Traunstein site (Germany), 4 tracks L / 5 tracks P, E-SAR, Capon

# Temporal variations at L-band (Capon)

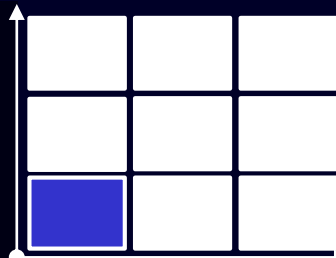
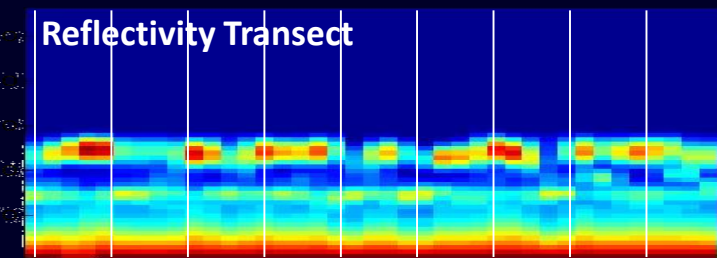
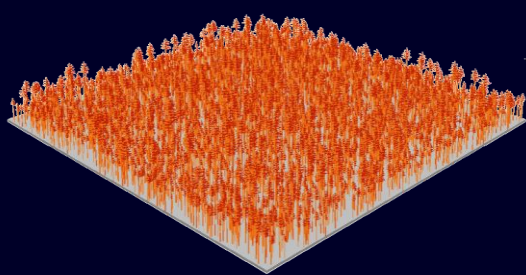


# Forest Structure Characterisation

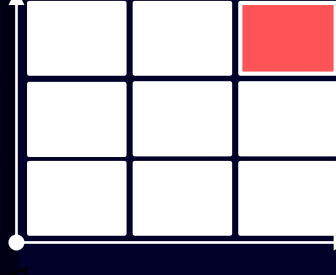
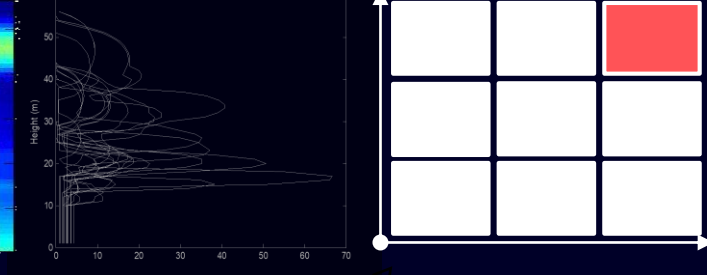
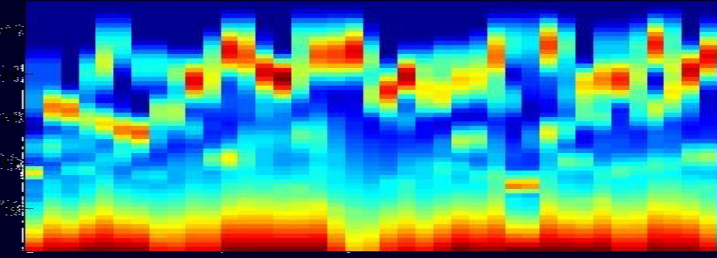
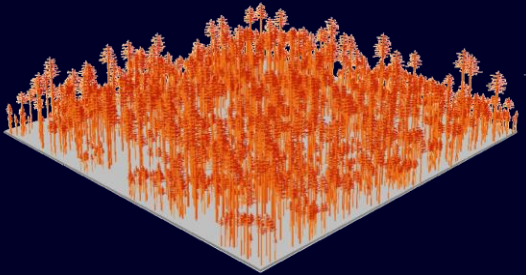


Helmholtz Alliance:  
Remote Sensing and Earth System Dynamics

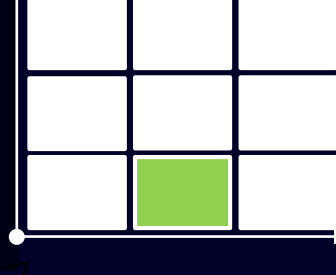
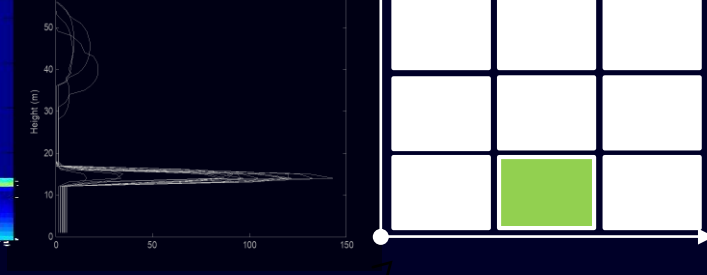
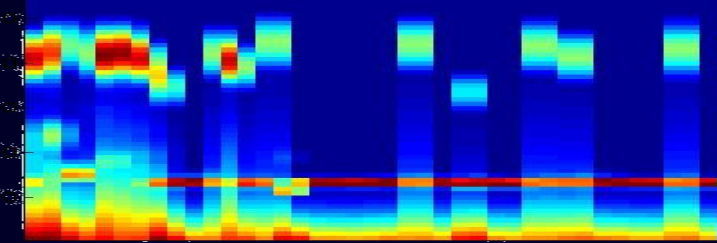
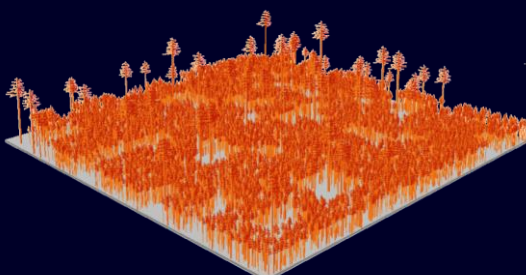
## ► Young forest, 50 years old



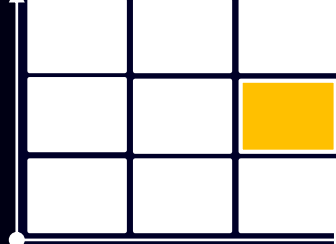
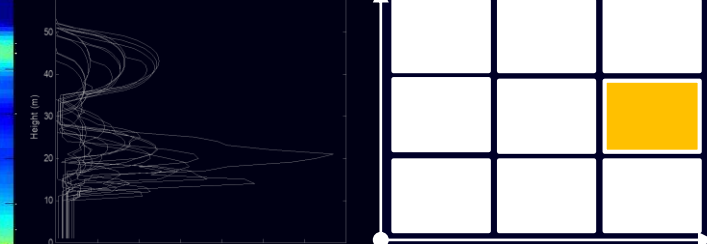
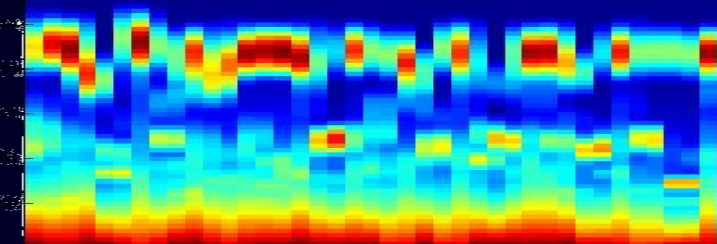
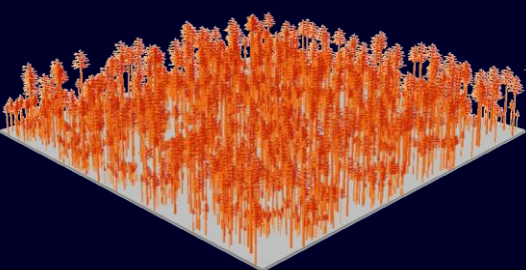
## ► Old forest, 500 years old

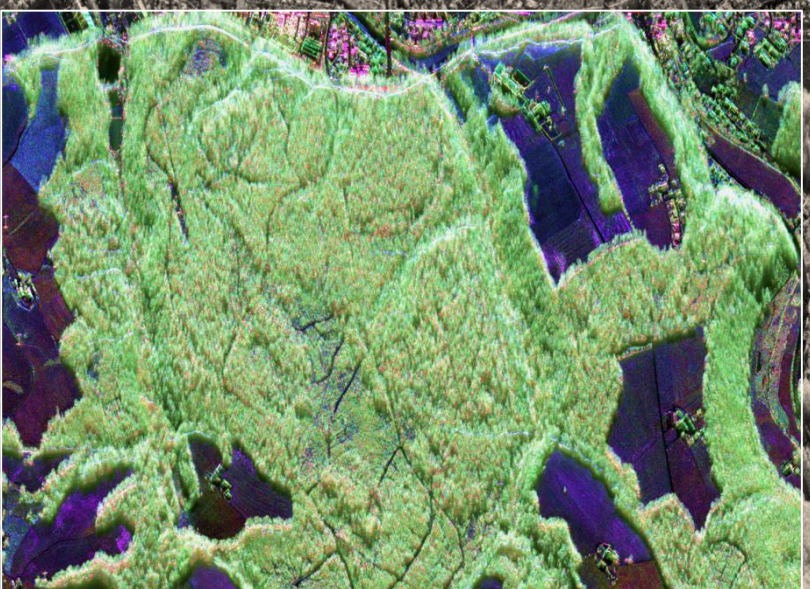


## ► Old forest, 10 years after a fire event

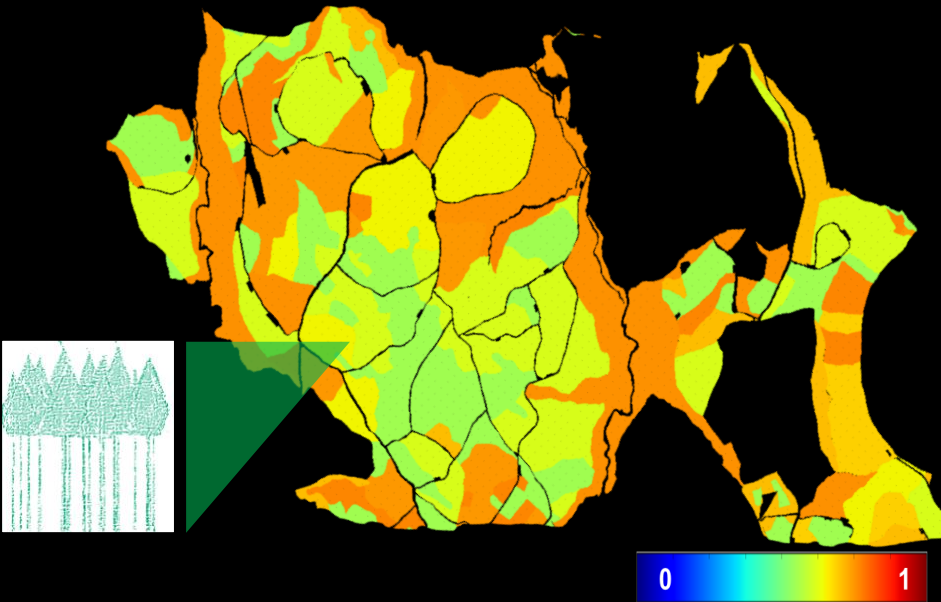


## ► Old forest, 200 years after a fire event

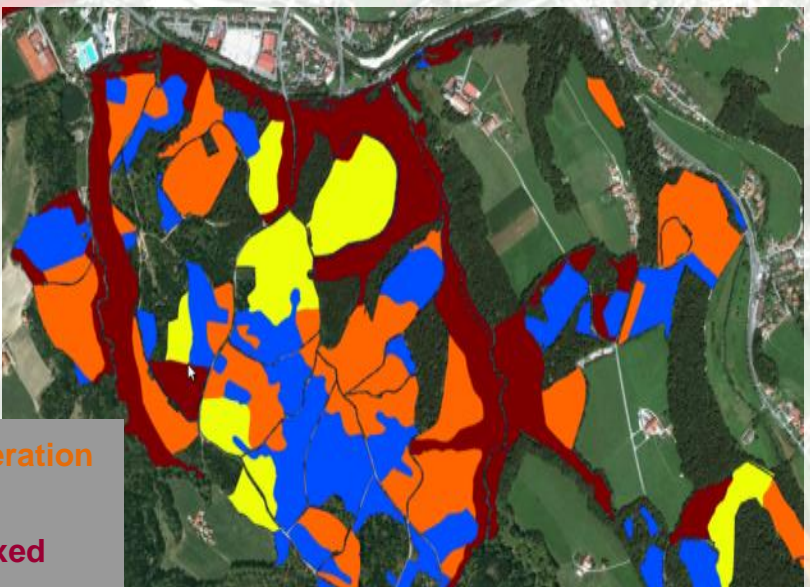




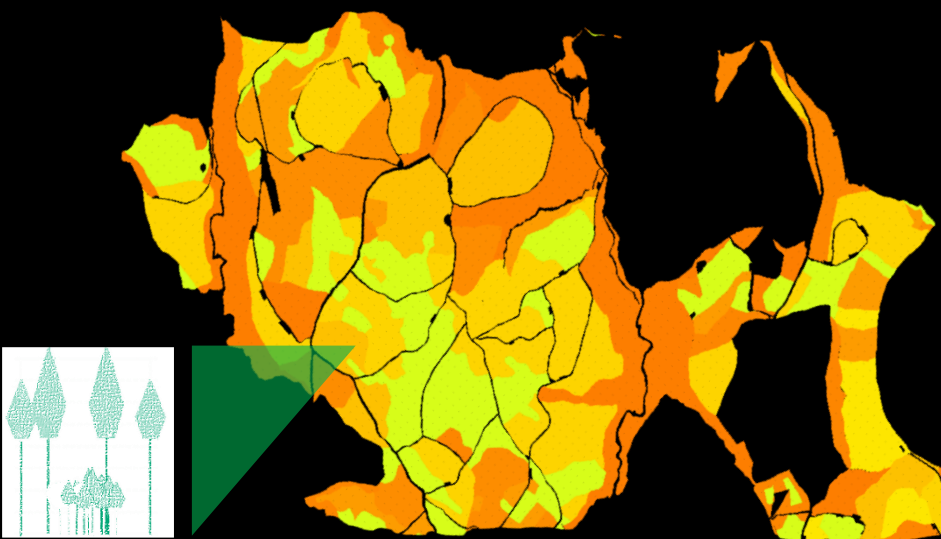
Vertical structure CM (Radar 2008)



Vertical structure CM (Radar 2012)

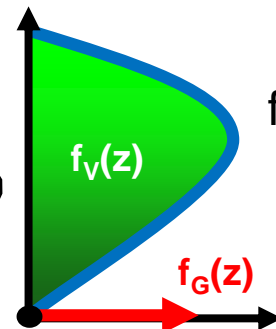
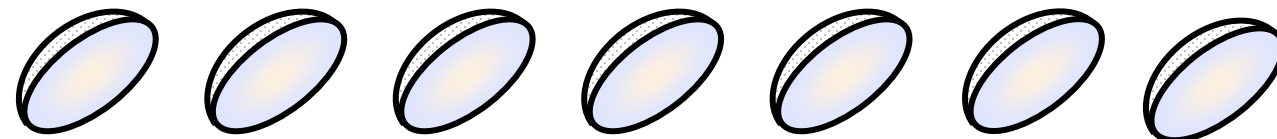


Regeneration  
Mature  
Old-mixed  
Young



Forest Structure Classification (25x25 m): Traunstein, Germany, 2008 / 2012

# SAR Tomography ... beyond profiles



Ground Layer Volume Layer

$$f(z) = P_G f_G(z) + P_V f_V(z)$$

Single-pol coherences

$$R = P_G \Gamma_G + P_V \Gamma_V$$

Assumption :  $f_G(z) = \delta(z - z_G)$

$P_G, P_V$  : backscattering powers (single-pol)

$\Gamma_G, \Gamma_V$  : multi-baseline coherence matrices

From single-pol to full-pol, Random volume assumption:

$$R_P = C_G \otimes \Gamma_G + C_V \otimes \Gamma_V$$

Sum of Kronecker Products (SKP)

$C_G, C_V$  : polarimetric covariance matrices

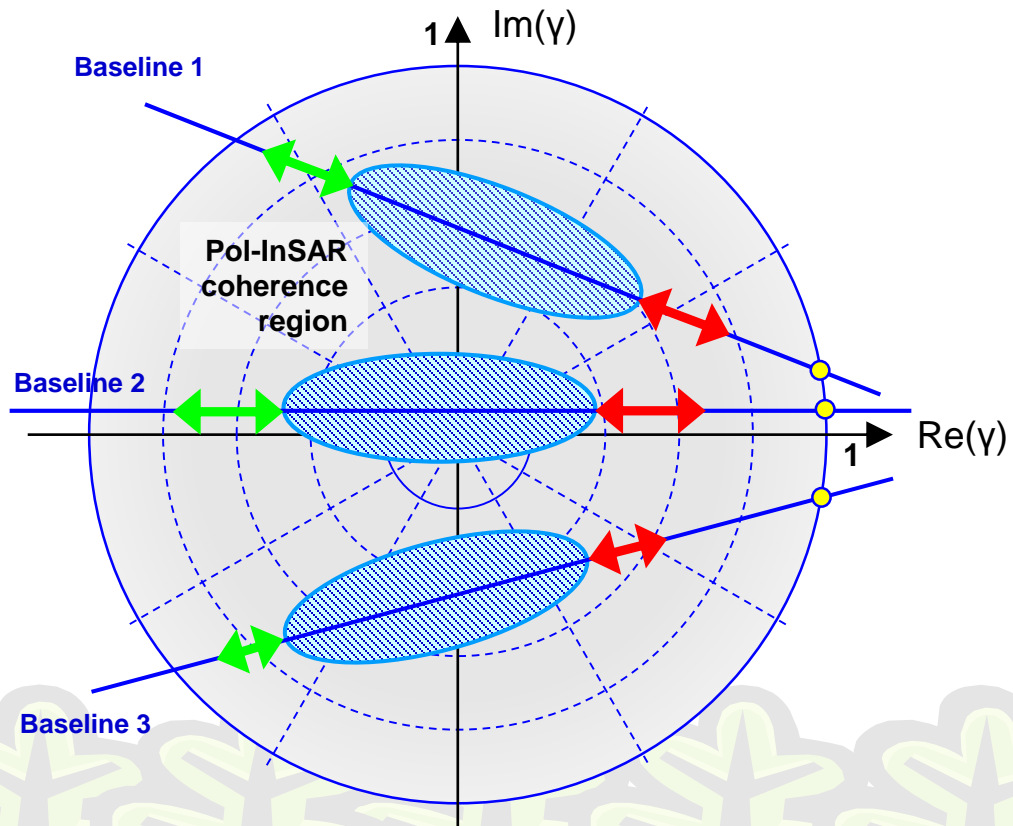
In both single and multi polarimetric cases, even under an RVoG assumption and independently on the number of baselines, the separation of ground / volume InSAR coherences and polarimetric covariances does not admit a unique solution !!

[T. Marzetta, IEEE-Proc. 1983 – S. Tebaldini, IEEE-TGARS 2009]



# The Sum-of-Kronecker-Products

- It extends Pol-InSAR concepts to TomoSAR
- Based on simple algebraic tools



$$\mathbf{R}_P = \mathbf{C}_G \otimes \Gamma_G + \mathbf{C}_V \otimes \Gamma_V$$

Sum of Kronecker Products (SKP)

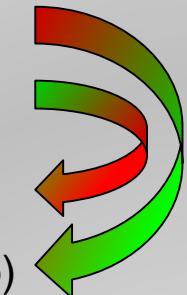
$$\hat{\Gamma}_{G,V}, \hat{\mathbf{C}}_{G,V} = \arg \min_{\Gamma_{G,V}, \mathbf{C}_{G,V}} \| \mathbf{R}_P - [\mathbf{C}_G \otimes \Gamma_G + \mathbf{C}_V \otimes \Gamma_V] \|_F^2$$

$$\Gamma_G = a \mathbf{R}_1 + (1 - a) \mathbf{R}_2$$

$$\Gamma_V = b \mathbf{R}_1 + (1 - b) \mathbf{R}_2$$

$$\mathbf{C}_G = [(1 - b) \mathbf{C}_1 - b \mathbf{C}_2] / (a - b)$$

$$\mathbf{C}_V = [-(1 - a) \mathbf{C}_1 + a \mathbf{C}_2] / (a - b)$$



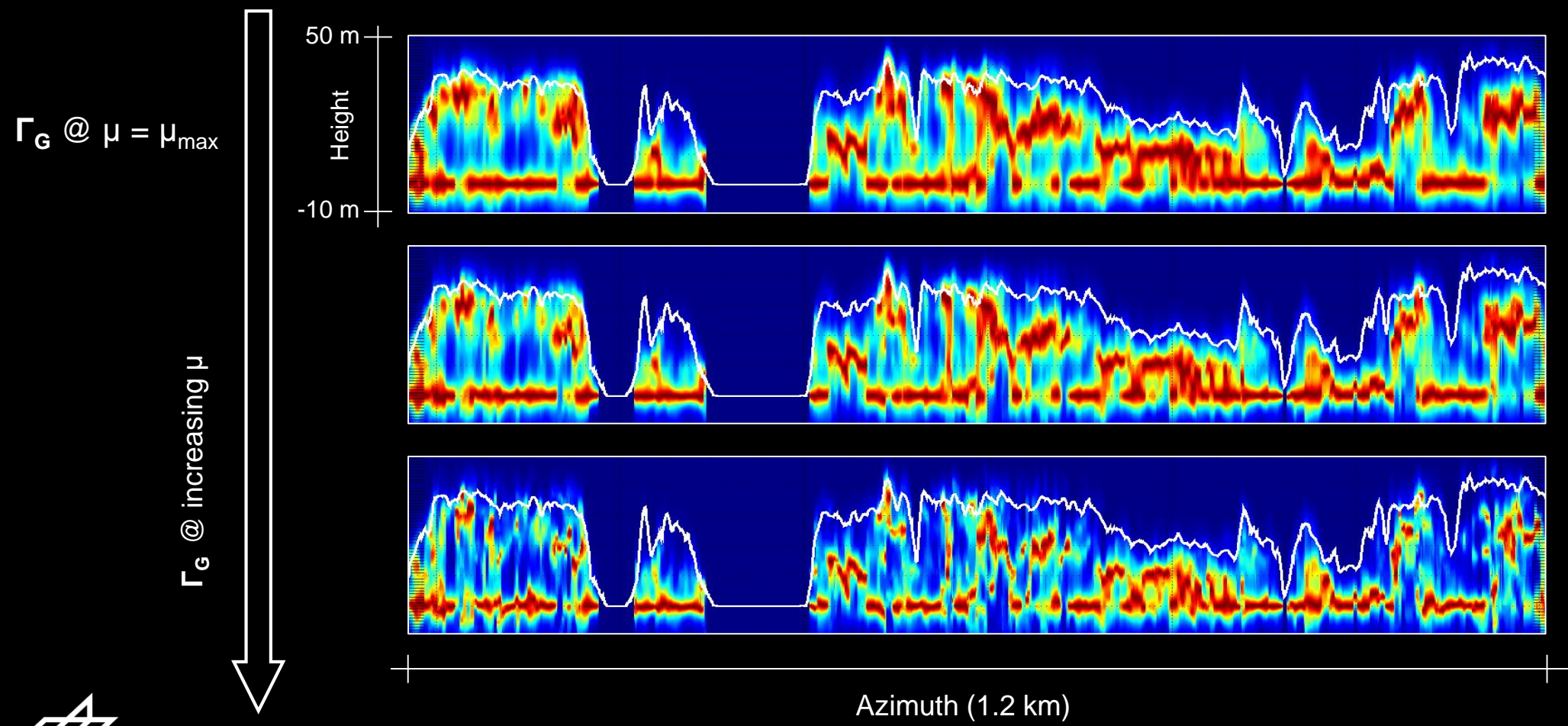
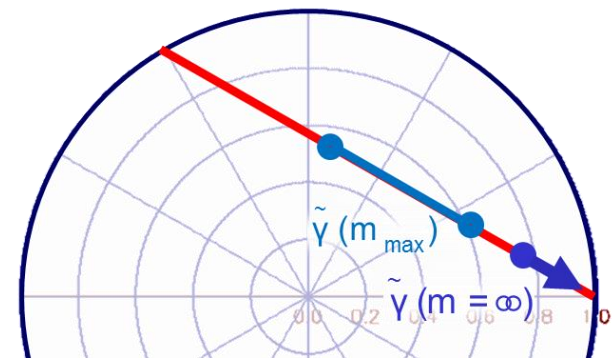
$\mathbf{R}_1, \mathbf{R}_2$  from SVD of a permutation of  $\mathbf{R}_P$

(a,b) are free parameters, bounded in order to provide positive (semi-)definite matrices

- It is an unconstrained Least Squares fitting, with no additional external knowledge
- The separation ambiguity is transferred to two unknowns scalar parameters

# Ground solutions

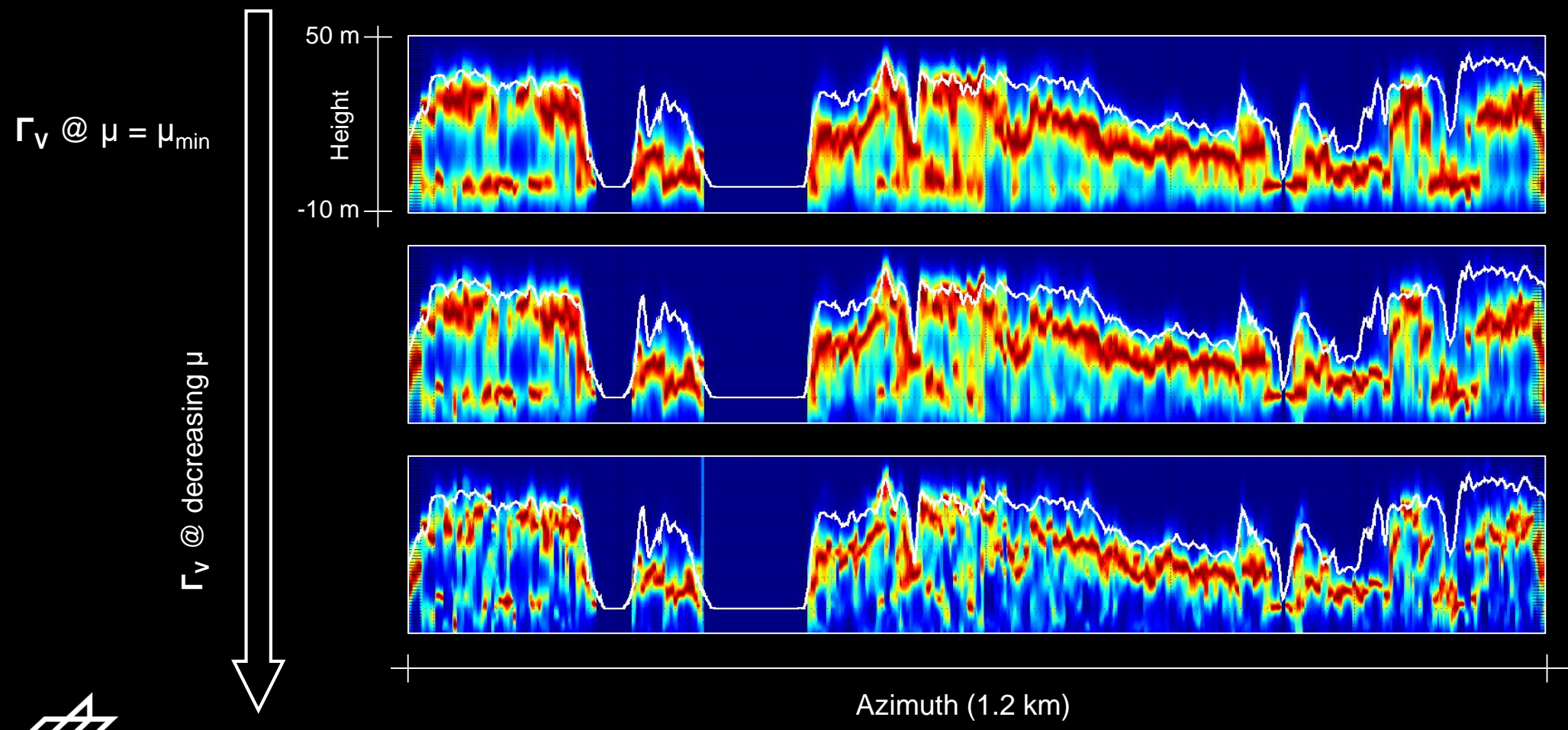
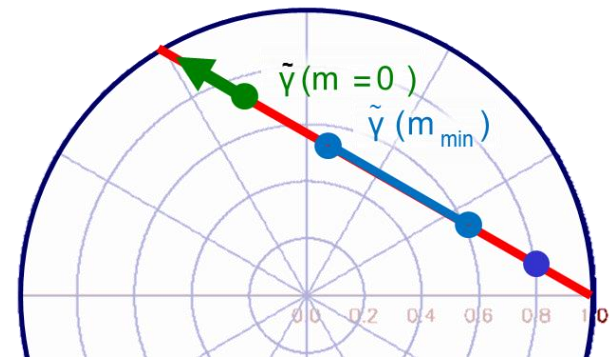
All the feasible ground coherence matrices are on the Pol-InSAR line segments outside the coherence region, under the positive (semi-)definiteness constraint.



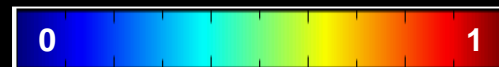
Traunstein forest (south of Germany) – L band – DLR's E-SAR, 7 tracks – Capon

# Volume solutions

All the feasible volume coherence matrices are on the Pol-InSAR line segments outside the coherence region, under the positive (semi-)definiteness constraint.

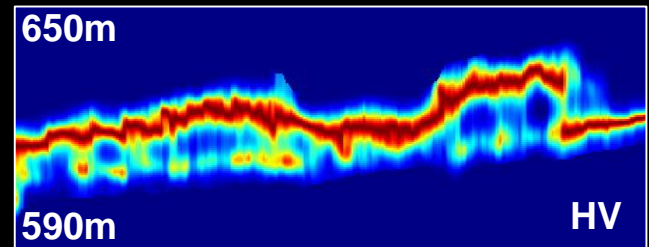
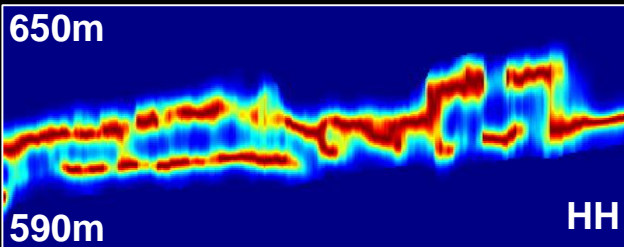


# Dependence on polarization & frequency

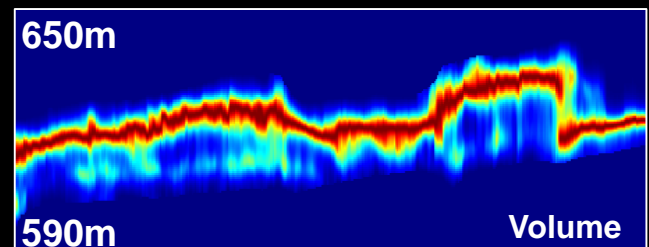
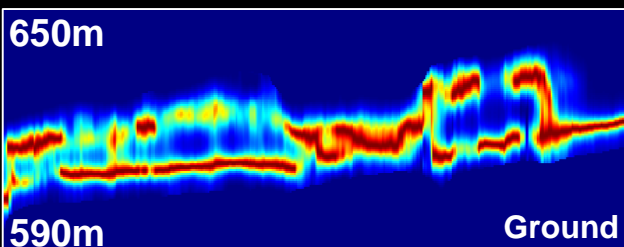


L-band

Lexicographic basis  
HH vs HV



Maximum ground vs  
Maximum volume

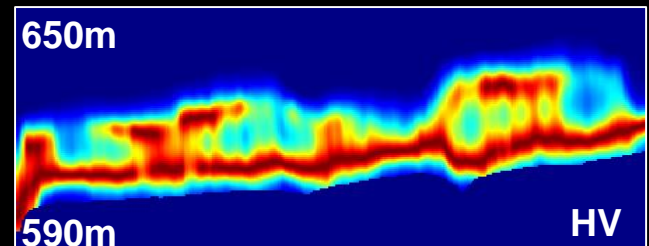
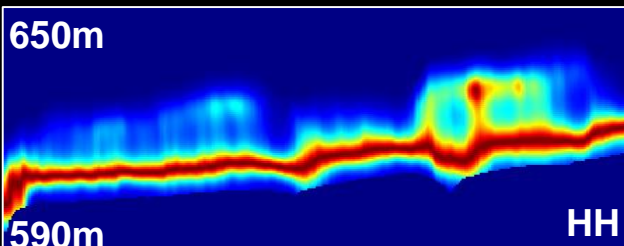


Slant range (~0.6Km)

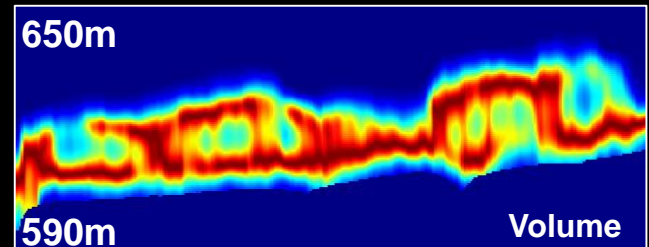
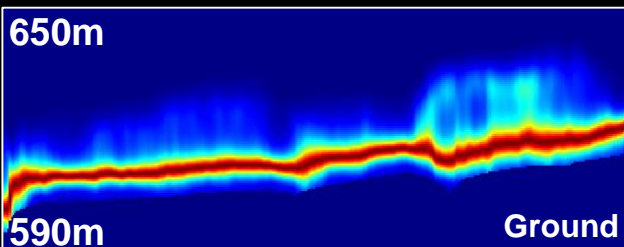
Slant range (~0.6Km)

P-band

Lexicographic basis  
HH vs HV



Maximum ground vs  
Maximum volume



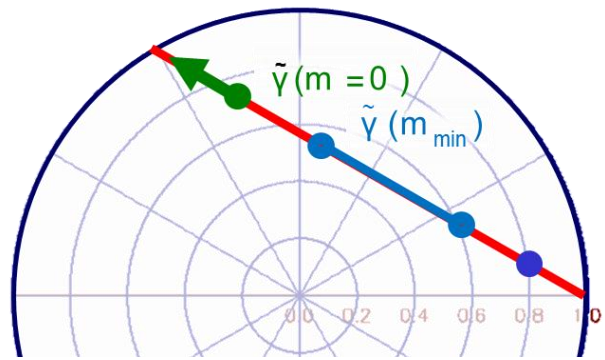
Slant range (~0.6Km)

Slant range (~0.6Km)

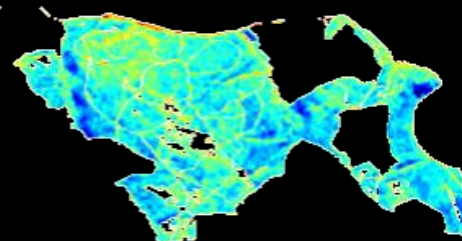
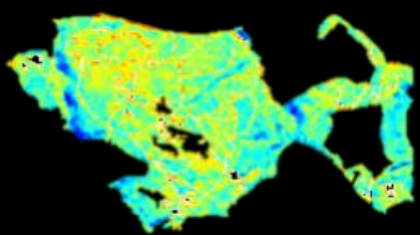


# Ground powers / polarimetry solutions

All the feasible ground covariance matrices are on the Pol-InSAR line segments outside the coherence region, under the positive (semi-)definiteness constraint.

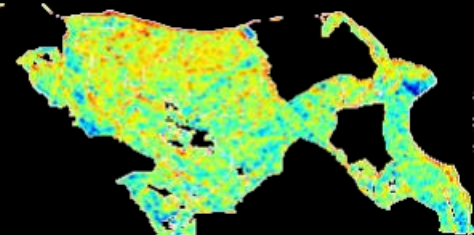


Capon estimates  
With known ground

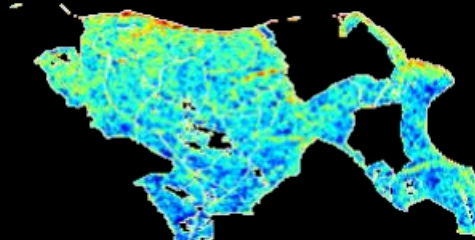


$\mathbf{C}_G @ \mu = \mu_{\min}$

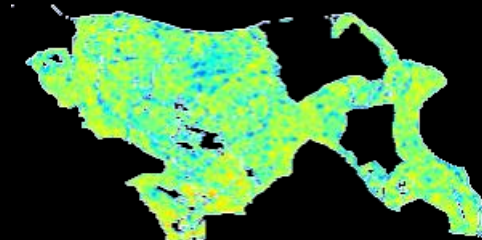
Ground power, HH



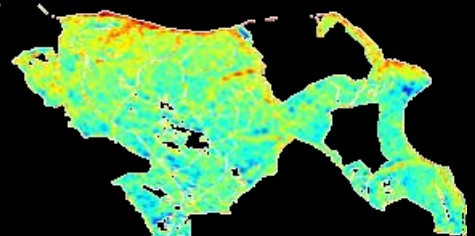
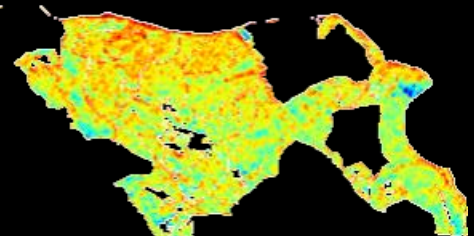
Ground power, HV



Ground entropy



$\mathbf{C}_G @ \text{decreasing } \mu$



-25 0 dB

0 1

Traunstein forest (south of Germany) – L band – DLR's E-SAR, 7 tracks – Capon

# Polarimetric SAR Interferometry

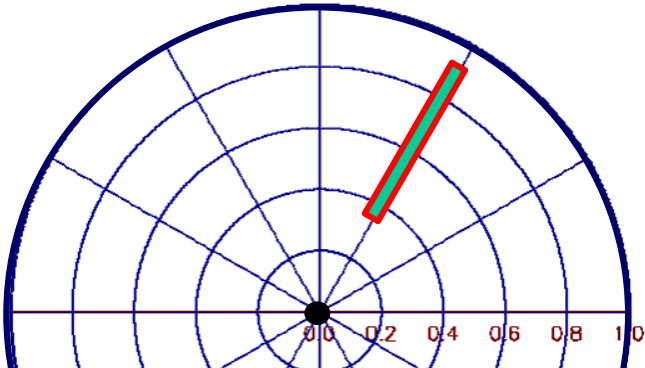
**Konstantinos P. Papathanassiou, Matteo Pardini**

German Aerospace Center (DLR)  
Microwaves and Radar Institute (DLR-HR)

[kostas.papathanassiou@dlr.de](mailto:kostas.papathanassiou@dlr.de)  
[matteo.pardini@dlr.de](mailto:matteo.pardini@dlr.de)

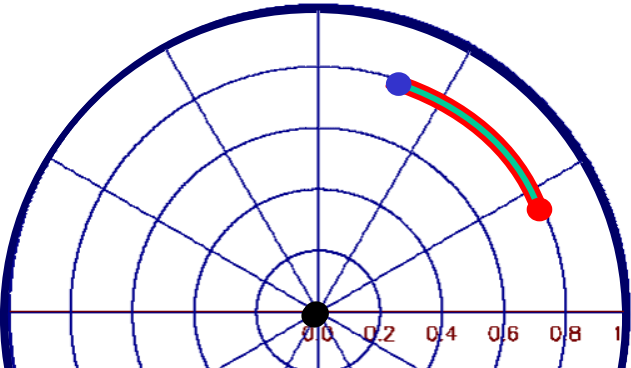


# Coherence Region (CR) Interpretation



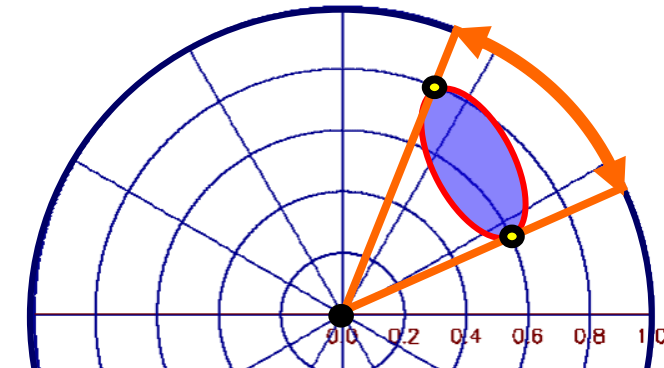
## Radial Shaped CR

i.e. InSAR coherence amplitude changes with polarisation but not the location of the phase center.



## Arc Shaped CR

i.e. InSAR phase center location changes with polarisation but not the absolute value of the coherence amplitude.

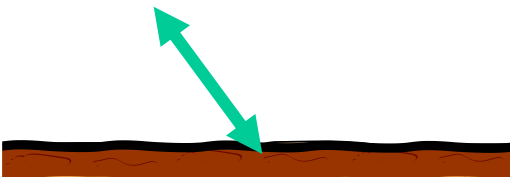


## Elliptical Shaped CR

i.e. InSAR coherence magnitude and phase center location changes with polarisation.

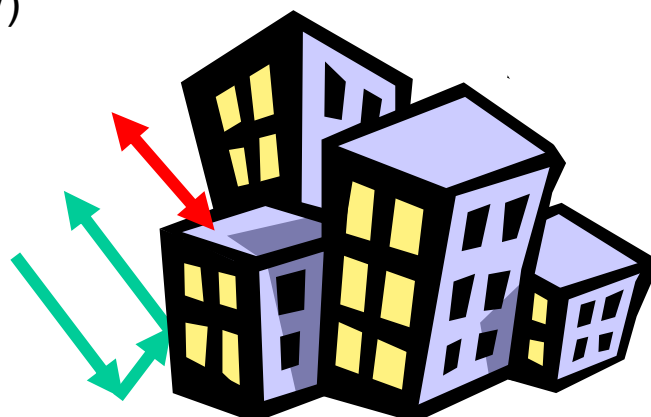
## Surface Scattering

$$\bar{\gamma}(\vec{w}) = \gamma_{\text{SNR}}(\vec{w}) \quad \bar{\gamma}_{\text{Vol}} := \gamma_{\text{SNR}}(\vec{w})$$



## (Polarised) Coherent scatterers

### at different heights



## (Depolarising) Scatterers

### at different heights

